An investigation of phase transformations in Pt-V coating systems

William Motsoko Makhetha

A dissertation submitted to the University of Cape Town, in fulfillment of the degree of Master of Science in Engineering

Centre for Materials Engineering

Department of Mechanical Engineering

July 2012

DECLARATION

- I know that plagiarism is wrong. Plagiarism is to use another's work and pretend that it is one's own.
- This dissertation An investigation of phase transformations in Pt-V coating systems is my own work.
- I have used the Institute of Electrical and Electronics Engineers (IEEE) System for referencing. Each contribution to, and quotation in, An investigation of phase transformations in Pt-V coating systems from the work(s) of other people has been attributed, and has been cited and referenced.
- I have not allowed, and will not allow, anyone to copy my work with the intention of passing it off as his or her own work.

Signature:..... Date ...../...../.....

Full Name: William Motsoko Makhetha

ACKNOWLEDGEMENTS

I would like to express my sincere gratitude to the following people:

My supervisor Prof. Candy Lang for the opportunity to work on this research project and for guiding me through to the end. I am grateful to have had you as my supervisor. You are the best any student could ask for. Thank you for being AWESOME beyond academics Prof.

My co-supervisor Dr. Mira Topic for your assistance throughout this research project. Your technical support has been AWESOME.

Dr. Mlungisi Nkosi at iThemba labs for making fabrication of thin-film coatings seem effortless.

Dr. Remy Bucher at iThemba labs for your help with XRD measurements and phase analysis.

Miranda from Electron Microscope Unit (EMU) at UCT for your assistance with SEM and EDS measurements.

Penny and Bev, thank you guys for organizing samples and materials used throughout this research project.

My fellow students who helped and were always there for moral support. You guys are fun people to work with.

My family and friends who helped and patiently believed in me to the completion of this task. Thank you for providing a shoulder to lean on. I am forever grateful to you guys.

ABSTRACT

Phase transformations in Pt-V coatings after heat treatment have been investigated. Five Pt-V ordered phases (PtV, PtV_3, Pt_2V, Pt_3V and Pt_8V) have been previously observed in bulk platinum-vanadium alloys. Phase formation in coatings is expected to be sequential and controlled by the lowest temperature eutectic (liquidus) composition; this allows control of experimental parameters for formation of desired ordered phases.

This investigation included fabrication of coatings, heat treatments, morphology characterization and phase analysis. Single and multilayer coatings ranging between 0.07 µm and 0.5 µm were deposited on vanadium and platinum substrates using E-beam deposition. The kinetics of phase transformation were studied by subjecting the coated layers to a variety of heat treatments in the temperature range 600°C to 900°C for 4 and 8 hours. Composition and morphology characterization was carried out using EDS and SEM respectively. XRD was used for phase analysis.

Four (PtV, PtV_3, Pt_2V, Pt_3V) out of the five Pt-V ordered phases exhibited in bulk alloys, were successfully formed from the coating system investigated in this project. The first phase formed, and the sequence of phase formation, was found to be different depending on which metal formed the substrate. The vanadium-rich ordered phase (PtV_3) was preferentially formed first on vanadium substrates and the sequence of phase formation progressed through ordered phases richer in platinum. The platinum-rich ordered phase (Pt_3V) was preferentially formed first on platinum substrates and the sequence continued towards formation of ordered phases richer in vanadium. An increase in heat treatment temperature from 600°C to 900°C resulted in rapid kinetics of phase transformation but affected the morphology of the coatings. An increase in coating thickness, number of coating layers, heat treatment time, and temperature resulted in an increase in overall total number of ordered phases and volume of ordered phases.

TABLE OF CONTENTS

1. INTRODUCTION

This research uses a model alloy system, platinum-vanadium, to investigate phase formation in coating systems. For this research, the advantage of coatings over bulk alloys is that they display sequential phase formation whereas bulk alloys display simultaneous phase formation [1]. The driving force for this kind of transformation is governed by changes in Gibbs free energy of the system: based on thermodynamic rules, the lowest possible energy of a system is achieved if phases form simultaneously in bulk alloys, but sequentially in coatings [1-4]. An understanding of the experimental parameters which influence sequential phase formation is clearly important for controlled formation of desired ordered phases.

The platinum-vanadium (Pt-V) alloy system exhibits five Pt-V ordered phases (PtV, PtV_3, Pt_2V, Pt_3V and Pt_8V) [5-7]. These have been successfully formed in bulk alloys, but not previously in coating systems. In the work presented here, a variety of different configurations of Pt-V coating systems, and a series of heat treatments, is used to investigate formation of Pt-V phases.

According to Pretorius *et al*. [1, 3, 4], phase formation in thin films (such as studied in this project) is controlled by the lowest temperature eutectic (liquidus) composition. This is in agreement with the rules governing the Gibbs free energy because it involves using changes in the heat of formation to determine phase formation. The rules for predicting phase formation in coatings use the Effective Heat of Formation (EHF) model, according to the following equation:

$$\Delta H' = \Delta H° \times \left(\frac{effective\ concentration\ of\ limiting\ element}{compound\ concentration\ of\ limiting\ element} \right)$$

which will be further explained in Chapter 2.

Platinum alloys frequently undergo diffusional ordering transformations; such transformations are commonly associated with an increase in hardness and strength [6, 8] and are accordingly of interest. The kinetics of these transformations may be slow in bulk alloys, if there is not enough energy for atoms of the alloying metal to rearrange and occupy preferred sites on the lattice to

form the ordered structures. Coating systems may offer faster transformation under the correct heat treatment conditions: a range of heat treatment temperatures and times was chosen for this research to determine the ordered phases formed.

Based on the advantages of coatings over bulk alloys in phase transformations, the aim of this project is to form ordered phases by heat treatments of platinum-vanadium coating systems. The focus of this research is to investigate coating thicknesses of up to 0.5 μm, known as thin films. The research project is limited to characterization of single and multilayer coatings on vanadium and platinum substrates. The following detailed objectives have been identified:

- To characterize the Pt-V coating system, as-coated and heat treated, in terms of phase transformations and morphology.
- To explore factors which influence the kinetics and thermodynamics of ordering transformations in Pt-V coatings.
- To evaluate prediction of first and subsequent phase formation using the EHF model.

There are six chapters in this dissertation. Following this Introduction, Chapter Two provides an overview of literature related to this research project: general views on diffusion and phase transformation, as well as the details on application of the EHF for predicting phase formation, are presented. Chapter Three deals with the protocol followed for gathering data. Analysis techniques and proposed treatment of the findings are also briefly discussed in this chapter. Results obtained from the experimental work are presented in Chapter Four and discussed in Chapter Five. Conclusions are finally drawn from this research in Chapter Six.

2. LITERATURE REVIEW

This literature review is laid out as follows: a general background to techniques used for deposition of thin film coatings and associated effects is presented first. A brief review on ordering transformations follows in section 2.2. An overview of the well known platinum-vanadium system is then presented in section 2.3. General reviews on phase transformation follow in section 2.4, then theories behind predicting phase formation in coating systems are presented in section 2.5.

2.1 THIN FILM COATING SYSTEMS

This section provides general background behind thin film coating techniques and thin film characterization in subsection 2.1.1, followed by a review of factors which determine adhesion between coating and substrate in subsection 2.1.2. Finally, stresses associated with thin film coatings, which are mostly a result of coating techniques used, are reviewed in subsection 2.1.3.

2.1.1 Preparation of thin film coatings

A thin film coating is a layer of material generally ranging from fractions of a nanometer to several micrometers in thickness. Thick films are generally greater than 100 microns in thickness [9-12]. The thicknesses of coatings investigated in this project range from 0.05 μm to 0.5 μm and are hence classified under thin-film coatings.

Several alternatives for deposition of thin film coatings exist, including oxidation, spin coating and plating [10-16], and each technique has advantages and disadvantages. Two common approaches are Physical Vapor Deposition and Chemical Vapor Deposition [10, 12].

Physical Vapor Deposition (PVD)

Films deposited by PVD are formed by atoms directly transported from source to the substrate through a gas phase. The physical vapor deposition can be achieved by the following processes:

- Evaporation
    - Thermal evaporation
    - Electron Beam (E-beam) evaporation
- Sputtering
    - DC sputtering
    - DC magneto sputtering
    - RF sputtering
- Reactive PVD

Chemical Vapor Deposition (CVD)

Films in CVD are formed by chemical reaction on the surface of a substrate. This can be achieved by the following processes:

- Low-Pressure CVD (LPCVD)
- Plasma-Enhanced CVD (PECVD)
- Atmosphere-Pressure CVD (APCVD)
- Metal-Organic CVD (MOCVD)

Table 2.1 shows a comparison of commonly-used PVD and CVD techniques. It can be seen that there is an inverse relationship between cost and coating quality.

Table 2.1: Comparison of typical deposition techniques [10-16].

Process	Uniformity	Impurity	Grain size	Deposition rate	Cost
Thermal evaporation	Poor	High	10 ~ 100 nm	1 ~ 20 A/s	Very low
E-beam evaporation	Poor	Low	10 ~ 10 nm	10 ~ 100 A/s	High
Sputtering	Very good	Low	~ 10 nm	~100 A/s	High
PECVD	Good	Very low	10 ~ 100 nm	10 ~ 100 A/s	Very high
LPCVD	Very good	Very low	1 ~ 10 nm	10 ~ 100 A/s	Very high

Thin film coatings for this research project were fabricated by E-beam deposition. As with all the PVD techniques, the E-beam process involves the following three phases [10, 13]:

Emissions from a vapor source

⇩

Vapor transport in vacuum

⇩

Condensation on substrates to be coated

Coatings are then characterized according to the surface, thickness, adhesion, morphology and composition. The general evaporation system requirements for E-beam are as follows [10]:

- Vacuum – preferably less than 1 X 10^{-4} Pa for medium quality films.
- Cooling water - required for thickness monitoring.
- Mechanical shutter – allows rapid modulation of evaporant flux: this is required because the evaporation rate is set by the temperature of the source material which cannot be turned on and off rapidly.
- Electrical power - either high current or high voltage - typically 1-10 kW.

Details of the evaporation parameters for the specific E-beam used in this research project are provided in chapter 3.

2.1.2 Adhesion of coating with substrate

The ability of a coating to remain attached to the substrate (also referred to as Bond Strength) determines adhesion between coating and substrate [11, 17-19]. Bond strength refers to interfacial forces which hold the two atoms together in a chemical bond. It determines the degree to which one atom contributes to the valency of the other atom [11, 17-19].

Increase in coating thickness results in increase in residual strains and this is usually associated with decrease in bond strength which therefore results in weak adhesion between coating and substrate [20]. Thin coatings are more likely to remain adherent with substrate.

The surface properties of a substrate may also contribute to adhesion with coating [17-19]. For instance, some materials might have an oxide film at the surface and some materials could be subjected to a final mechanical treatment such as polishing. The geometrical properties of surfaces are therefore very important and are not only determined by the substrate but also by factors such as contamination or poor vacuum during deposition process. Morphology and structure of the coating is determined by the method used to fabricate such a coating and each method is specific for desired morphology [12, 13]. For instance, thick coatings are likely to remain in place if the desired application involves sliding contact, while thin ones might be removed quickly from the substrate.

A determining factor on whether an atom or molecule will stick to a substrate is how well it can equilibrate with the substrate surface [11, 17-19]. Good adhesion is achieved if the energy is decreased to a point where the atoms will not subsequently be desorbed [11, 17-19]. Therefore, depending on the coating thickness and deposition rate, hardness and different amounts of energies and stresses can be expected in coated specimens.

2.1.3 Stresses in thin-film coatings

Different types of stresses are encountered in thin film coatings, some of which are as follows [17-19, 21-25]:

- Thermal stresses – these arise during post-deposition cooling and are caused by the difference of linear thermal expansion coefficients of film and substrate.
- Internal stresses – these may arise due to non-equilibrium conditions during deposition. Depending on the deposition technique used, these stresses are affected by the rate of cooling, geometry of sputtering, impurities, etc. In E-beam deposition for instance, the deposition rate determines the amount of residual stress in thin films [10, 12, 13, 26]. In this case, the stresses are expected to increase with an increase in the deposition rate. This occurs because intergranular porosity increases as the deposition rate increases, creating larger tensile stresses [26].

Stresses in thin film coatings are important because they contribute to the driving force for diffusion. Stresses which exist between coating and substrate are similar to those existing in grain boundaries, which are primarily responsible for the mass transport in thin films [17-19, 21, 22]. The interaction between coating and substrate can therefore be considered as a point of high stress concentration which may lead to an increase in total diffusion flux. Activation energy for diffusion may therefore change depending on the magnitude of stress between coatings with substrate. The greater is the stress and the thinner is the coating, the greater are effective coefficients of diffusion.

2.2ORDERING TRANSFORMATIONS

During metal alloying, different atoms which make up the alloy rearrange and the solute atoms can occupy preferential sites on the lattice forming an ordered lattice known as a superlattice [6, 7, 27]. This type of ordering is known as long range ordering (LRO) [6-8, 27-29]. Ordered alloys which undergo long range ordering are generally stable below a critical ordering temperature (T_c). Interdiffusion between substrate/coating couples can also result in the formation of superlattice structures.

Different superlattices can be formed during long range ordering transformations and these superlattices are characteristic of each particular alloy being studied. According to Parker [30], some superlattices can be fabricated through E-beam evaporation of alternating thin-films. These superlattices are explained as multilayered periodic structures having dimensions which approach the atomic spacing of the constituent materials comprising them. But the superlattice properties differ from those of their constituent elements.

2.3THE PLATINUM-VANADIUM SYSTEM

Platinum, as with other transition metals, has strong interatomic bonds which are characteristic of its crystalline structure and physical properties [6]. The platinum-vanadium system is well established in bulk alloys, but not in thin-film coatings. Some properties of platinum and vanadium are shown in table 2.2.

Table 2.2: Properties of platinum and vanadium metals [6, 31]

Platinum (Pt)	Vanadium (V)
• Face-centered cubic structure • Density of about 21.45 g.cm^{-3} • Melting point of about 1768°C • Outstanding catalytic properties • Excellent high-temperature characteristics • Chemical resistant • Suitable for fine jewelry • Appearance:  Grayish white metal.	• Body-centered cubic structure • Relatively low density (6.0 g.cm^{-3}) • Melting point of about 1910°C • Superconducting • Low-temperature ductility • Good fabricability • Corrosion resistant • Appearance:  Blue-silver gray metal.

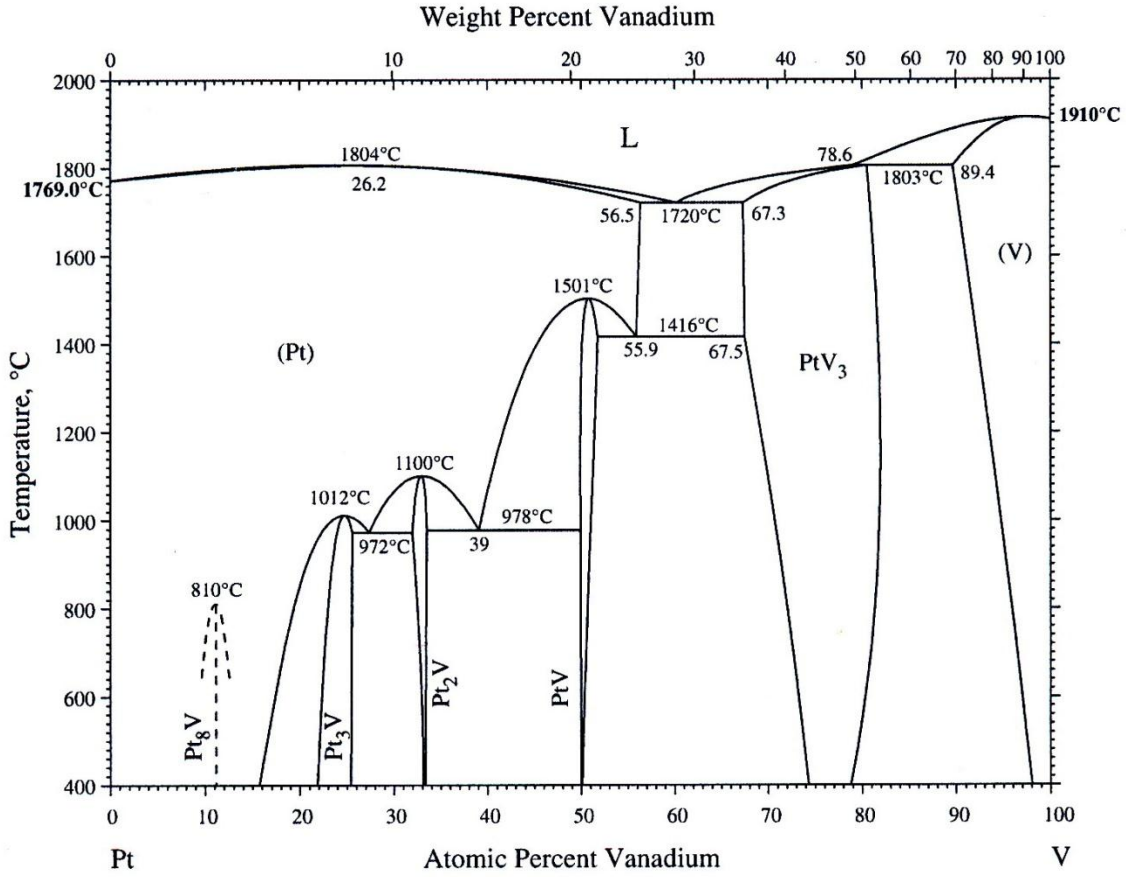

Figure 2.1: Equilibrium phase diagram of platinum-vanadium system (after Waterstrat [32] with Pt_8V information by Nxumalo *et al* [6]).

The platinum-vanadium (Pt-V) alloy system exhibits five Pt-V ordered phases (PtV, PtV_3, Pt_2V, Pt_3V and Pt_8V) as shown in figure 2.1 [5-7, 32]. The Pt-V phase diagram shows that ordering transformations take place at lower temperatures towards the platinum-rich side. But towards the vanadium-rich side, PtV_3 is stable at higher temperatures. Tables 2.3 and 2.4 present crystal structures and lattice parameters of Pt-V intermediate phases [6, 32].

Table 2.3: Crystallographic data for stable Pt-V phases.

Phase	Lattice structure	a [nm]	b [nm]	c [nm]
Pt_8V	Face-centered tetragonal	-	-	-
Pt_3V	Body-centered tetragonal	0.384600	-	0.779600
Pt_2V	Body-centered orthorhombic	0.272	0.835	0.379
PtV	Orthorhombic	0.442	0.269	0.476
PtV_3	Cubic	0.4808	-	-

Table 2.4: Crystallographic data for metastable phases observed in Pt-V system.

Phase	Structure	a [nm]	b [nm]	c [nm]
Pt_3V	Cubic	0.3879	-	-
PtV	Tetragonal	0.381	-	0.388
PtV_3	Cubic	0.3918	-	-

Diffusional ordering transformations such as those observed in the platinum-vanadium system are commonly associated with an increase in hardness and strength [6, 8, 33] and are accordingly of interest where enhanced mechanical properties are desirable. The kinetics of these transformations may be slow in bulk alloys, particularly if diffusion distances are long and heat treatment times are short. Platinum-vanadium coated systems may offer faster transformation under the correct heat treatment conditions, but the five ordered Pt-V phases have not previously been successfully formed in coated systems.

2.4PHASE TRANSFORMATIONS IN SOLID-STATE MATERIALS

Solid-state phase transformations modify microstructure and can thus be used in tuning of the properties of materials [34-36]. In addition to the change in structure, phase transformations can also involve changes in local composition for multi-phase systems. In order for a diffusional phase transformation to take place, rearrangement and redistribution of atoms via diffusion is required. The characteristics of diffusional phase transformations are as follows [2, 21, 23, 36, 37]:

- A decrease in the free energy of the system (G). At constant pressure and temperature, phase transformations occur spontaneously when the free energy of the system decreases.
- Nucleation and growth. These are diffusion-controlled processes which determine the kinetics of phase transformations and they are dependent on time and temperature. Controlling time and temperature results in nucleation and growth of stable particles for the formation of a new phase.

Some of the reasons as to why diffusion is important are as follows [2, 21, 23, 34-37]:

- Diffusion enables phase transformation as mentioned above.
- The diffusion process takes place from a high to a low element potential and is therefore generally driven by a concentration gradient.
- Diffusion is very important because it puts the system in equilibrium hence formation of stable phases.
- Diffusion coefficient (*D),* relates a net flux of atoms per unit area (*J)* to an atom concentration gradient (*dc/dx)* according to Fick's first law, which is expressed by [2, 37, 38].

$$J = - D \left(\frac{dc}{dx}\right) \qquad \text{Equation 1}$$

- In steady-state diffusion, there is a constant concentration gradient and as a result, the flux of atoms is independent of time and distance. Fick's first law holds for steady-state diffusion.
- In non steady-state diffusion, the flux of atoms changes with time and distance because there is changing composition gradient. Fick's second law is applicable because it takes into account time and jump distance and is expressed as follows:

$$dc/dt = D(d^2c/dx^2) \qquad \text{Equation 2}$$

- Diffusion varies with composition and for non-cubic materials, the atomic jump frequency and distance also varies with crystallographic direction resulting in anisotropic diffusivity.
- Diffusion occurs by means of lattice imperfections including vacancies.
- Diffusion is more likely when temperature goes up because the equilibrium concentration of vacancies in a lattice increases. Increasing temperature also helps provide atoms with energy to overcome energy barriers during diffusion.

A phase transition is typically brought about by a change in temperature of the system; the temperature at which the change of phase occurs is called the transition temperature [38]. Atomic migration throughout the whole volume of the crystal lattice predominates at high temperatures [38]. At temperatures well below the absolute melting temperature of a metal, atomic migration occurs primarily at surfaces, dislocations, and grain boundaries. For ordered phases, temperatures higher than the critical temperature (T_c) lead to a disordered state [2, 37]. This therefore suggests that heat treatments are only required to start the process of diffusion by providing atoms with enough energy to break bonds with their neighbors and migrate. The rate of diffusion will therefore be determined by how high the heat treatment temperature is below T_c (ΔT below T_c).

Solid-state reactions taking place in thin film coatings follow a non-equilibrium phase formation [3]. It is non-equilibrium because growth of new phases takes place at a moving interface. Upon heat treatment of coated specimens, phase transformation takes place and new ordered structures

form. The reaction is controlled by mechanisms of diffusion similar to bulk alloys, hence heat treatments are required to enable atoms to break bonds with their neighbors and migrate.

2.4.1 Mechanisms of diffusion in solid materials

Substitutional

In this mechanism, equilibrium vacancy concentration is required for diffusion to take place [2, 35, 36, 38]. As-received materials always have defects but the equilibrium vacancy concentration increases with increase in temperature resulting in high diffusion rate.

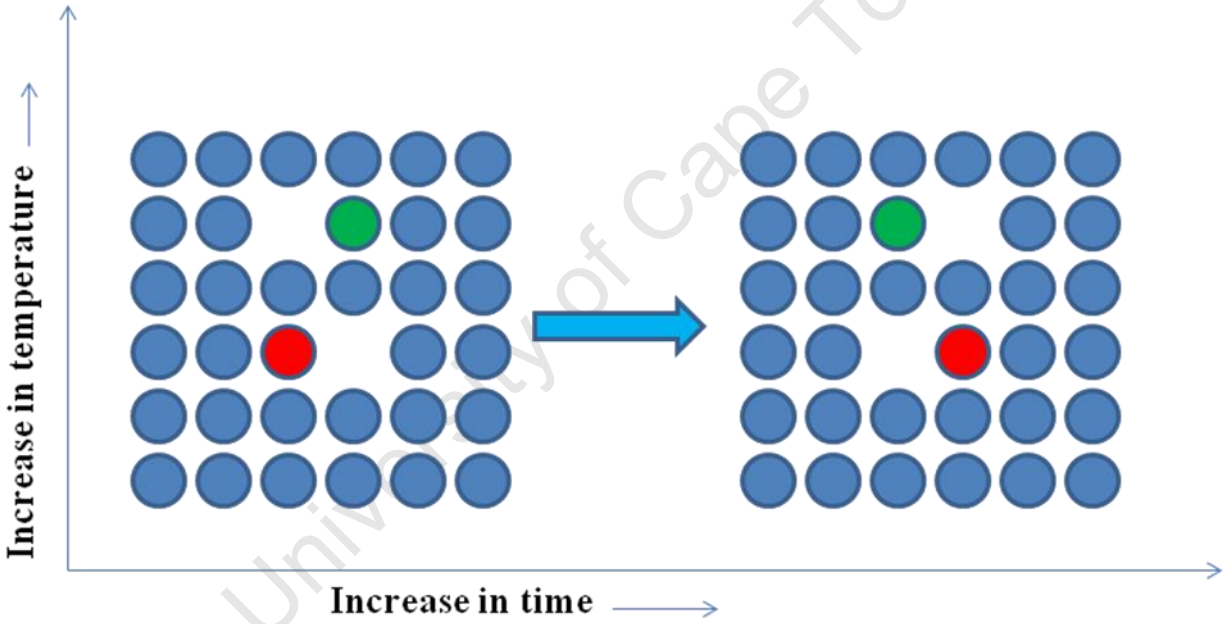

Figure 2.2: Schematic representation of substitutional diffusion mechanism as a result of increase in time and temperature [2, 35, 36, 38].

All substitutional atoms adjacent to a vacant space have equal chances of jumping into the vacancy [35, 36]. The process is faster at high temperature because equilibrium vacancy concentration increases with increase in temperature.

Other diffusion mechanisms are **Interstitial** and **Intersticialcy**. The interstitial mechanism refers to the jumping of very small atoms from one interstitial site to another without directly involving the remainder of the lattice [2, 38]. Typical atoms which diffuse via the interstitial mechanism in metals include H, O, N, and C. The jump frequency of atoms in this mechanism is very high because the atoms always have neighboring vacant sites. Diffusion rate through this mechanism is therefore very high. The intersticialcy mechanism involves an interstitial atom and an atom on a regular lattice site moving in unison [2, 38]. In this mechanism, an atom on a regular site can be replaced by one from an interstitial site.

2.4.2 Phase stability in solid-solid phase transformations (reaction between two solids)

Thermodynamically stable phases are almost always produced in liquid-solid transformations but not necessarily in solid-solid transformations (between two different solids) [16, 30, 39]. This is because in solid-liquid interactions, the transformations occur by fast liquid state diffusion, and the kinetics of the transformations can always keep pace with the thermodynamic requirements. In solid-solid transformations however, diffusion is generally several orders of magnitude slower than liquid-solid diffusion [16, 39]. So with solid-solid diffusion transformations being much more sluggish than their liquid-solid counterparts, deviations from the Gibbs' rule are expected (The Gibbs rule is explained further in section 2.4.3). Nonetheless, the solid-solid transformations are still able to occur, but over a range of temperatures (which sometimes could be several hundred degrees) rather than at one specific temperature. The Pt-V phase diagram (in figure 2.1) shows for example that five different ordered phases are stable below 800°C for different compositions. Accordingly, solid-solid transformations between Pt and V are best displayed on a time-temperature-transformation (TTT) diagram, in which different products and the kinetics of the reaction are shown as a function of temperature [16, 39].

Due to the sluggishness of the solid-solid transformation, metastable transitional phases may be produced in preference to the equilibrium phases. This situation arises because the system has to lose a given amount of free energy (the driving force of transformation) to form the stable

reaction product [16, 39-42]. The system can lose the energy faster by forming a series of metastable phases, which progressively give rise to the formation of stable products [16, 39-42].

Many solid-solid transformations are known to pass through several distinct intermediate stages to maximize the rate of decrease of the free energy of the system before arriving at their equilibrium states [40]. As a result, the magnitude of the free energy change of solid-solid transformation can be varied by allowing the transformation to proceed at different temperatures. It is therefore possible to obtain in any given alloy several different reaction products resulting from different reaction mechanisms, and this is depending on the actual transformation temperature employed.

2.4.3 Thermodynamics of solid-solid reactions

Atoms form stable structures when they are at their lowest possible energy state [2, 3, 37]. The driving force for the solid-solid reaction that leads to the formation of these stable structures is governed by the Gibbs' free energy, expressed as follows:

$$\Delta G^o = \Delta H^o - T\Delta S^o \qquad \text{Equation 3}$$

where ΔG^o is determined by the change in enthalpy (ΔH^o) and the change in entropy (ΔS^o) at temperature (T) during the reaction. The change in entropy is small during solid-solid formation of ordered compounds, usually only about ±0.001 kJ/deg per mole of atoms [4] and therefore the heat of formation term (ΔH^o) becomes a good measure of the change in Gibbs' free energy [43] according to the following equation:

$$\Delta G^o = \Delta H^o \qquad \text{Equation 4}$$

This is only true at low temperatures and very high enthalpy changes, such that ΔH^o term of the equation dominates the $-T\Delta S^o$ term.

2.4.4 Kinetics in solid-solid reactions

The diffusion coefficient is dependent on temperature [2, 3, 37]. Diffusion rate increases with increase in temperature. Given enough time at temperature, atoms are able to migrate from their high concentration to their low concentration, with certain exceptions such as in ternary diffusion whereby atoms can diffuse up a concentration gradient [2].

This refers mostly to bulk alloy reactions. But similar conditions can be expected in coating systems because for thermally activated solid-solid transformations, the rate at which the interfaces migrate is a function of the transformation temperature [23, 24, 26, 44, 45]. For instance, the diffusion coefficient (D) increase with increase in temperature and the change in free energy of a system (ΔG) decreases with increase in temperature. As a result, the phase with the lowest ΔG will be the most stable.

2.5PREDICTION OF PHASE FORMATION IN COATINGS

The advantage of coatings over bulk alloys for this research is that they display sequential phase formation whereas bulk alloys display simultaneous phase formation [1, 3, 4, 46-50]. This happens because based on thermodynamic rules; the lowest possible energy of a system is achieved if phases form simultaneously in bulk alloys, but sequentially in coatings. Experimental parameters which influence sequential phase formation are therefore important for controlled formation of desired ordered phases in coating systems. Rules for predicting phase formation have therefore been formulated to assist in control of the experimental parameters.

2.5.1 Walser and Benè (W-B) model for predicting phase formation

One of the early models for predicting phase formation sequence in thin films was formulated by Walser and Benè [49] who stated the rule for first phase formation as follows:

"The first compound nucleated in planar binary reaction couples is the most stable congruently melting compound adjacent to the lowest-temperature eutectic on the bulk equilibrium phase diagram."

This means that the first phase nucleated in metal-metal thin film reactions is the ordered intermetallic phase immediately adjacent to the low-temperature eutectic in the binary equilibrium phase diagram.

The rule governing the Walser and Bené model for subsequent phase formation was stated as follows [49]:

"The second phase is the compound with the smallest ΔT that exists in the phase diagram between the composition of the first phase and unreacted element,"

ΔT in this case is the temperature difference between the liquidus curve and the peritectic or peritectoid point, which is zero for congruently melting compounds.

The nucleation of a new phase, according to the W-B model, is favoured for similar melting phases while skipping the nucleation of dissimilar melting phases. This is because there is a higher energy barrier associated with dissimilar melting phases during rearrangement in short-rage order and the energy associated with similar melting states is small [3]. Therefore, predicting the phase formation sequence using the W-B model was achieved through the use of temperature change as a measure of stability. This is applicable where there is no similarity in melting compounds between the first phase and the remaining element. If only non-congruent phases are left, the one with the smallest ΔT usually forms [3]. This is because, "the larger the ΔT between the liquidus curve and the peritectic (or peritectoid) point for non-congruent phase the more difficulty it has to nucleate at the moving interface."

According to Pretorius *et al*. [1] however, the W-B model did not make direct use of thermodynamic data and was therefore only relatively successful in predicting phase formation. Thermodynamic data could be used directly to predict first and subsequent phase formation sequence after Pretorius *et al*. [1] proposed the effective heat of formation (EHF) model. The EHF (ΔH´) model enables the calculation of heats of formation as a function of concentration [43] and has been successful in predicting phase formation sequence as well as explaining how the presence of impurities such as oxygen can alter phase formation sequence.

2.5.2 Effective Heat of Formation (EHF) model

It has been found that in thin films, phase formation is controlled by the lowest eutectic (liquidus) [1, 3, 4, 46-50] and that the effective concentrations at the growth interface are expected to be as close as possible to that of the lowest temperature eutectic (liquidus) within the concentration range of the two interacting phases. Based on this, it is expected that phases will react with each other to form a phase with a composition between those of the interacting phases and closest to that of the lowest eutectic (liquidus) composition.

As shown in Section 2.4.3, the heat of formation is a good measure of the change in Gibbs free energy. The EHF model makes use of the heat of formation to predict phase formation. The EHF is expressed by the following equation:

$$\Delta H' = \Delta H° \times \left(\frac{effective\ concentration\ of\ limiting\ element}{compound\ concentration\ of\ limiting\ element} \right) \quad \text{Equation 5}$$

Pretorius *et al*. [3] stipulated that the heat of formation can only be used to predict phase formation when activation or nucleation barriers do not exist, since a system will always prefer to go to its lowest possible free energy state, therefore making it easier for phases to be stable.

During solid-solid interactions, phase formation at an interface is a non-equilibrium process [1, 3, 4]. This as explained by Pretorius *et al*. [1, 3] , means that only one compound phase forms at a particular interface. This is different from the bulk equilibrium process whereby a simultaneous formation of a mixture of phases leads to the lowest free energy state for the system.

The phase transformation at a growth interface is regarded as a dynamic nonequilibrium process [3] in that the excess atoms, left from the previous phase formation, are looked upon as being available for the formation of the next increment of the compound at the moving interface. The heat released is dictated by the effective concentration of the limiting element and the concentration of the limiting element in the compound to be formed.

Pretorius *et al*. [1, 3] explain the phase formation expected in metallic systems (such as platinum and vanadium) as follows. The initial condition when dealing with thin films of one metal deposited onto a thick substrate is such that there is more of one element (substrate) than the other (coating). For example, if the reaction is started with two elements A (thick substrate) and B (thin film coating), during the reaction, B atoms are expected to be used up while A atoms are expected to be in excess. A simplified equation to illustrate this point at the reaction interface is as follows:

$A + B = A\ (Excess) + B\ (Limiting) + A_xB\ (New\ phase)$

The reaction continues until the entire limiting element B is completely consumed such that the equation above ends up as;

$A + B = A\ (Excess) + A_xB\ (New\ phase)$

It is important to note that, there is a possibility of more than one new phase formed, but the concept is still the same in that the new phases are formed at the expense of the limiting element. Also, in the case where the limiting element is completely consumed, some of the ordered phases formed will be consumed at the expense of new ordered phases forming.

Therefore, the B element is regarded as a limiting element and the availability of the excess A atoms will result in the initiation of the formation of the next phase. This is explained further in section 2.5.3 below. For subsequent phase formation, the reaction between the remaining element A and the phase previously formed will result in the formation of a new phase. The growth of a particular phase at any point, increases until one of the previous two elements or phases, is completely consumed.

Therefore, using equation 5, the effective heat of formation of any compound can be calculated as a function of the concentration of the reacting species. It is therefore crucial to know the effective concentration at the interface of the two reacting species in thin films to be able to use equation 5 to predict phase formation.

2.5.2.1 EHF model for first phase formation

Since the thin-film solid-solid interaction is a nonequilibrium process, when predicting phase formation using EHF model, the effective concentrations at the growth interface are independent of the relative thicknesses of the interacting components [3]. But knowledge of the effective concentrations of the two reacting species at the interface is required [46, 47].

However, Petrorius *et al.* [3] point out that it is not possible to calculate the actual effective concentrations of the reactants at the growth interface during solid-solid interaction. Brown and Ashby [49] nonetheless, showed that activation energy can be used to estimate the effective concentrations. They explained that, for a given structure and bond type, the activation energy for solid-solid diffusion is directly proportional to the melting point of the solid. Activation energy can therefore determine mobility. The greatest mobility of the atoms and hence the most effective mixing at a reaction interface upon heating is expected to take place at the composition of the lowest eutectic (or liquidus) of the binary system [1, 3, 46, 47]. The effective concentrations of the interacting atoms are therefore chosen to be that of the lowest temperature eutectic (or liquidus). For instance, figure 2.3 below shows the lowest liquidus temperatures of three different binary systems.

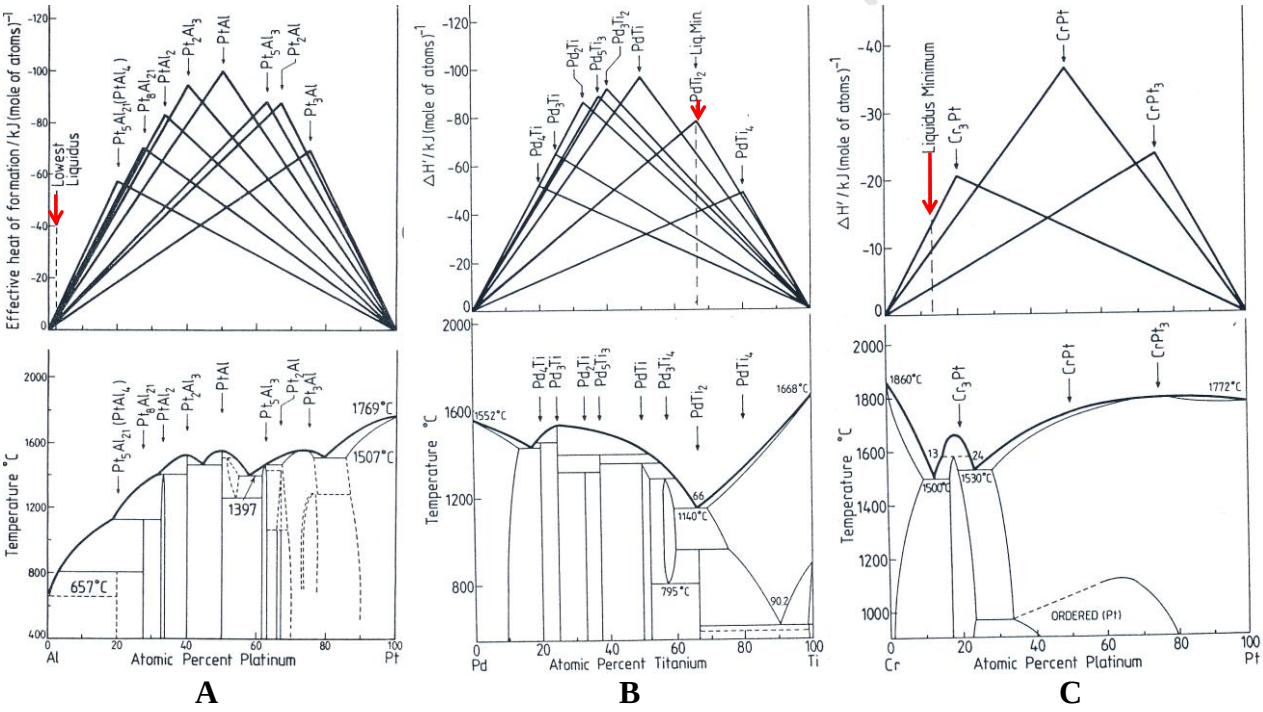

Figure 2.3: Phase diagrams and corresponding effective heat of formation diagrams of Pt-Al (A), Pd-Ti (B) and Pt-Cr (C) systems (After Pretorius *et al.* [1, 3]).

The effective concentrations in each case are therefore assumed to be 98 at. % Al, 2 at. % Pt in (A), 32 at. % Pd, 68 at % Ti in (B) and 88 at. % Cr, 12 at % Pt in (C) as indicated by arrows in figure 2.3.

According to Petrorius *et al.* [3], effective instead of actual concentrations are used in prediction of phase formation in the EHF model because many factors such as lowest eutectic, impurities, atomic mobility, diffusing species, etc, could affect the actual concentrations that are available for interaction at the growth interface. This therefore makes the lowest temperature eutectic become the determining factor at a growth interface when effective concentrations are used. This led to the proposal of the first phase formation rule which was stated as follows [1, 3]:

"*The first compound phase to form during metal-metal interaction is the phase with the most negative, effective heat of formation (ΔH´) at the concentration of the lowest temperature eutectic (liquidus) of the binary system."*

Therefore according to this rule, high EHF (ΔH´) means the formation of such a phase leads to the largest change in free energy (release of the most energy from the system) hence that phase would be formed first. But for phases with a large number of atoms per unit cell, high (most negative) ΔH´ does not necessarily mean that the particular phase will form first. This according to Petrorius *et al.* [3] happens because these phases are difficult to nucleate at the moving interface. In the Pt-Al binary system for instance, Pt_5Al_{21} (416 atoms per unit cell) and Pt_8Al_{21} (116 atoms per unit cell) were predicted to have the most negative ΔH´. But these phases would be skipped hence the EHF rule predicts first phase formation of either $PtAl_2$ (12 atoms per unit cell, ΔH' *-5.05 kJ(mol at.)*$^{-1}$) or Pt_2Al_3 (5 atoms per unit cell, ΔH´ *-4.75 kJ(mol at.)*$^{-1}$) depending on assumed effective concentrations.

2.5.2.2 EHF model for subsequent phase formation

Pretorius *et al.* [1] formulated the second rule governing the EHF model for the phase formation sequence and this rule was stated as follows:

"After the first phase formation in metal-metal binary systems, the next phase to form at the interface between the compound phase and the remaining element is the next phase richer in the unreacted element, which has the most effective heat of formation."

The effective heat of formation rule correctly predicts phase formation sequence in elements such as nickel, palladium, platinum, gold and aluminides [1, 3, 50]. But certain phases are skipped for Pt, Pd and Au and these phases are skipped because they are difficult to nucleate. The difficulty to nucleate is usually indicated by a large number of atoms per unit cell as mentioned in section 2.5.2 or by noncongruency. This is especially so in a nonequilibrium situation, such as in thin-film systems, where growth has to take place at the moving interface.

The phase formation sequence in binary metal thin films depends on the overall composition of the structure [3]. This can be illustrated using the EHF rule to predict phase formation sequence as follows:

During the reaction of two elements A and B, for a thin coating B on thick substrate A (B < A), the first phase to form will be the one predicted by the EHF rule as shown in section 2.5.3, which will be a B-rich phase as illustrated next.

$A + B = A\ (Excess) + B\ (limiting) + AB_x\ (B\text{-rich phase})$

The above step represents nucleation and growth of the first phase. The effective concentration of element B is expected to decreases at this stage. The first phase continues to grow until the entire B element is consumed to complete the formation as follows:

$A + B = A\ (Unreacted) + AB_x\ (B\text{-rich phase})$

The effective concentration of the atoms at the reaction interface is then expected to move towards the formation of a phase that leads to the biggest change in free energy (most negative effective heat of formation within the concentration range of the two interacting phases). This

would be a phase richer in A (unreacted) element since at this point all the B element is completely consumed. The reaction will proceed as follows:

A (Unreacted) + AB_x (B-rich) = A (Unreacted) + AB_x (B-rich) + A_yB (A-rich phase)

The above step represents nucleation and growth of the second phase and which continues until all of the first phase is used up to complete the second phase formation according to:

A (Unreacted) + AB_x (B-rich) = A (Unreacted) + A_yB (A-rich phase)

The process continues with subsequent phases richer in A (unreacted element) until the most A-rich phase is formed as follows:

A (Unreacted) + A_yB (A-rich phase) = A (Unreacted) + A_zB (Most A-rich phase) + A_yB (A-rich phase)

The final reaction would be:

A (Unreacted) + A_yB (A-rich phase) = A (Unreacted) + A_zB (Most A-rich phase)

In the case of thin A-coating on thick B-substrate (B > A), the first phase to form is still the phase predicted by the EHF rule. After the first phase formation, the effective concentration is still expected to turn towards the unreacted element leading to formation of the adjacent phase which in this case is more B-rich. Again this process continues until the most B-rich phase is formed.

A complicated scenario is encountered if the most B-rich phase, in the case of B > A (limiting), is the first phase to form. According to Pretorius *et al.* [3], no subsequent phase formation takes place in this case because, the effective concentration of the limiting element at the growth interface decreases after formation of the first phase. The complete consumption of the limiting element therefore results in the effective concentration favoring formation of phases richer in the

unreacted element (B). Since the most B-rich phase would have formed already, no subsequent phase formation takes place.

The EHF model had limitations in that it could only characterize successfully the intermetallic formation sequence and not the superlattice formation sequence seen in Pt-based alloys like Pt-V system [3]. As a result, the alternative model for predicting phase formation sequence was one formulated by Walser and Bené, which is stated in section 2.5.1 above.

2.5.2.3 Summary of EHF model on first and subsequent phase formation

Whatever the configuration of a specific sample, mixing at the interface will always be controlled by the lowest temperature eutectic of the system and the effective concentrations will be expected to be as close as possible to that of the lowest eutectic within the concentration range of the two interacting phases [3]. This is expected to take place even if the eutectic composition does not lie between the compositions of the interacting phases.

In general, phases are expected to react with each other to form a phase with the most negative effective heat of formation with composition lying between that of the interacting phases. Reactions which form a phase outside this composition range lead to an increase in free energy, as it leads to less bond formation.

3. EXPERIMENTAL PROCEDURE

The four sections in this chapter provide details of experimental procedure followed for investigation of the platinum-vanadium coating system in this project. Section 3.1 presents the sample preparation procedure carried out before coating deposition. Single and multilayer coatings were deposited onto substrates as described in section 3.2. Several heat treatment temperatures were explored at different heat treatment times as shown in section 3.3. The procedure for characterization of morphology, composition and phase structure is outlined in section 3.4.

3.1SAMPLE PREPARATION

Platinum and vanadium sheets were used as substrates in this experiment. The vanadium sheet was received as annealed, whereas the platinum was received as a button, which was cold rolled into a sheet. Both sheets were cut into 10 mm x 10 mm squares as shown below.

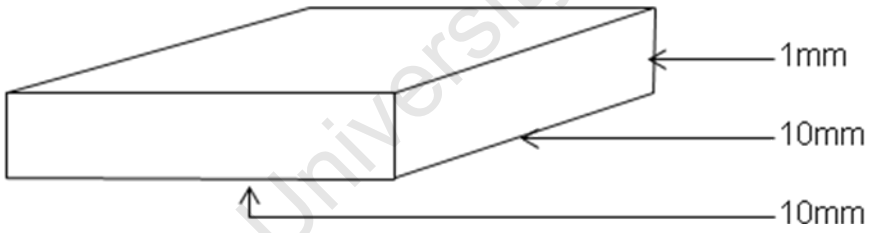

Figure 3.1: Schematic representing the dimensions of substrates prior to deposition.

These substrates were then mounted in resin to allow grinding and polishing to be carried out, using silicon carbide 500, 800 and 1200 grit paper and 3 µm, 1 µm and ¼ µm diamond paste respectively. Prior to E-beam deposition, thorough cleaning of substrates is required for good adhesion of the coating with substrate. Accordingly, the substrates were demounted and cleaned in a stepwise technique as described below.

Specimens were immersed and sonicated sequentially in:

Methanol

Acetone

Trichloroethylene

Acetone

Methanol

De-ionized water

5% Hydrofluoric acid solution

Each of these steps is recommended to be carried out for 5 minutes in an ultrasonic bath. In this project, it was found that leaving the substrates in the ultrasonic bath for 20 minutes at each step resulted in improved coated specimens after deposition. Following the cleaning sequence, samples were immediately loaded into the E-beam and put under vacuum overnight.

3.2COATING PROCEDURE

An electron beam (E-beam) physical vapour deposition technique was used for deposition of coatings onto substrates. The substrates were mounted onto rotating sample holders inside the evaporator, and a vacuum was created in the evaporator prior to deposition, to eliminate contamination of specimens. The parameters of materials to be deposited were first entered into the film thickness monitor and the deposition was monitored and physically controlled until the desired thickness parameters were reached.

The overall E-beam evaporation conditions were as follows:

- Deposition rate of platinum coatings was 1.8 – 2.4 A^0/s at a vacuum pressure of 1 x 10^{-4} Pa.
- Deposition rate of vanadium coatings was 2.4 – 3.0 A^0/s at a vacuum pressure of 8 x 10^{-5} Pa.

Due to the possibility of thickness variation, the rate of deposition was gradually slowed down towards the end of deposition to obtain near accurate thickness.

Different thicknesses of single layer coatings were deposited on substrates as shown in table 3.1. Alternating thicknesses and schematic representation of multilayer coatings on substrates were as shown in table 3.2.

Table 3.1: Single layer coatings and schematic representation of coated layers.

Type of substrate	Thickness of deposited layer	Schematic representation
Vanadium	0.1 µm Pt	
	0.2 µm Pt	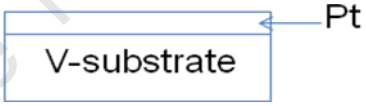
	0.3 µm Pt	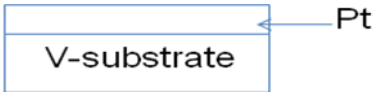
Platinum	0.3 µm V and 0.07 µm Pt	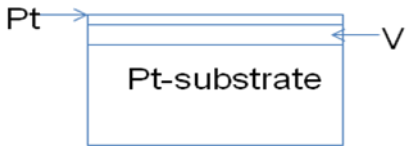

Note: The single layer of vanadium on platinum substrate needs to be covered by a layer of platinum because vanadium oxidizes easily if left as the topmost layer, hence the layer of platinum seen in table 3.1 above.

Table 3.2: Multilayer coatings and schematic representation of coated layers.

Type of substrate	Thickness of deposited layer	Schematic representation
Vanadium	Three layers (**3L**); at a sequence of 0.1 µm Pt, 0.05 µm V and 0.1 µm Pt.	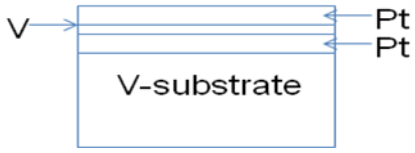
	Five layers (**5L**); at a sequence of 0.1 µm Pt, 0.05 µm V, 0.1 µm Pt, 0.05 µm V and 0.1 µm Pt.	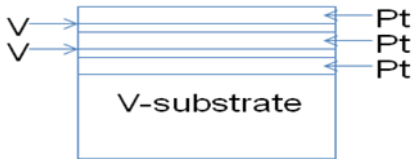
Platinum	Four layers (**4L**); At alternating 0.3 µm V and 0.07 µm Pt.	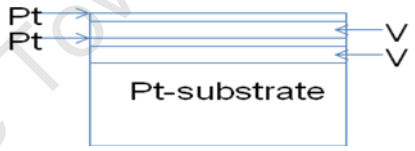
	Six layers (**6L**); At alternating 0.3 µm V and 0.07 µm Pt.	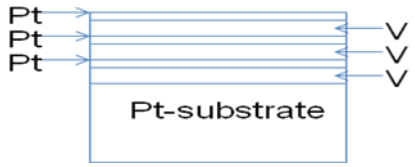

3.3HEAT TREATMENT PROCEDURE

All heat treatments were carried out in a vacuum furnace according to the plan shown in table 3.3. The heat treatments were followed by fast fan-cooling to minimize the possibility of further transformation occurring during slow cooling.

Table 3.3: Heat treatment procedure.

Heat treatment temperature	Heat treatment time	Number of specimens
600ºC	4 hours	1
	8 hours	1
700ºC	4 hours	1
	8 hours	1
800ºC	4 hours	2
	8 hours	2
900ºC	4 hours	2
	8 hours	2
Total number of specimens per configuration		12

Therefore:

- Number of specimens for configuration Pt on V, 0.1 µm Pt single layer = 12
- Number of specimens for configuration Pt on V, 0.2 µm Pt single layer = 12
- Number of specimens for configuration Pt on V, 0.3 µm Pt single layer = 12
- Number of specimens for configuration Pt on V, 3L multilayer = 12
- Number of specimens for configuration Pt on V, 5L multilayer = 12
- Number of specimens for configuration V on Pt, 0.3 µm Pt single layer = 12
- Number of specimens for configuration V on Pt, 4L multilayer = 12
- Number of specimens for configuration V on Pt, 6L multilayer = 12

Note: A total of 96 specimens were studied. One specimen for each configuration heat treated at 600ºC and 700ºC was studied because XRD results showed minor peak intensities; hence only the heat treatments at 800ºC and 900ºC were duplicated for confirmation of results.

3.4CHARACTERIZATION TECHNIQUES

The following equipment was used for data collection to assist in analysis of coating/substrate couples:

- SEI Nova NanoSEM, at 20.0 kV accelerating voltage, was used to obtain micrographs of as-deposited and post-heat treated samples for morphology characterization. SEM measuments were done for all configurations (96 specimens) but the images presented in the results section were for emphasis on coating and temperature effect on morphology.
- Energy Dispersive X-ray Spectroscopy (EDS or EDX) was used for elemental analysis of samples. The Pt excitation energy is 9.441 and that of V is 4.952. The primary voltage setting for EDS measurement therefore needs to be double or more than Pt and V excitation energies; hence 20.0 kV was used for these measurements. For thin coatings and depending on density of the coating material, the EDS interaction depth can be expected to be more than the interdiffused zone, which renders the results inconclusive because information from the substrate will have been picked up. EDS measuments were done for all configurations (96 specimens) but only a few results are presented for emphasis on heat treatment temperature effect.
- X-ray Diffraction (XRD) was used for phase analysis. The measurements were carried out using Bruker D8-Advance diffractometer with CuK_{α} radiation at 40 kV. The scan step size for these measurements was 0.02° at a 2θ range between 10° and 100°. The XRD interaction/penetration depth changes with angle of measurement according to the schematic diagram in figure 3.2 and summarized in figure 3.3 respectively.

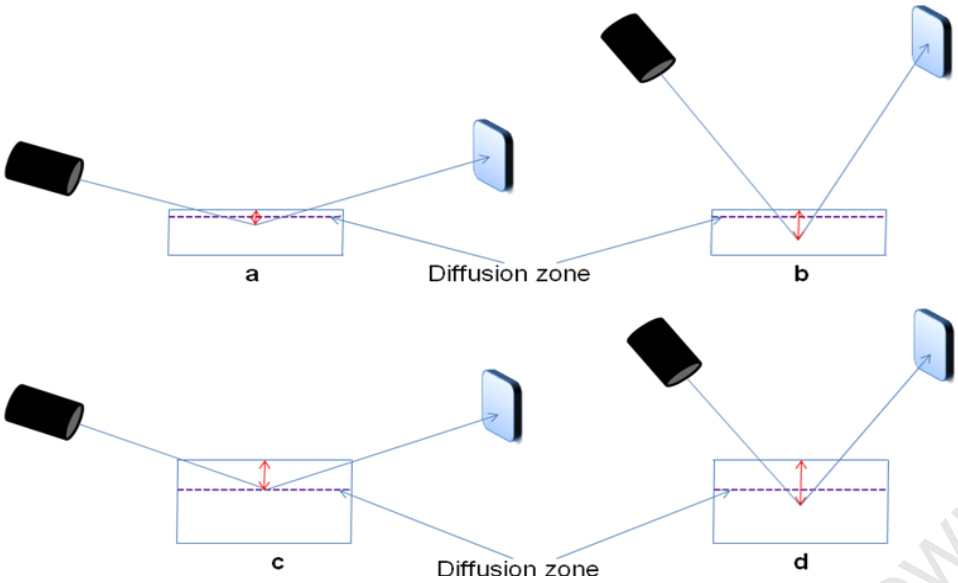

Figure 3.2: A schematic representation of XRD interaction depth (a – b = thin coatings, c – d = thick coatings, a – c = low angles and b – d = high angles).

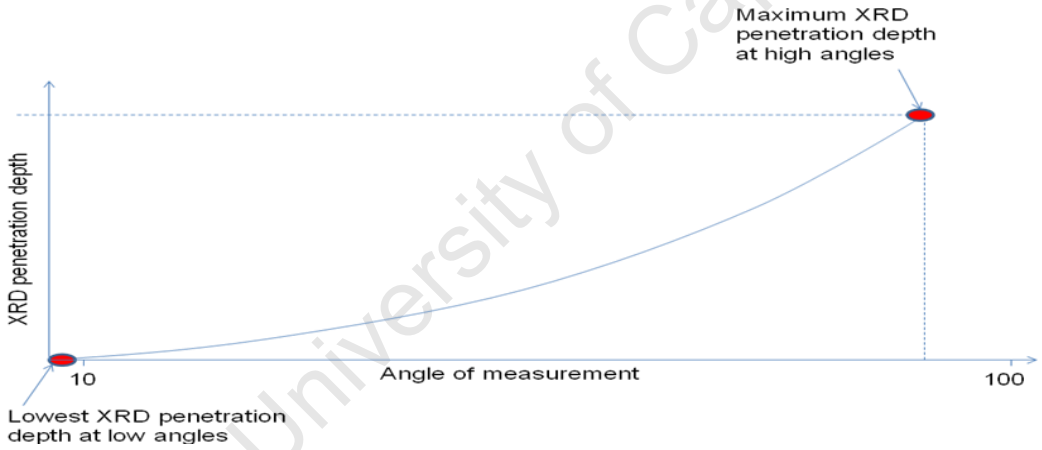

Figure 3.3: A schematic graph showing increase in XRD penetration depth with increase in angle of measurement.

The XRD interaction depth is small at low measuring angles (figure 3.2 a and c) and large at high measuring angles (figure 3.2 b and d). Finally, interaction depth is also determined by absorption of ordered phases which in turn depends on density of each individual phase.

4. RESULTS

The results obtained in this research are presented in this chapter and for every figure presented, a short description of what the results mean is provided underneath. Detailed discussion of these results is dealt with in chapter Five.

4.1MORPHOLOGY CHARACTERIZATION

Morphological characterization is divided into three sections. In section 4.1.1 the effects of sample pre-treatment prior to deposition of coatings are presented. The SEM images in section 4.1.2 show surface morphology arising from different heat treatment temperatures and coating thicknesses. Finally, composition analysis measured by EDS is presented in section 4.1.3.

4.1.1 Pre-treatment of substrates

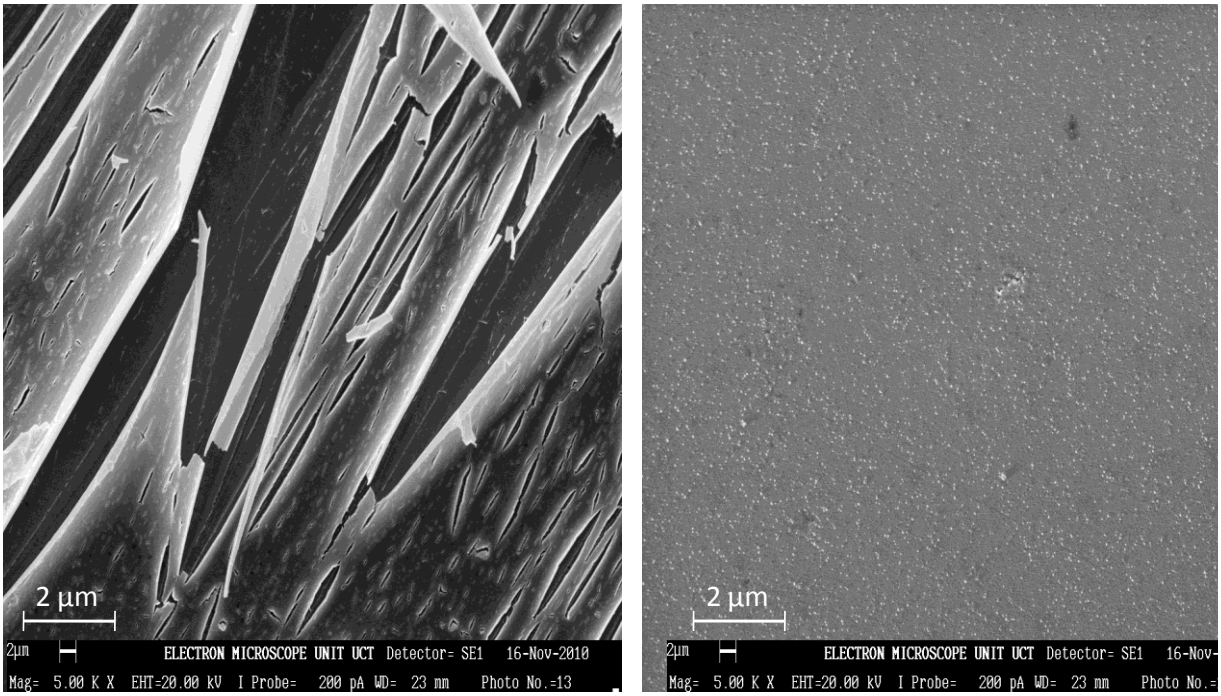

a b

Figure 4.1.1: As-deposited single layer of 0.1 µm Pt coating on V substrate.

Figure 4.1.1 shows SEM images of samples with two different pre-treatments. Image (a) shows an as-deposited sample with no chemical cleaning before deposition. The resulting morphology exhibits ineffective adhesion of coating and substrate, as shown by the delamination and curling up of the coating. The sample in image (b) was chemically cleaned before deposition and shows relatively even adhesion of coating and substrate.

4.1.2 Temperature and thickness effects

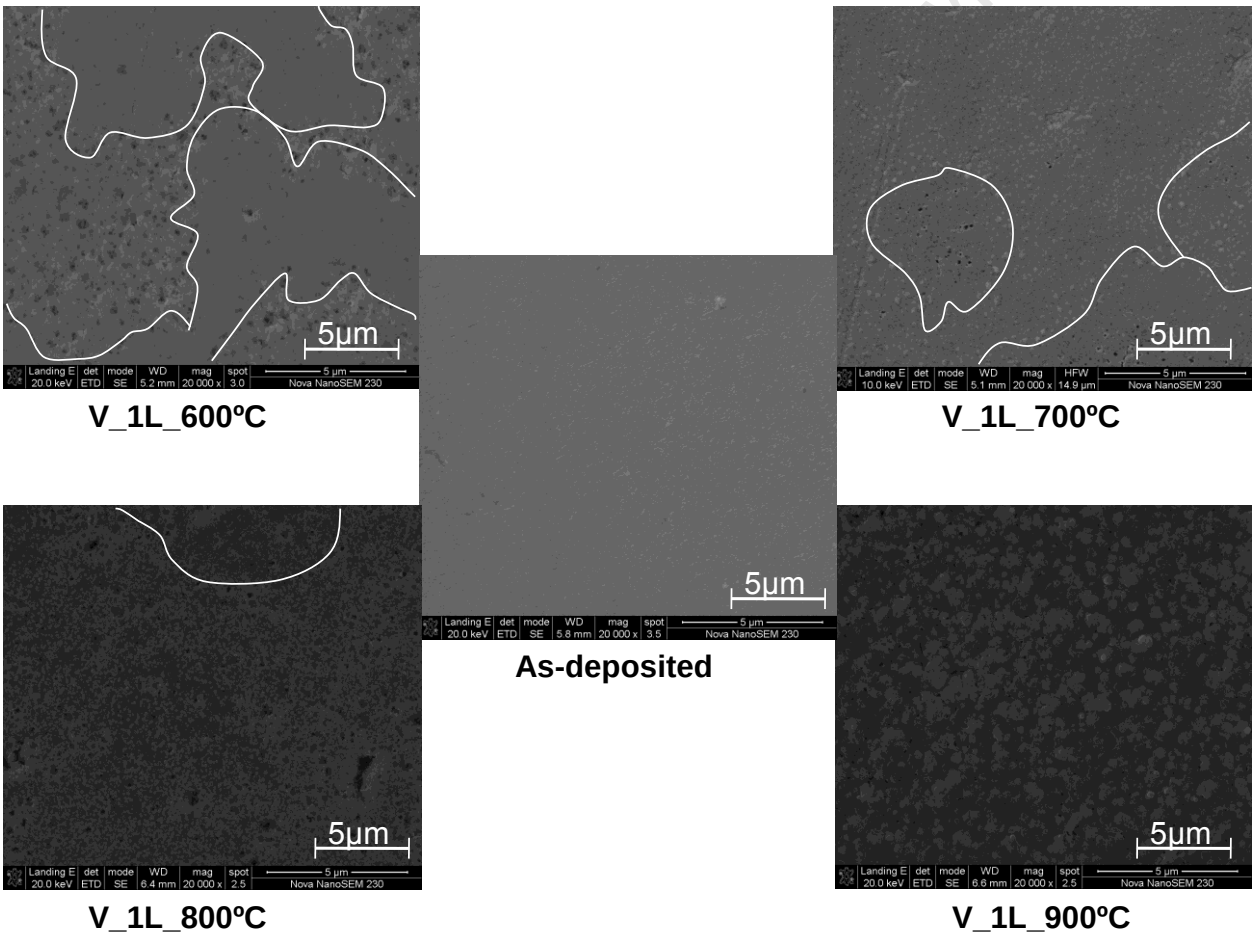

Figure 4.1.2: Single layer of 0.1 µm Pt coating on V substrate.

Figure 4.1.2 shows SEM images of single layer coated samples after heat treatment at 600ºC to 900ºC for 8 hours. The white borders are included to show distinct morphological features. Heat treatment at 600ºC shows a large area displaying relatively smooth morphology within the white borders and few rough areas. The smooth morphology is reduced in size at 700ºC and is further reduced at 800ºC and is being replaced by the rough morphology. Morphology at 900ºC is uniformly rough with small granules. Compared to the as-deposited morphology, roughness increases with an increase in heat treatment temperature.

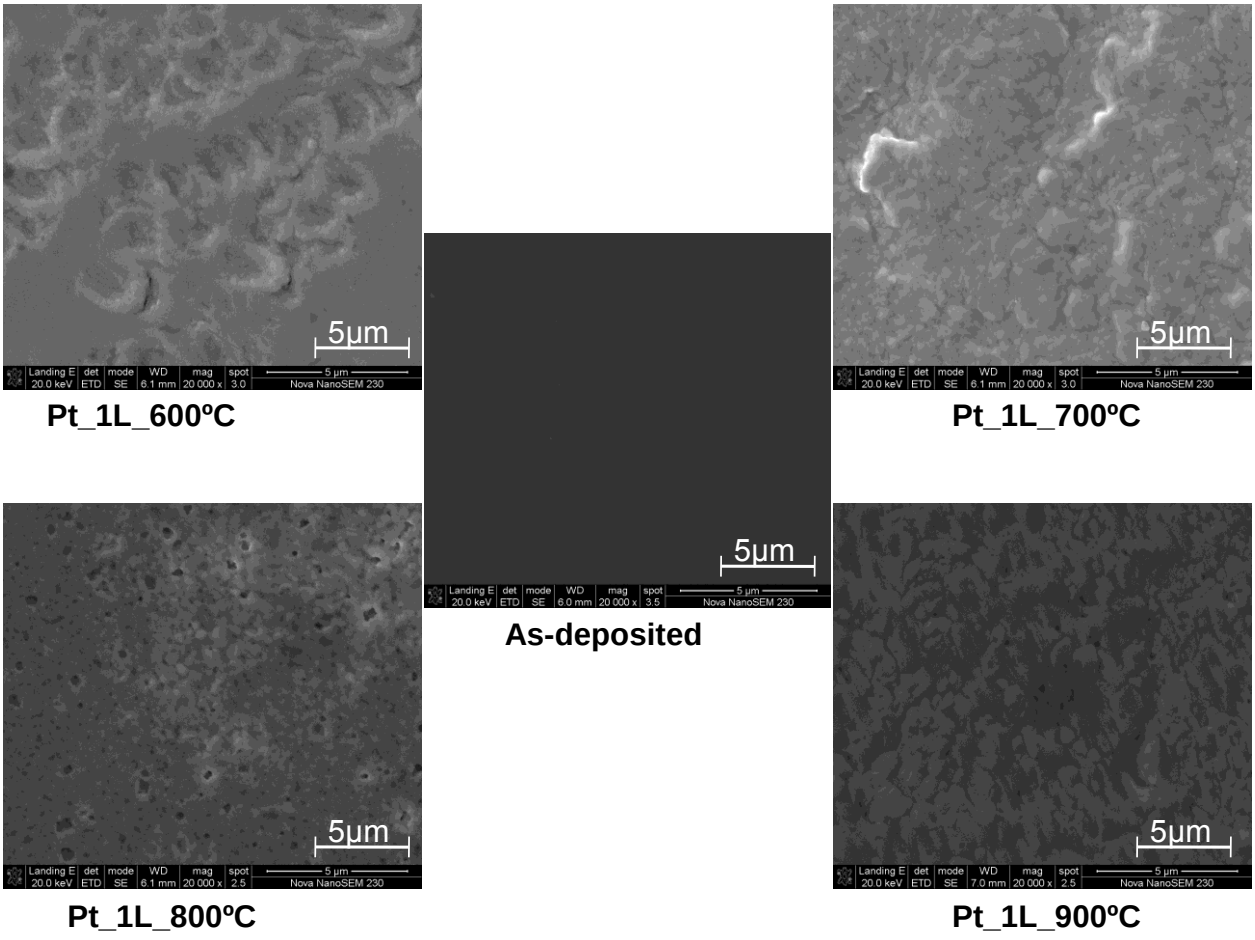

Figure 4.1.3: Single layer of 0.3 µm V coating on Pt substrate.

Using Pt as a substrate, a single layer of 0.3 µm V coating shows no distinct morphological boundaries after heat treatment at 600ºC to 900ºC for 8 hours, as shown in figure 4.1.3. Instead, a globular morphology was observed after the heat treatments. At 600ºC, bigger and fewer

globules were seen; an increase in temperature resulted in smaller globules observed after heat treatment at 700ºC, 800ºC and 900ºC. Comparing micrographs for all heat treatments with the as-deposited coating, roughness generally increases with an increase in heat treatment temperature.

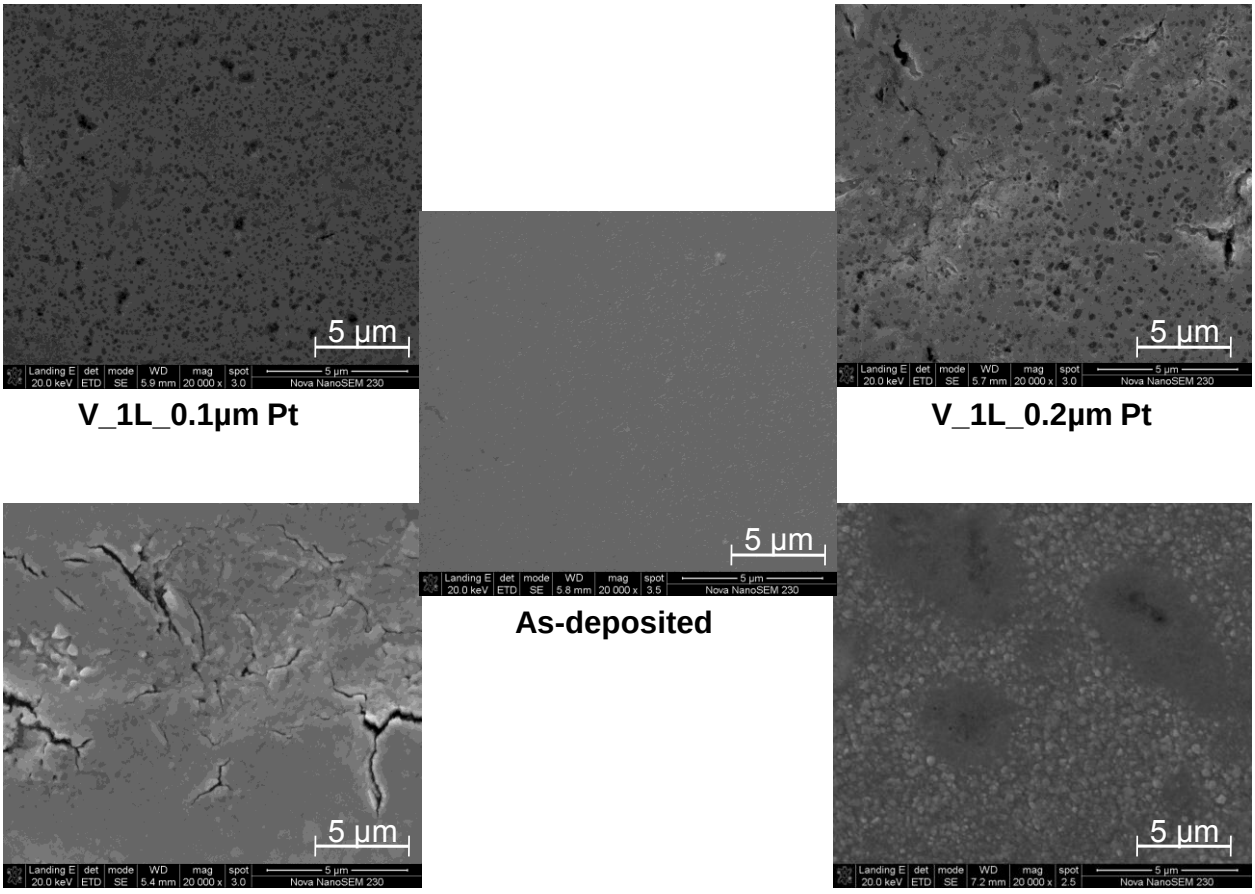

Figure 4.1.4: Different thickness, single layers of Pt coating and a multilayer (5L) on V substrate; all heat treated at 800ºC/8hrs.

The SEM images in figure 4.1.4 show the effect of increasing Pt coating thickness on morphology after heat treatment at 800ºC for 8 hours. A coating of 0.1 µm Pt shows no crack formation after heat treatment, whereas a few cracks were seen in the 0.2 µm Pt coating after heat treatment. At 0.3 µm Pt coating, multiple cracks were observed compared to 0.2 µm Pt. The 5L multilayer (at the coating sequence of 0.1 µm Pt, 0.05 µm V, 0.1 µm Pt, 0.05 µm V and 0.1

μm Pt) was included to differentiate between single and multilayers; and displays no crack formation but shows a light/rough continuous morphology separated by dark/smooth islands.

4.1.3 Composition analysis

Section 4.1.3 shows results from EDS analysis of coated samples. The EDS technique is performed on the surface of the coating, so as-deposited coatings, such as the Pt coating in figure 4.1.5, show only the Pt coating in compositional analysis. The results presented in section 4.1.2 showed that morphology changed considerably after heat treatments. For EDS the composition from the lowest heat treatment temperature is compared here to that of the highest temperature, for both V and Pt substrates. Then the composition of morphological features such as crack development is presented and finally, the composition of dark and smooth areas is compared to that of light and rough granules formed after heat treatments.

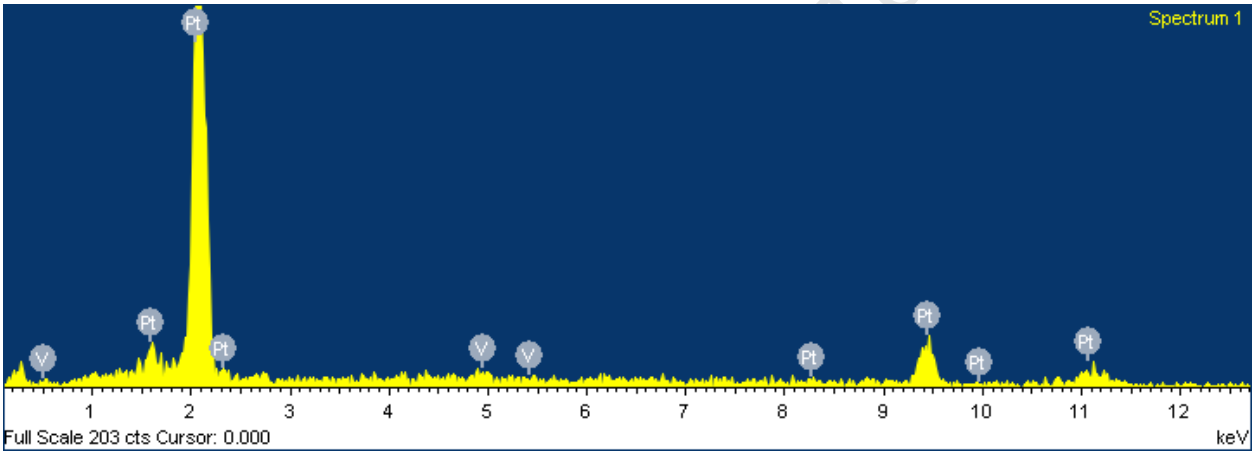

Element	Weight%	Atomic%
V	0.00	0.00
Pt	100.00	100.00
Totals	100.00	

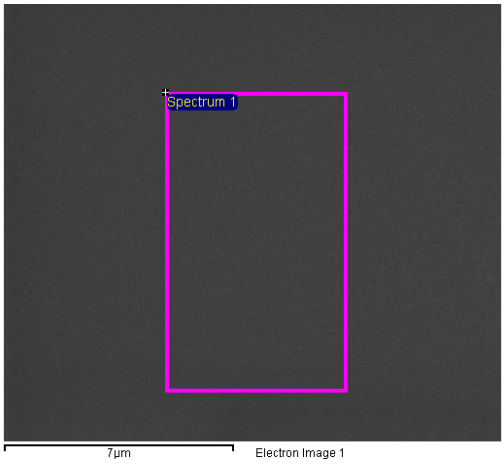

As-deposited

Figure 4.1.5: As-deposited single layer of 0.3 µm Pt on V substrate.

V coatings on Pt substrate were coated with thin layers of Pt to avoid oxidation. The as-deposited (V plus Pt) coated samples accordingly showed 100% Pt.

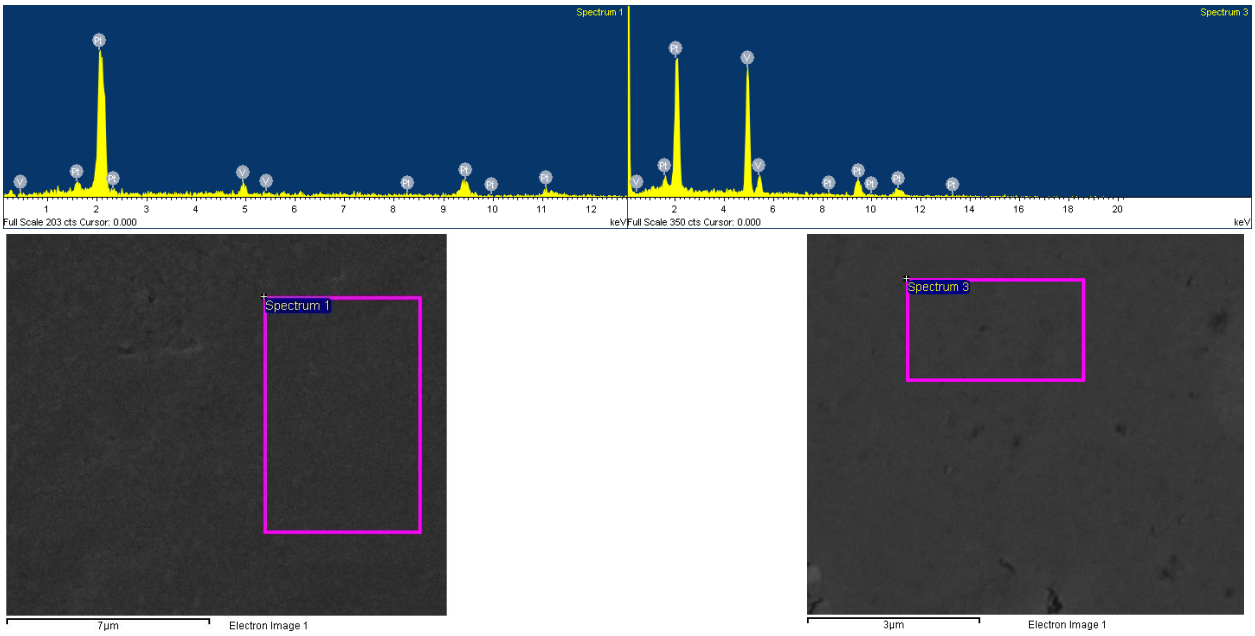

Element	Weight%	Atomic%
V	6.84	21.94
Pt	93.16	78.06
Totals	100.00	

600ºC/8hrs

Element	Weight%	Atomic%
V	46.05	76.58
Pt	53.95	23.42
Totals	100.00	

900ºC/8hrs

Figure 4.1.6: Single layer of 0.3 µm Pt on V substrate, heat treated at different temperatures

Figure 4.1.6 shows a comparison of composition analysis of 0.3 µm Pt on V substrate after heat treatment at 600ºC and 900ºC for 8 hours. The lowest and highest heat treatment temperatures were chosen for comparison to show the effect of temperature on composition of the coatings. Compared to the as-deposited sample in figure 4.1.5, both heat treatments show considerable reduction in Pt concentration. A greater reduction in Pt concentration is seen after the heat treatment at 900ºC compared to the heat treatment at 600ºC.

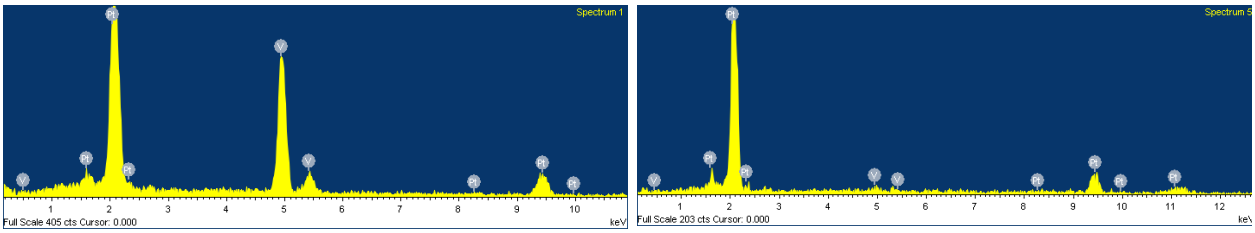

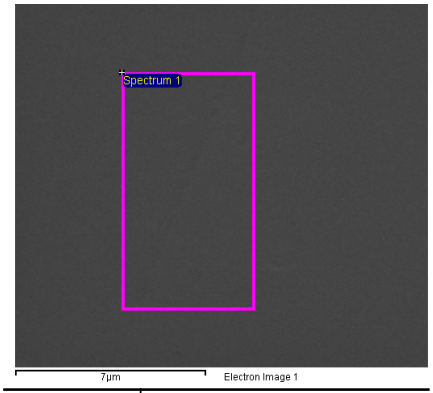

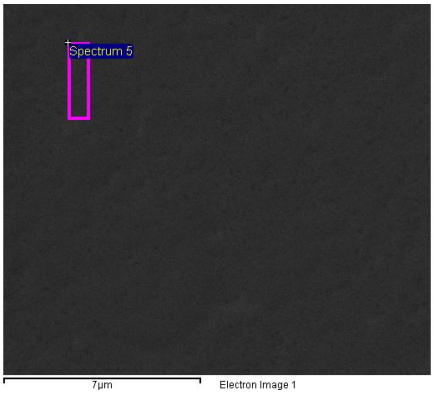

Element	Weight%	Atomic%
V	39.74	71.63
Pt	60.26	28.37
Totals	100.00	

600ºC/8hrs

Element	Weight%	Atomic%
V	0.00	0.00
Pt	100.00	100.00
Totals	100.00	

900ºC/8hrs

Figure 4.1.7: Single layer of 0.3 µm V (coated with a thin layer of 0.07 µm Pt) on Pt substrate, heat treated at different temperatures.

A single layer of 0.3 µm V on Pt substrate heat treated at 600ºC for 8 hours shows a higher concentration of V than Pt. But V is no longer evident after heat treatment at 900ºC: the resulting composition showed 100% Pt concentration as shown in figure 4.1.7.

It is noteworthy that a Pt substrate with a single layer coating of 0.3 µm V resulted in 71.63 at.% V after heat treatment at 600ºC and 0.0 at.% V after 900ºC as shown in figure 4.1.7; whereas a single layer of 0.3 µm Pt on V substrate resulted in 78.06 at.% Pt after heat treatment at 600ºC and 23.42 at.% Pt after 900ºC as shown in figure 4.1.6. This gives an indication that vanadium diffuses faster than platinum. This is further considered in Chapter 5.

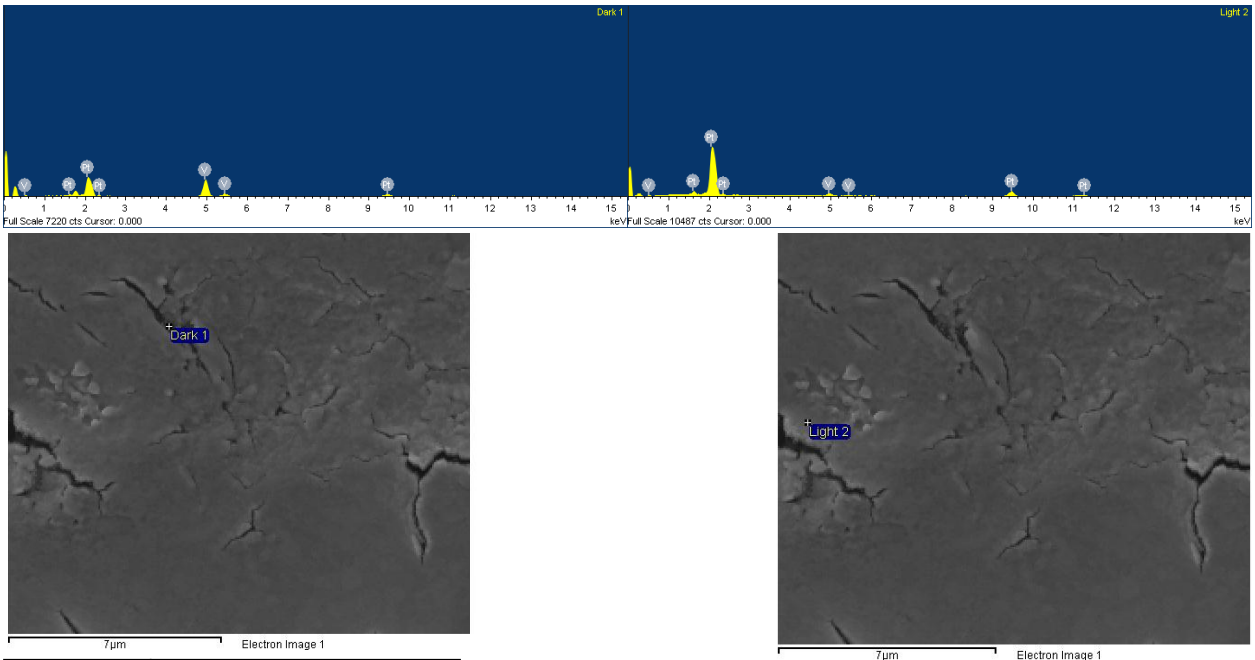

Element	Weight%	Atomic%
V	44.32	75.30
Pt	55.68	24.70
Totals	100.00	

Element	Weight%	Atomic%
V	4.72	15.95
Pt	95.28	84.05
Totals	100.00	

Figure 4.1.8: Single layer of 0.3 µm Pt on V substrate heat treated at 800ºC for 8 hours.

Figure 4.1.8 is included in this section to show composition analysis of morphology which displayed cracked features. With V used as a substrate, the dark area within a crack in a 0.3 µm Pt coating showed a higher concentration of V than Pt. The area adjacent to the crack showed a higher concentration of Pt than V. Coatings on Pt substrate showed no cracks after all heat treatments.

Figure 4.1.9 and figure 4.1.10 show results from EDS measurements from multilayers of V and Pt substrates respectively. The heat treatment of 800ºC for 8 hours was chosen because the resulting morphology showed very similar features, whereby a light continuous area is separated by smooth dark islands. In both figures, the composition of light areas is compared to that of dark islands.

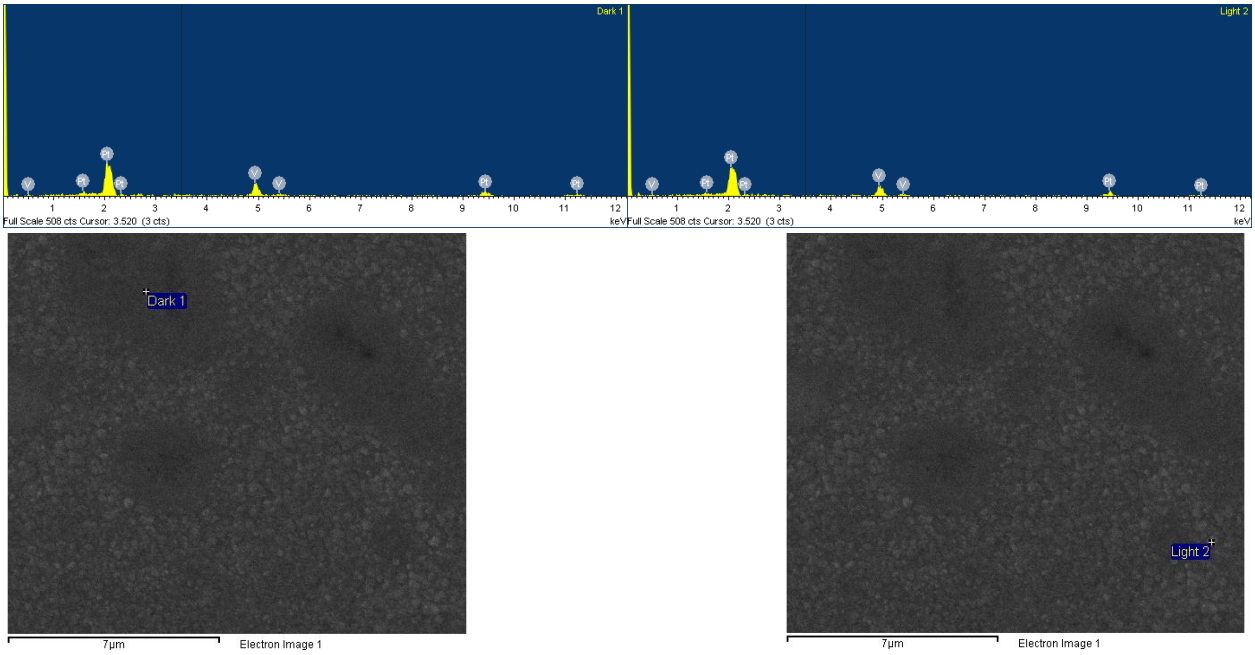

Element	Weight%	Atomic%
V	24.00	54.73
Pt	76.00	45.27
Totals	100.00	

Element	Weight%	Atomic%
V	22.16	52.17
Pt	77.84	47.83
Totals	100.00	

Figure 4.1.9: V substrate with multilayer coatings (5L at alternating 0.1 µm Pt and 0.05 µm V) heat treated at 800ºC/8hrs, comparing dark islands (left) to light areas (right)..

The continuous light area in figure 4.1.9 showed a composition ratio of about 52 at.% V to 47 at.% Pt after the 5L multilayer on V substrate was heat treated at 800ºC for 8 hours. Analysis of the dark islands showed a composition ratio of about 55 at.% V to 45 at.% Pt. Figure 4.1.9

therefore shows approximately 50/50 concentration of both Pt and V after the heat treatment of 5L multilayer on V substrate.

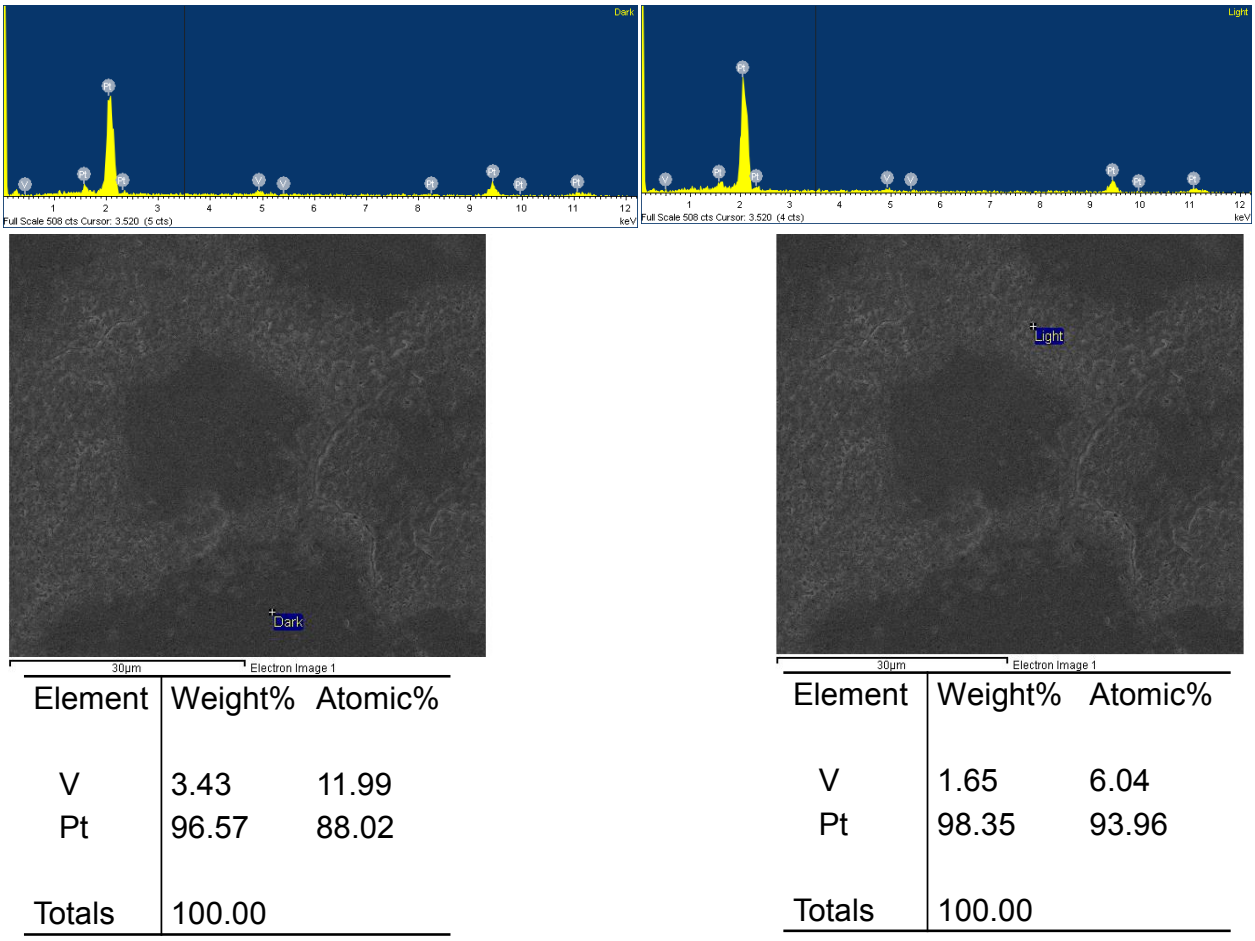

Element	Weight%	Atomic%
V	3.43	11.99
Pt	96.57	88.02
Totals	100.00	

Element	Weight%	Atomic%
V	1.65	6.04
Pt	98.35	93.96
Totals	100.00	

Figure 4.1.10: Pt substrate with multilayer coatings (4L at alternating 0.3 µm V and 0.07 µm Pt) heat treated at 800ºC/8hrs.

In figure 4.1.10, the continuous light area on the surface of multilayer coatings on a Pt substrate showed a composition ratio of about 6 at.% V to 94 at.% Pt after heat treatment at 800ºC for 8 hours. The separating dark islands showed a composition ratio of about 12 at.% V to 88 at.% Pt.

Figure 4.1.10 therefore shows that the concentration of Pt and V in both dark and light areas is roughly the same after the heat treatment at 800ºC for 8 hours.

4.2XRD PHASE ANALYSIS

In this section, sets of XRD spectra are presented on the same axes to facilitate comparison between, for instance, different heat treatment temperatures and different coating thicknesses at temperature. Each spectrum is thus shifted on the intensity axis; the relative intensity of the spectra, however, is unchanged. Some peaks are very small but labeled because they were identified as positive indication of phase formation after removal of background and K_β peaks. A general term, "volume fraction", is used to estimate the relative proportions of peaks of ordered phases. For all sets of XRD spectra, overlapping peaks are labeled on the topmost spectrum.

4.2.1 Vanadium substrate with single Pt layer

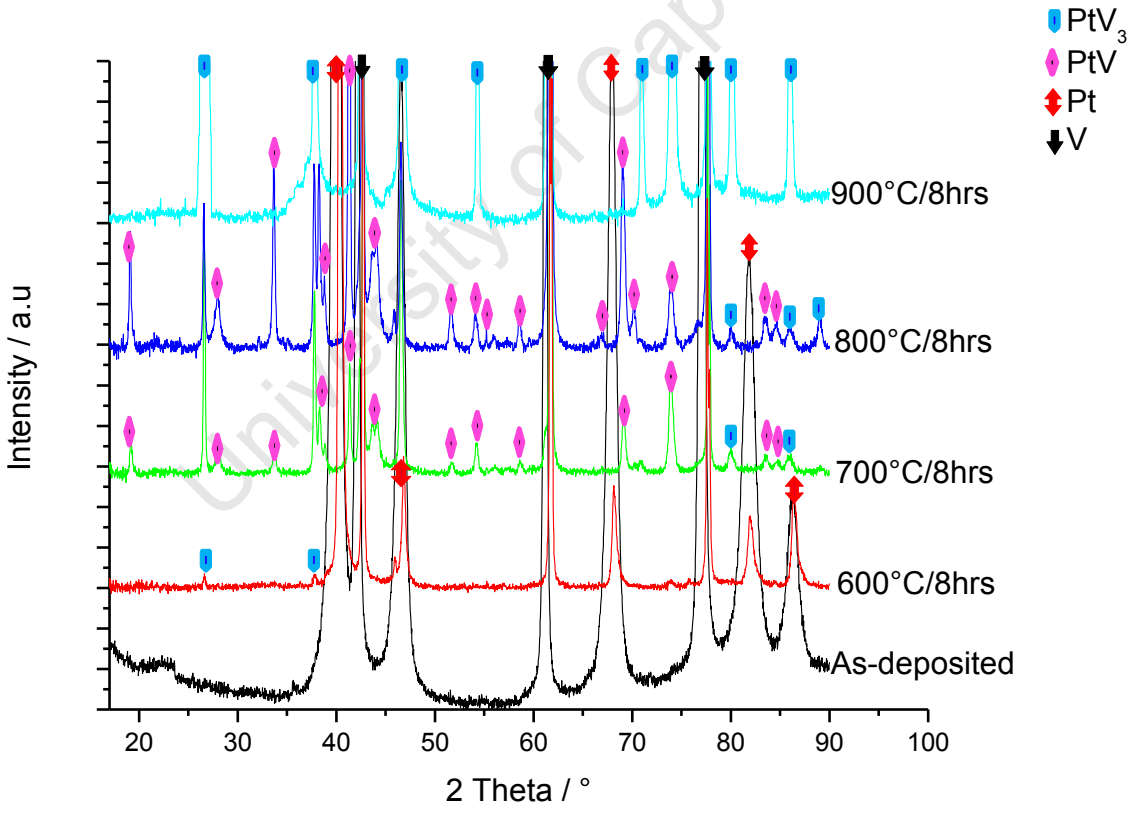

Figure 4.2.1: Single layer of 0.1 µm Pt coating on V substrate.

The graph in figure 4.2.1 shows the XRD spectra from V substrate with a 0.1 µm Pt coating, after heat treatment at 600°C to 900°C for 8 hours. Heat treatment at 600°C results in little change except for the appearance of two minor peaks of the PtV_3 phase. Heat treatment at 700°C and 800°C results in growth of the PtV_3 phase peaks and the appearance of new PtV_3 peaks; and the appearance of multiple PtV phase peaks. At 900°C, the PtV_3 peaks continued to grow but the PtV peaks are absent.

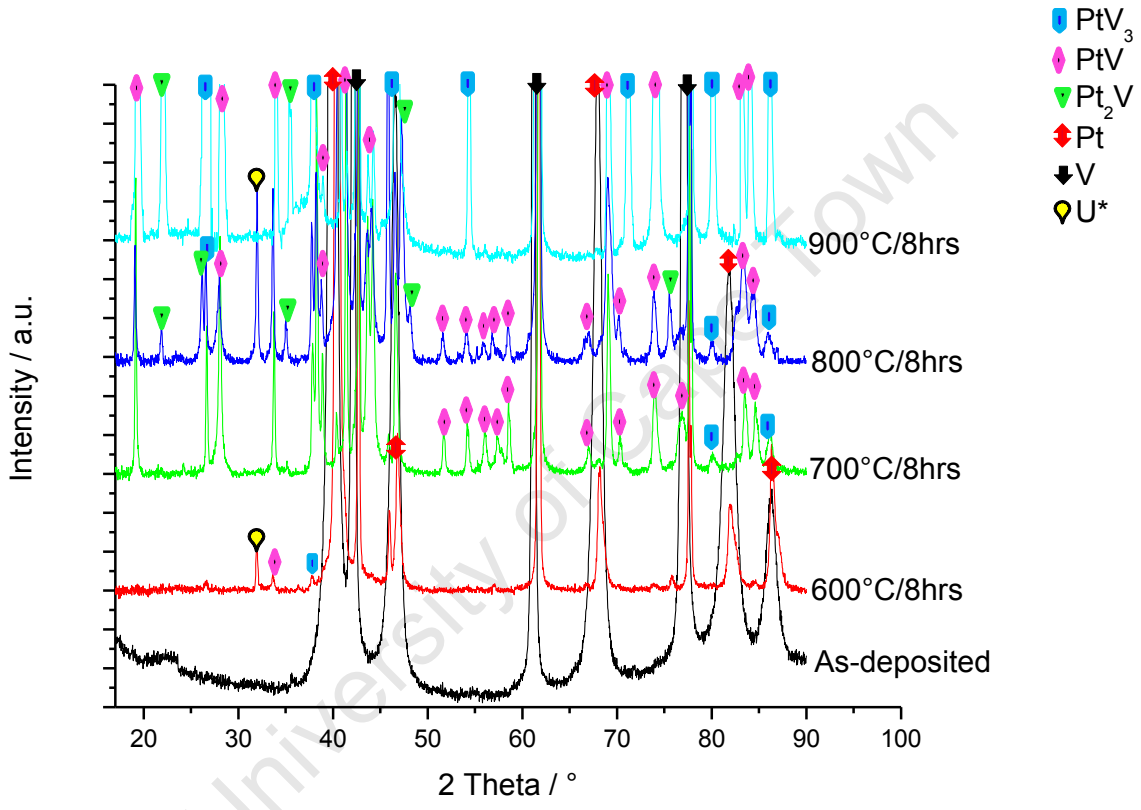

Figure 4.2.2: Single layer of 0.2 µm Pt coating on V substrate (U* = Unknown peak).

Figure 4.2.2 shows the spectra from V substrates with a coating of 0.2 µm Pt. At this coating thickness, heat treatment at 600°C results in minor peaks indicating a small change after heat treatment. In addition to the minor PtV and PtV_3 peaks, a new unknown peak (U*) started to develop at 600°C. The peak for this unknown phase remained very small at 700°C but increased significantly at 800°C. Unlike the results shown for a thinner coating in figure 4.2.1, the PtV phase started forming at 600°C, growing after the heat treatment at 700°C. The intensity of most

PtV peaks decreased at 800 °C and some of these peaks disappeared after the heat treatment at 900 °C (e.g. between angle 50° and 60°. The PtV_3 ordered phase was stable from 600°C to 900°C. For the thicker 0.2 µm Pt coating, the Pt_2V ordered phase was formed after heat treatment at 800°C and 900°C.

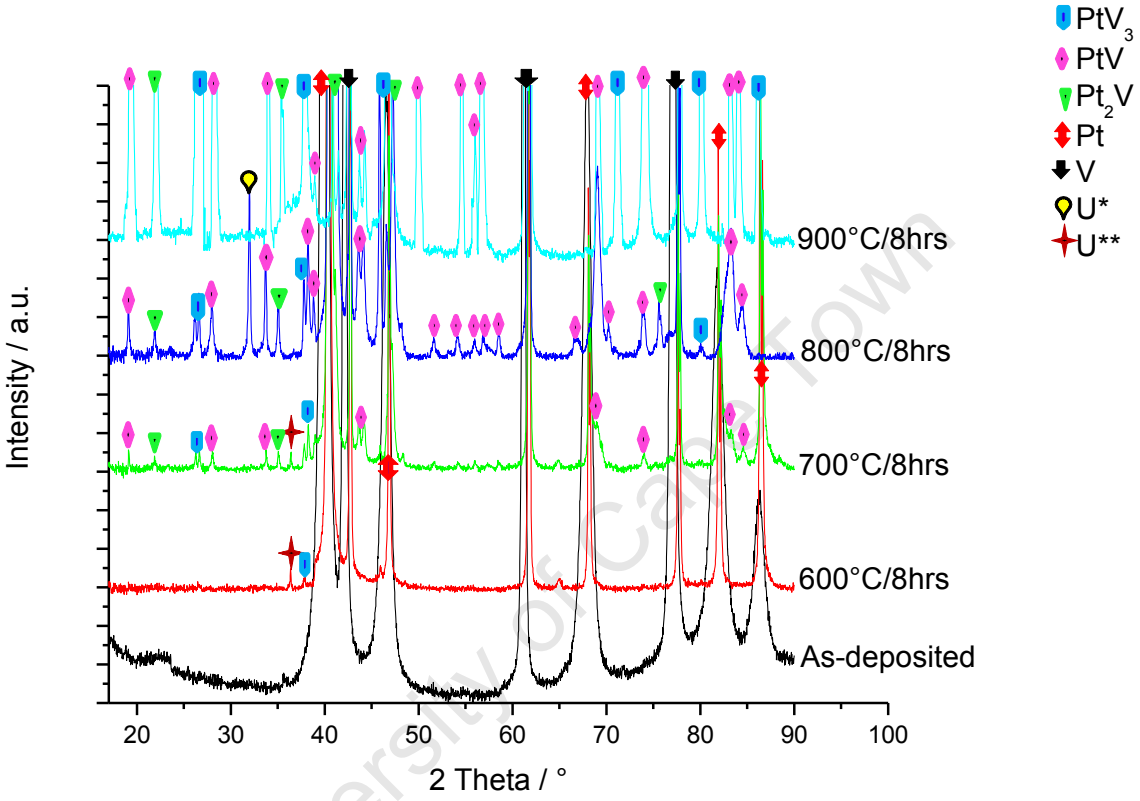

Figure 4.2.3: Single layer of 0.3 µm Pt coating on V substrate.

The major difference between 0.2 µm Pt and 0.3 µm Pt coatings is that heat treatment at 600°C, 700°C and 800°C resulted in smaller changes in peak intensities at 0.3 µm Pt. Figure 4.2.3 shows three Pt_2V peaks at 700°C, unlike figure 4.2.2 in which the Pt_2V peaks only became visible from 800°C. Most of the PtV peak intensities decreased with increase in heat treatment temperature at 0.2 µm Pt whereas the PtV_3 peak intensities increased; but at 0.3 µm Pt, both PtV and PtV_3 peak intensities started developing at 600°C and increased with increase in temperature.

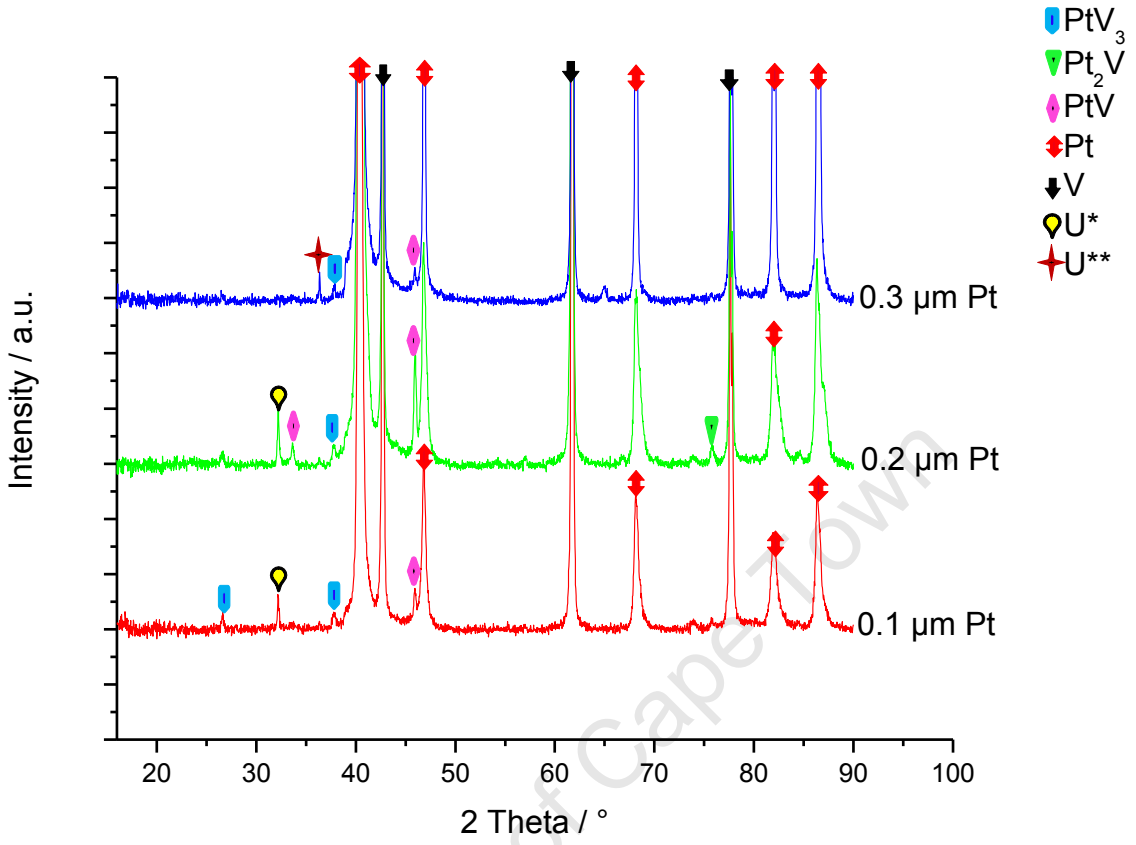

Figure 4.2.4: Single Pt layers heat treated at 600°C for 8 hours.

Figure 4.2.4 shows a comparison of different coating thicknesses after heat treatment at 600°C for 8 hours. Heat treatment at 600°C resulted in very minor changes in phase structure – some possibly nucleation of new phases - at all three coating thicknesses as shown.

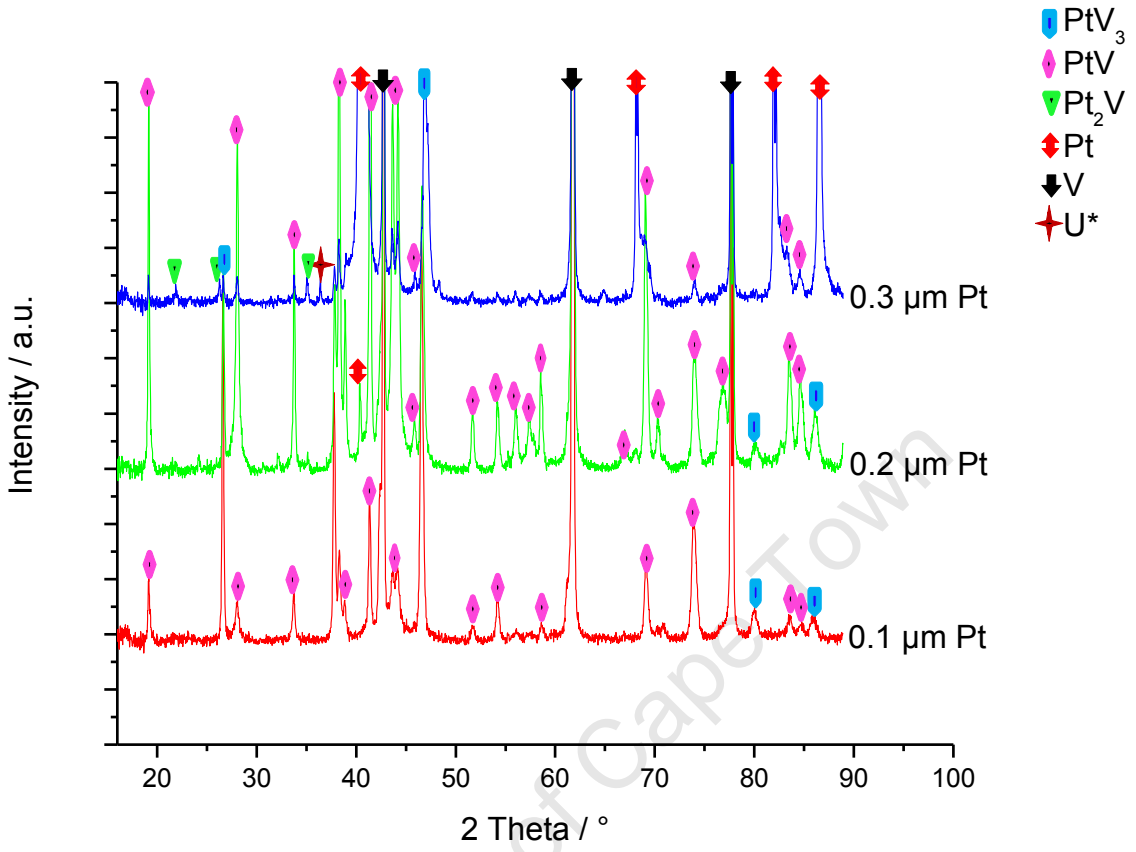

Figure 4.2.5: Single Pt layers heat treated at 700°C for 8 hours.

Heat treatment at 700°C, as shown in figure 4.2.5, results in an increase in peak intensities of both PtV_3 and PtV phases as coating thickness increases from 0.1 µm Pt to 0.2 µm Pt. The graph for 0.2 µm Pt also shows the appearance of additional PtV peaks as a result of increased coating thickness. The same heat treatment on 0.3 µm Pt coating thickness, however, shows almost invisible peaks of the ordered phases compared to the 0.2 and 0.1 µm Pt coatings.

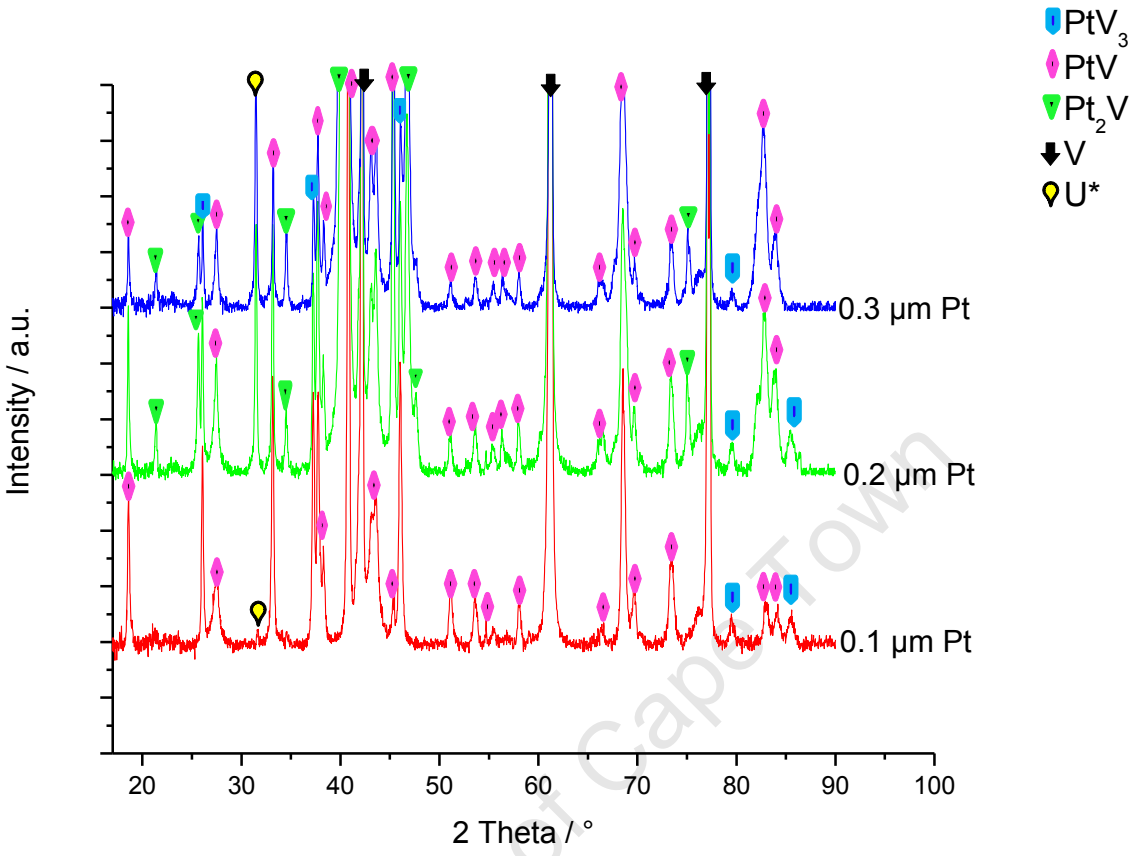

Figure 4.2.6: Single Pt layers heat treated at 800°C for 8 hours.

Figure 4.2.6 shows that for heat treatment at 800°C for 8 hrs, a number of phases formed. The peak intensity of phases formed at 0.1 µm Pt coating, slightly increased at 0.2 µm Pt coating for the same heat treatment. New peaks, especially those indicating the formation of Pt_2V phase, were observed at 0.2 µm Pt coating and not at 0.1 µm Pt coating. At the heat treatment shown in figure 4.2.6, the peak intensity of ordered phases formed at 0.2 µm Pt was almost the same at 0.3 µm Pt.

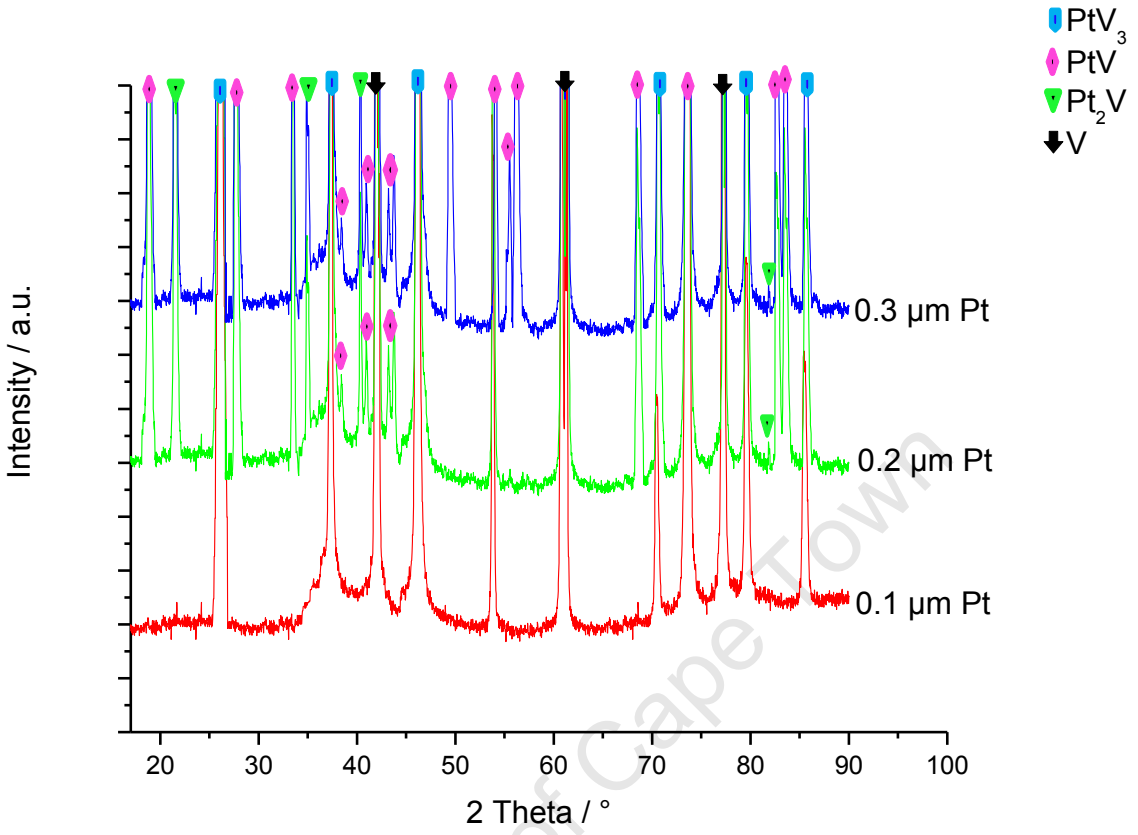

Figure 4.2.7: Single Pt layers heat treated at 900°C for 8 hours.

Heat treatment at 900°C for 8hrs results in additional peaks for each increase in coating thickness from 0.1 µm Pt to 0.2 µm Pt and to 0.3 µm Pt. The 0.2 µm Pt coating shows the peaks of both PtV and Pt_2V phases (in addition to PtV_3 peaks), which were not seen at 0.1 µm Pt. The graph for 0.3 µm Pt also shows the appearance of additional PtV peaks which were not seen in the graph for 0.2 µm Pt. In addition to the development of new peaks with each increment in coating thickness, the intensity also increased with increased coating thickness.

4.2.2 Platinum substrate with single V layer

Section 4.2.1 showed that heat treatments at 600°C and 700°C mostly resulted in formation of small peaks of ordered phases. Significant peak formation was seen after heat treatment at 800°C and 900°C. For comparison purposes, Pt substrates with a V coating were heat treated at 800°C and 900°C as shown below. The Pt substrates, coated with a single layer of 0.3 µm V, were coated with a thin layer of 0.07 µm Pt to prevent oxidation of the V coating. Results for all heat treatments are presented on a single axis in figure 4.2.8.

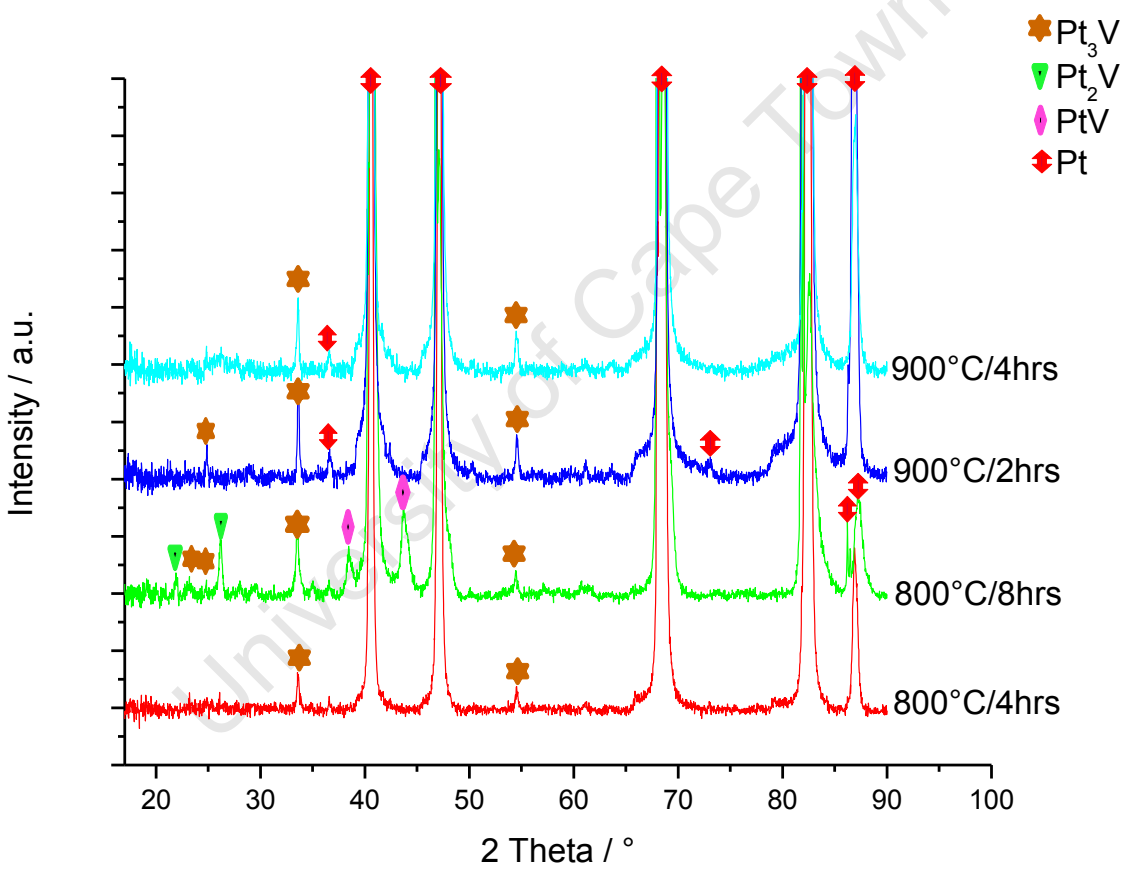

Figure 4.2.8: Single V layers heat treated at 800°C and 900°C for 2, 4 and 8 hours.

Changing the substrate to Pt resulted in a change in phase formation as shown in figure 4.2.8. Peaks for the Pt rich phase (Pt_3V) are observed for all heat treatments. Minor peaks for both Pt_2V

and PtV are seen only after heat treatment at 800°C/8hrs. New peaks for the Pt solid solution became apparent (at about 36° and 86°) after heat treatment at 800°C and 900°C.

4.2.3 Multilayer coatings on V substrate

Sections 4.2.3 and 4.2.4 present the XRD spectra of results from multilayered specimens, to show the effect of multilayer coatings on phase formation.

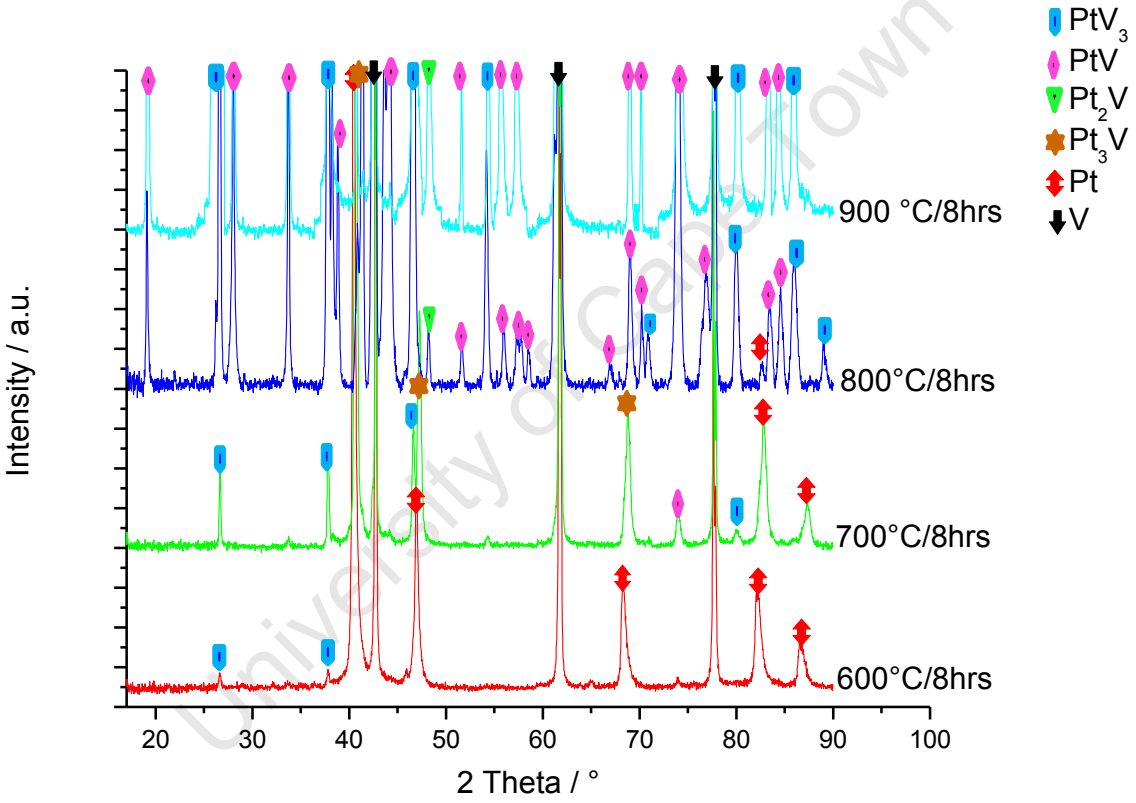

Figure 4.2.9: V substrate with multilayers (3 layers (3L) at the coating sequence of 0.1 µm Pt, 0.05 µm V and 0.1 µm Pt).

The graph in figure 4.2.9 shows the XRD spectra of 3L multilayers on V-substrate heat treated at 600°C to 900°C for 8 hours. The peaks for all four Pt-V ordered phases (PtV_3, PtV, Pt_2V and Pt_3V) were formed. Peaks of ordered phases started nucleating at 600°C and continued to grow

with increase in temperature as shown by the increase in peak intensity of ordered phases. The intensity of Pt peaks decreased with increase in heat treatment temperature. A Pt_2V peak was observed at 48° after heat treatment at 800°C/8hrs and increased at 900°C/8hrs. Both PtV_3 and PtV peaks started forming at 700°C/8hrs and increased in intensity at 800°C/8hrs and 900°C/8hrs along with multiple new peaks for both ordered phases.

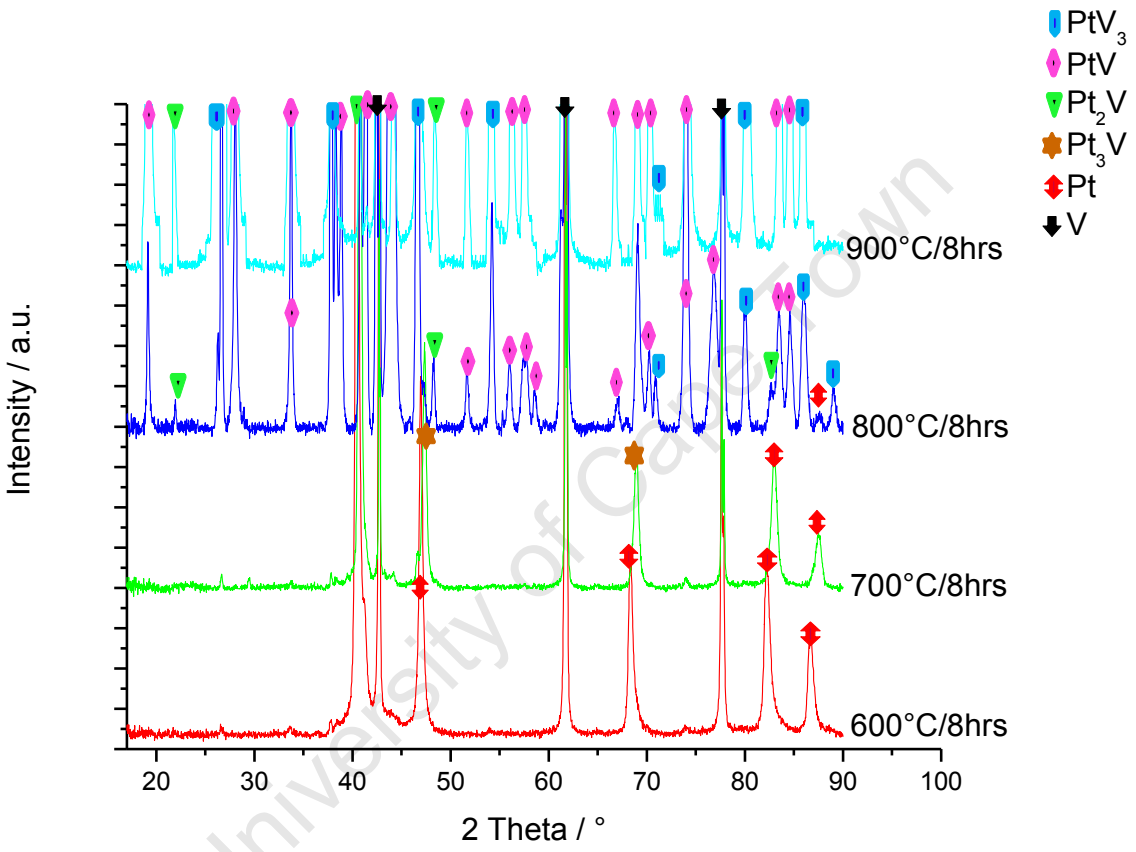

Figure 4.2.10: V substrate with multilayers (5L at the coating sequence of 0.1 µm Pt, 0.05 µm V, 0.1 µm Pt, 0.05 µm V and 0.1 µm Pt)

Figure 4.2.10 shows that increasing the number of layers from 3L to 5L did not result in significantly different results. Comparing 3L to 5L multilayer coatings, it can be seen that Pt_3V peaks were only formed after heat treatment at 700°C for 8 hours and that for both multilayer coatings, the Pt3V peaks were seen at the same 2 theta angles. Pt_2V peaks were still nucleated after heat treatment at 800°C but compared to the 3L multilayer; a total number of Pt_2V peaks

was higher at 5L multilayer coatings. PtV_3 and PtV peaks only started forming at 800ºC and the peak intensities for these phases increased at 900ºC.

In both 3L and 5L multilayers, Pt_3V peaks were also formed, making an overall of four Pt-V ordered phases formed in multilayer coatings as opposed to an overall total of three in single layer coatings.

4.2.4 Multilayers on platinum substrate

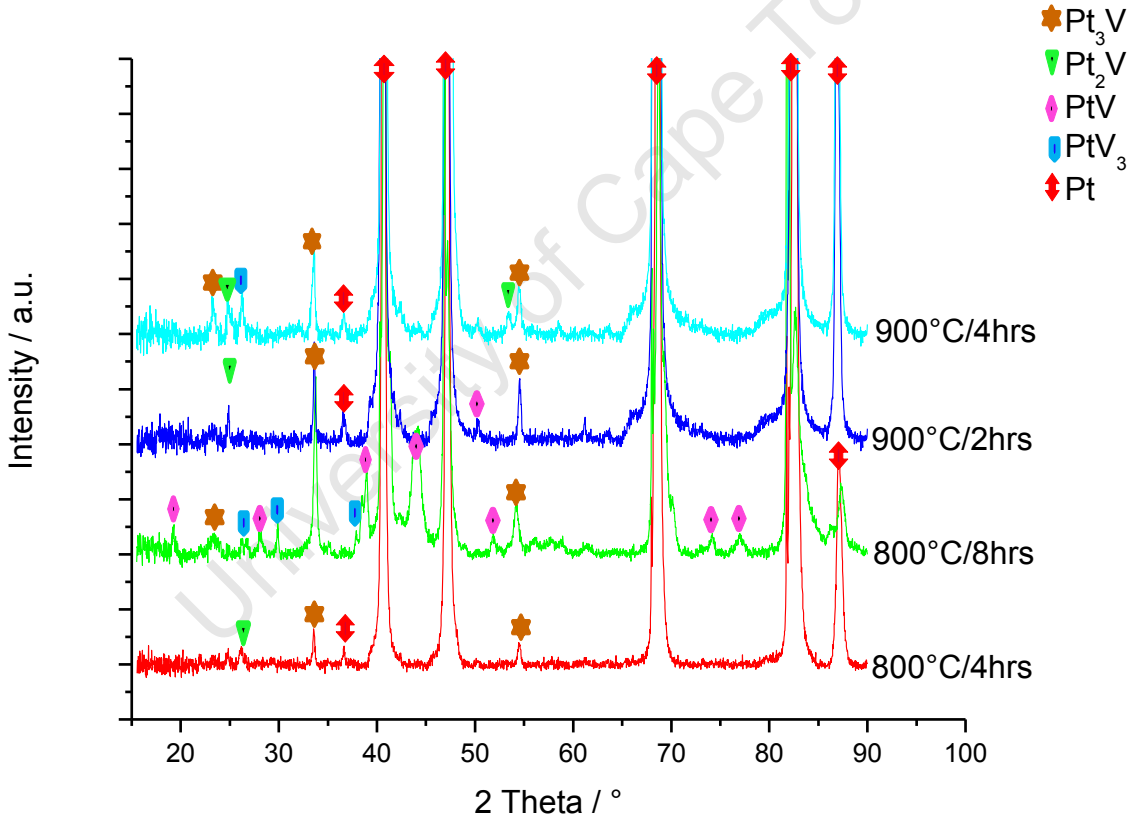

Figure 4.2.11: Pt substrate with multilayer coatings (4L made up with alternating 0.3 µm V and 0.07 µm Pt).

Heat treatments of Pt substrate multilayers resulted in the formation of more PtV peaks compared to Pt substrate single layers. It can also be seen in figure 4.2.11 that compared to the single layers, small peaks of PtV_3 were seen after heat treatment at 800ºC/8hrs and 900ºC/4hrs. The similarity between single and multilayers of Pt substrate lies in the observation of Pt_3V peaks at around 34º and 54º. The increase in number of layers also resulted in the formation of additional small Pt_3V and Pt_2V peaks.

The similarity between Pt substrate and V substrate multilayers was that the four Pt-V ordered phases were observed after the heat treatment of multilayers and not of single layers.

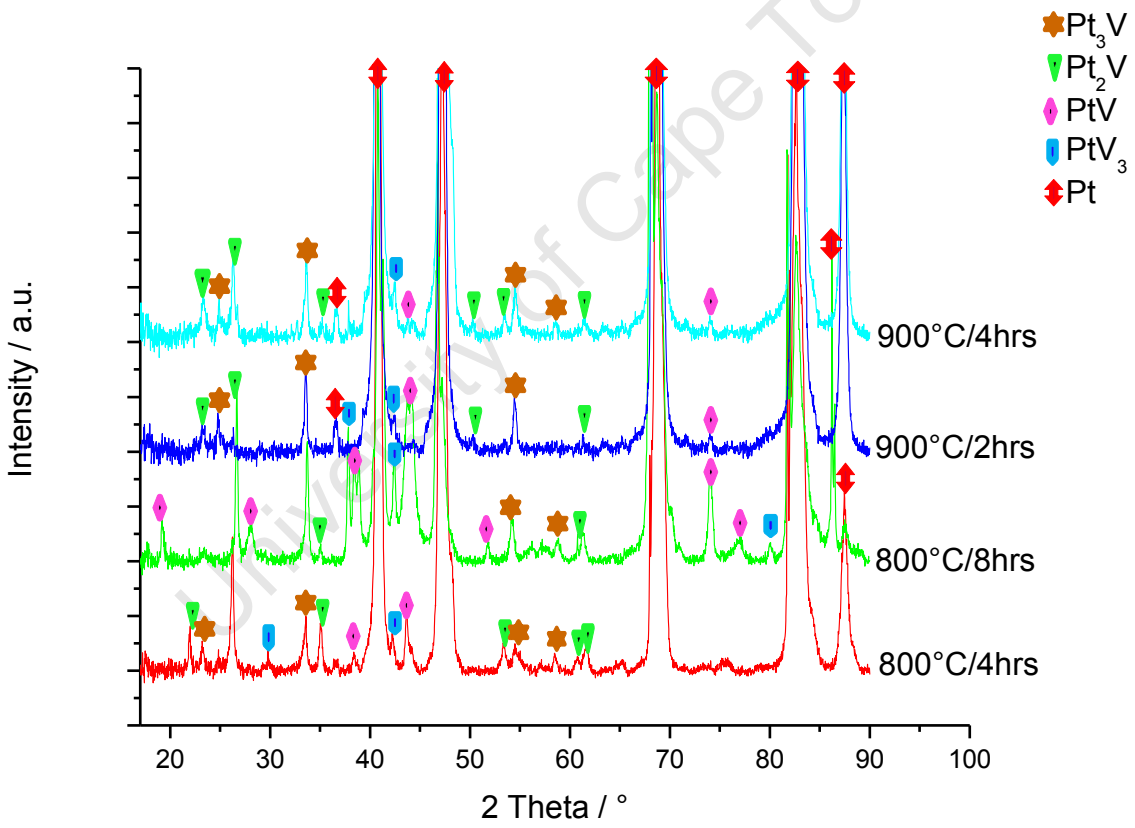

Figure 4.2.12: Pt substrate with multilayer coatings (6L made up with alternating 0.3 µm V and 0.07 µm Pt).

As with all multilayers studied in this project, the 6L Pt substrate multilayers resulted in the formation of peaks for all four Pt-V ordered phases. The intensity of most peaks showing ordered phases in figure 4.2.12 is slightly greater for the set of 6L compared to the 4L shown in figure 4.2.11. Heat treatment of the 6L also resulted in the development of additional new peaks for Pt_3V, Pt_2V, PtV and PtV_3 phases.

5. DISCUSSION

Four sections make up the discussion chapter. Composition and morphology characterization are discussed in section 5.1. XRD phase analysis is discussed in section 5.2. The Pt-V phase diagram is presented again in section 5.3 and the phase formation in this work is discussed in relation to the phase diagram. Finally, discussion on phase formation exhibited in Pt-V system is evaluated in section 5.4.

5.1MORPHOLOGY CHARACTERIZATION

Morphology discussion is subdivided into two sections. The importance of substrate pretreatment is discussed first and followed by discussion on the effect of heat treatment temperature and coating thickness on morphology.

5.1.1 Pre-treatment of substrates

The chemical washing technique is recommended before deposition of coatings to avoid contamination and poor adhesion with substrate. As shown in figure 4.1.1 (a), the coating is easily delaminated if the recommended cleaning technique is not implemented on substrates. In this project, it was found that good adhesion of coating and substrate is achieved if each step of the cleaning technique is carried for 20 minutes, instead of the recommended 5 minutes, in an ultrasonic bath.

Prior to deposition, contamination of substrates was minimized by reducing the exposure of substrates to oxidizing environment during the interval between cleaning and deposition procedure. This was done by immediately loading the substrates into the E-beam straight after the last step of the cleaning sequence. Deposition was also carried out under vacuum to help minimize contamination. Contamination post-deposition was minimized by making Pt the

topmost layer because it Pt oxidizes less readily compared to V. But because this is an evaporated Pt, the coatings can be expected to be as badly contaminated; hence the phase formation sequence as predicted by the EHF model might be compromised.

5.1.2 The effect of temperature and coating thickness

In general, the surface morphology of heat treated coatings is rough compared to that of as-deposited samples, as seen in the SEM images in figure 4.1.2. The mixture of smooth and rough surface regions, seen after heat treatment at lower temperatures, changes to a uniformly roughened surface after higher temperature heat treatments. This increase in surface roughness with increasing heat treatment temperature was seen for all Pt coatings on V substrates; V coatings on Pt substrates also showed increased roughness as temperature increases, but the surface features in this case were more globular (Fig. 4.1.3) as opposed to the granular features seen in Fig. 4.1.2.

Increased coating thickness also results in increased surface roughness, but the most frequently observed morphological feature of increased coating thickness is cracking. Figure 4.1.4 shows that cracks become more prevalent as coating thickness increases. The relative coefficients of linear thermal expansions of Pt and V are 9.0×10^{-6} K^{-1} and 8.0×10^{-6} K^{-1} respectively. The cracking and delamination of coatings such as this can therefore be attributed to mismatch of thermal expansion coefficients between substrate and coating. The mismatch causes residual strains which can result in the coating separating from the substrate after synthesis, or cracking as a result of heat treatment. Depositing coatings in to multilayers instead of thick single layers can help reduce the kind of cracking as shown in figure 4.1.4: the surface of a 5L multilayer (total thickness of Pt is 0.3 μm) shows no formation of cracks, compared to the surface of a 0.3 μm single layer of Pt after the same heat treatment.

5.2XRD PHASE ANALYSIS

Factors such as heat treatment temperature, time at temperature, coating thickness and number of coating layers, were found to affect phase formation in coated substrates. These factors are discussed separately in subsections for each type of substrate. The effect of these factors, measured at 0.02° step size at a 2θ range between 10° and 100°, is evaluated according to the volume fraction of ordered phases formed, which is estimated by height to width ratio of peak intensities of the ordered phases. Overall, acquisition and interpretation of results are not influenced by XRD measurement angles because all specimen, (thin, thick and multilayers), were scanned at low and high angles (between 10º and 100º). The only difference is that at high measuring angles on thin coatings, the XRD interaction depth can be expected to be more than the coated layer, in which case, substrate peaks are expected to be seen on XRD spectra. But for thick coatings at high measuring angles, the substrate peaks will not necessarily be seen on XRD spectra. Therefore, for every set of XRD spectra acquired in this project, each labeled peak is considered to be positive identification of phase formation. Volume fraction is calculated automatically by the XRD machine by taking into consideration height to width ratio of peak intensity which therefore gives a good qualitative determination of ordered phases. This is a better estimation than counting the number of peaks of one ordered phase in relation to other ordered phases which might be inconclusive because of the limiting range (10º to 100º) of measurement.

Single and multilayers of Pt coatings on V substrates are discussed in section 5.2.1. The discussion on single and multilayers of V coatings on Pt substrates follows in section 5.2.2. All heat treatments are considered in each of these sections, but the two temperatures, 800°C and 900°C, for which results are shown in figure 5.2.3 (for V substrates) and figure 5.2.6 (for Pt substrates), were chosen for emphasis because they showed greater XRD peak intensities compared to lower heat treatment temperatures.

5.2.1 Single and multilayer coatings on vanadium substrates

A couple of unidentified peaks (labeled Unknown U* and Unknown U** in chapter 4) were formed but only from single layer coatings of Pt on V substrates. Judging by the random appearance of these peaks, contamination was the most likely reason for development of these peaks. The rest of the XRD peaks were correctly identified for phase formation and are discussed next.

5.2.1.1 The effect of temperature on phase formation

Heat treatment of coated substrates at low temperatures (600°C and 700°C) resulted in no significant binary phase formation. The lowest temperature studied was 600°C and for all heat treatment times, the XRD spectra either showed no new peaks or very few, low intensity peaks in addition to the dominant elemental (substrate and coating) peaks. In figure 4.2.4, XRD spectra for Pt single layer coatings heat treated at 600°C for 8 hours show that only very small new peaks were formed. This XRD result suggests that the mixed phases PtV_3, PtV and PtV_2 have started to nucleate but there is no evidence of significant point of nucleation. According to the Pt-V phase diagram, these ordered phases are all expected to form at temperatures below 1012°C. . Heat treatment of multilayer coatings at 600°C showed similar results. Diffusion rate at 600ºC for 8 hours is therefore not high enough for phase transformation.

Figure 4.2.5 shows that the intensity of PtV_3 and PtV peaks is slightly higher after heat treatment at 700°C than at 600°C. This evidence of growth of stable ordered phases is expected, as the diffusion rate at 700°C is higher than at 600°C due to increased atomic mobility and increased equilibrium vacancy concentration.

The observations above were similar for coating thicknesses of 0.1 µm Pt and 0.2 µm Pt. At 0.3 µm Pt however, the elemental substrate and coating peaks remained dominant after heat treatment at 600°C and 700°C, with only minor peaks from ordered phases.

Heat treatment of single layer coatings at 800°C and 900°C, as shown in figures 4.2.6 and figure 4.2.7 respectively, result in XRD peaks of greater intensity than heat treatments at 600°C and 700°C. Since the ordered phases are stable at all heat treatment temperatures, this can be attributed to the expected increase in diffusion rate with increasing temperature. Even for the 0.3 µm thickness Pt coating, significant peaks of ordered phases were observed after heat treatment at 800°C and 900°C compared to the same coating thickness heat treated at 600°C and 700°C. Higher temperatures provide energy for atoms to diffuse a greater distance, which results in a larger interdiffused zone between coating and substrate as schematically shown in figure 5.2.1. This zone results in formation of a larger volume of ordered phases after heat treatment at 900°C compared to 700°C.

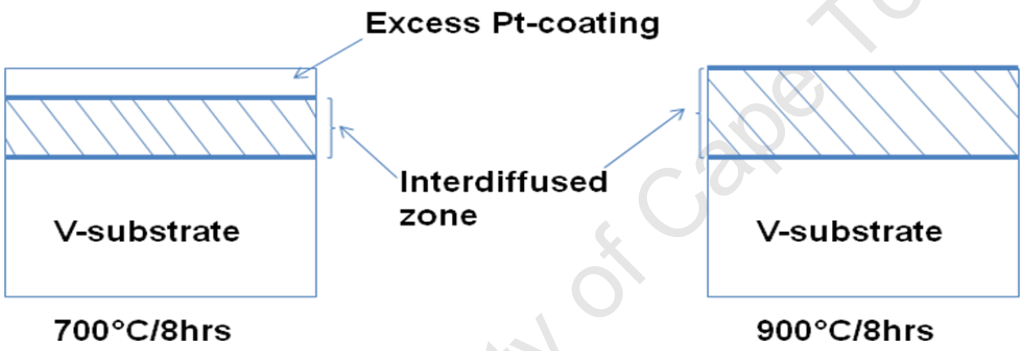

Figure 5.2.1: Idealised schematic diagram showing diffusion zone after heat treatment of 0.3 µm Pt coating at 700°C and 900°C for 8 hours.

Elemental Pt peaks were not seen after heat treatment of 0.1 µm Pt and 0.2 µm Pt at 700°C as shown in figure 4.2.5. But for the same heat treatment temperature, significant peaks of elemental Pt were seen after heat treatment 0.3 µm Pt. This therefore suggests that there was a high volume of unreacted Pt in the 0.3 µm coating as illustrated by the excess Pt coating shown in figure 5.2.1 above. The volume fraction of peaks of ordered phases increased with increase in coating thickness from 0.1 µm Pt to 0.2 µm Pt at 700°C, but decreased at 0.3 µm Pt for the same heat treatment temperature. Investigation of cross-sectioned specimens showed that there was poor adhesion of the 0.3 µm Pt coating with the substrate, as shown by the SEM image in figure 5.2.2 below.

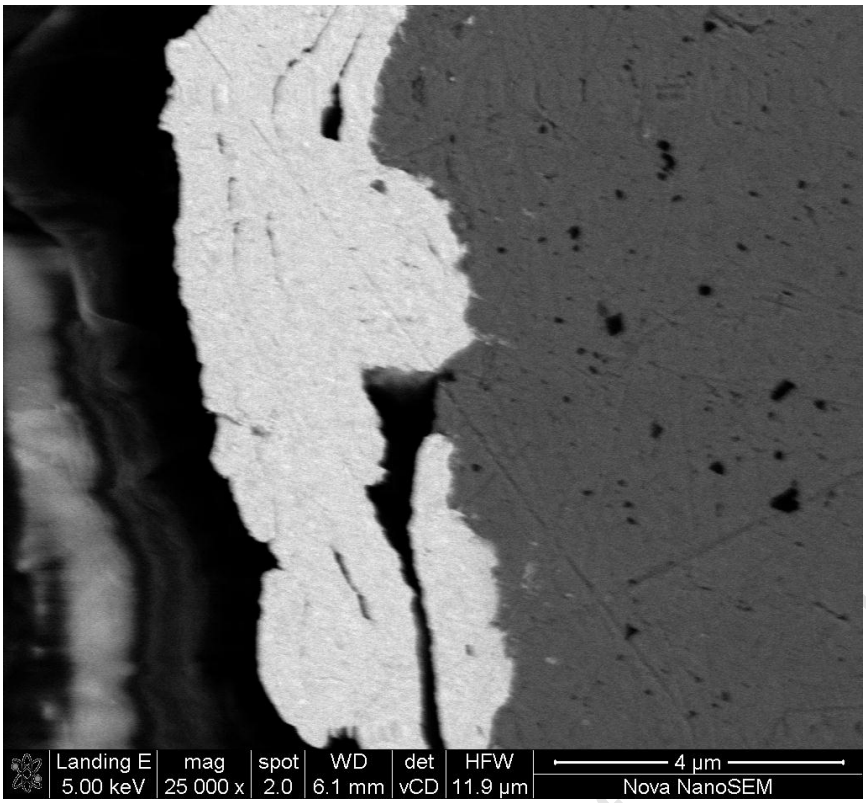

Figure 5.2.2: SEM image showing a cross-section of 0.3 µm Pt on V substrate, heat treated at 700ºC for 8 hours.

It is concluded that the presence of voids (delamination) between the 0.3 µm Pt coating and the substrate, resulted in little or no interdiffusion and hence no significant formation of ordered phases at low temperatures. (With good adhesion, the interdiffused zone at 0.3 µm Pt would be expected to be relatively larger or at least the same as in 0.2 µm Pt). After heat treatment at 900°C in all coating thicknesses however, no elemental Pt peaks remain (figure 4.2.7); the entire Pt coating appears to have interdiffused with the substrate. It can therefore be seen that, for the same coating thickness (0.3 µm Pt) heat treated at two different temperatures (700°C and 900°C), the interdiffused zone is larger at the higher temperature (in spite of the voids) ; a larger volume of ordered phases is therefore formed at 900°C than at 700°C.

Finally, for heat treatments at low temperatures (700°C for instance), the Pt_2V phase was only nucleated in the 0.3 µm Pt coating as shown in figure 4.2.5. At higher temperatures however, it nucleated and grew for the 0.2 µm Pt coating. This is evidence of the temperature effect on phase formation: the concentration of Pt provided by a 0.2 µm Pt coating is sufficient for formation of Pt_2V above 700°C, but this phase was not formed at lower temperatures for the same thickness.

5.2.1.2 The effect of time at temperature on phase formation

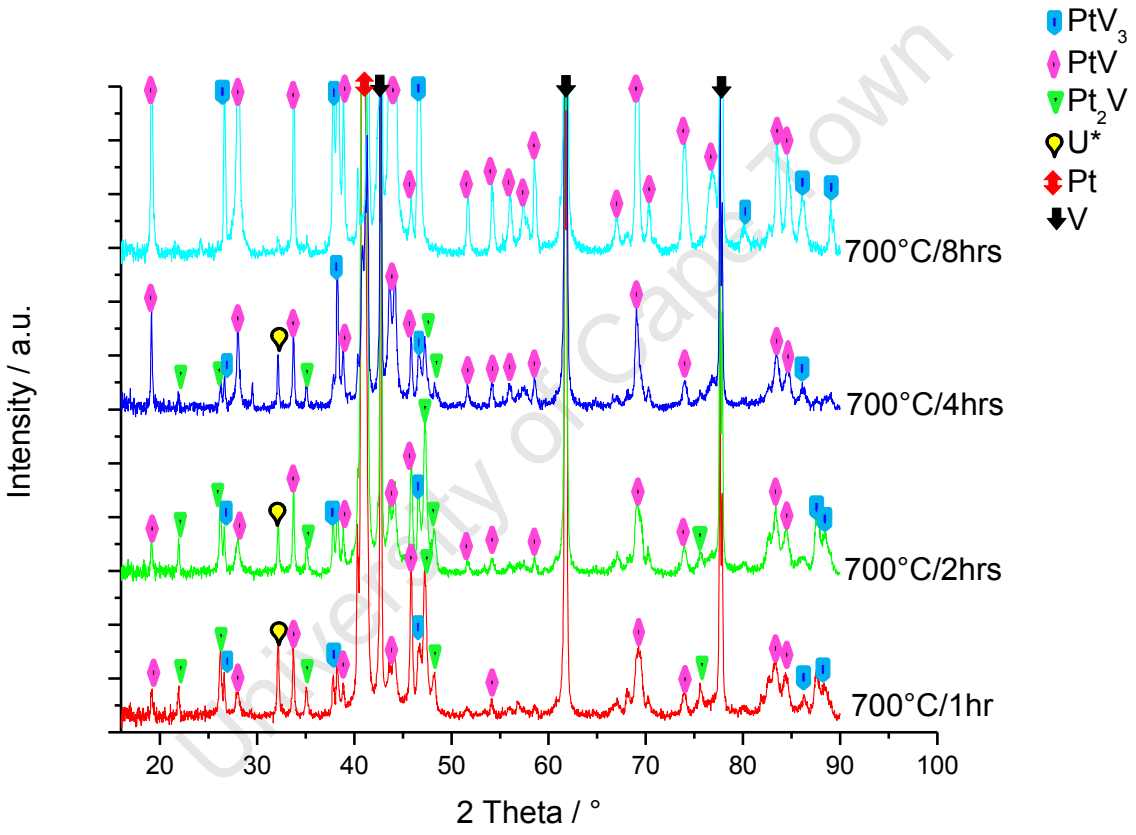

Figure 5.2.3: Single layer of 0.2 µm Pt on V substrate after increasing time at 700°C.

Three noticeable effects of increased heat treatment time at temperature can be seen in figure 5.2.3. First, the volume fraction of peaks of ordered phases increases with increased heat treatment time. Secondly, additional peaks of PtV_3 and PtV appear and grow as time at temperature increases; and finally, although PtV_3 and PtV peak intensities increase with time, those of the Pt_2V phase decrease (and ultimately disappear) with increased time at temperature.

The first observation is expected because increased time at temperature allows enough time for atoms to rearrange and form stable structures, hence the increase in volume fraction of peaks of ordered phases formed. The increase in intensity of PtV_3 and PtV peaks shows that these ordered phases increase in volume with increased heat treatment time at temperature for the same reason. Pt_2V peaks are formed during the early stages of heat treatment; but as heat treatment time increases, the peak intensities of the Pt_2V phase decrease, suggesting that the growth of the PtV_3 and PtV phases occurs at the expense of the Pt_2V phase. This behavior is expected in thin film studies such as carried out in this project, based on the EHF model for sequence of phase formation. Later sections (section 5.3.3 and section 5.3.4 respectively) on first phase and subsequent phase formation discuss this behavior in relation to the EHF model.

5.2.1.3 The effect of coating thickness on phase formation

An increase in thickness of the Pt coating from 0.1 µm to 0.2 µm resulted in peak growth and additional peaks due to nucleation and growth of ordered phases at 700°C, as shown in figure 4.2.5. This suggests that phase formation continues with an increase in thickness of Pt coating. (A further increase in thickness of the Pt coating to 0.3 µm, however, showed no significant phase formation after heat treatment at 700°C for 8 hours, due to inadequate adhesion as seen in figure 5.2.2.)

At higher temperatures (800°C and 900°C) the volume fraction of ordered phases formed, increased with increased thickness of Pt coating as shown in figure 4.2.6 and figure 4.2.7. At each point of increase in Pt coating thickness, additional peaks of ordered phases were observed. PtV and PtV_3 phases were formed at all single layer thicknesses. These results show that phase formation in general is directly proportional to the Pt coating thickness. Formation of more Pt rich ordered phases is also directly proportional to the Pt coating thickness: as shown in figure 4.2.6 and 4.2.7: the Pt_2V phase was only formed at 0.2 µm Pt and 0.3 µm Pt but not at 0.1 µm Pt for the same heat treatment temperature and time. The increase in Pt coating thickness enables increased phase formation because the amount of Pt is enough for formation of new ordered

phases. According to Pretorius *et al.* [3], phase formation increases until the limiting element (Pt in this case) is completely consumed. Therefore with limited Pt such as in the 0.1 µm coating, phase formation is limited; hence the increase in Pt thickness to 0.2 µm and 0.3 µm results in formation of high peak intensity of ordered phases.

5.2.1.4 The effect of number of coating layers on phase formation

Since there was more consistency in phase formation after heat treatments at 800°C and 900°C, the following comparison between single and multilayer coatings is based on results obtained from these two temperatures as shown in figure 5.2.3 and figures in chapter 4.

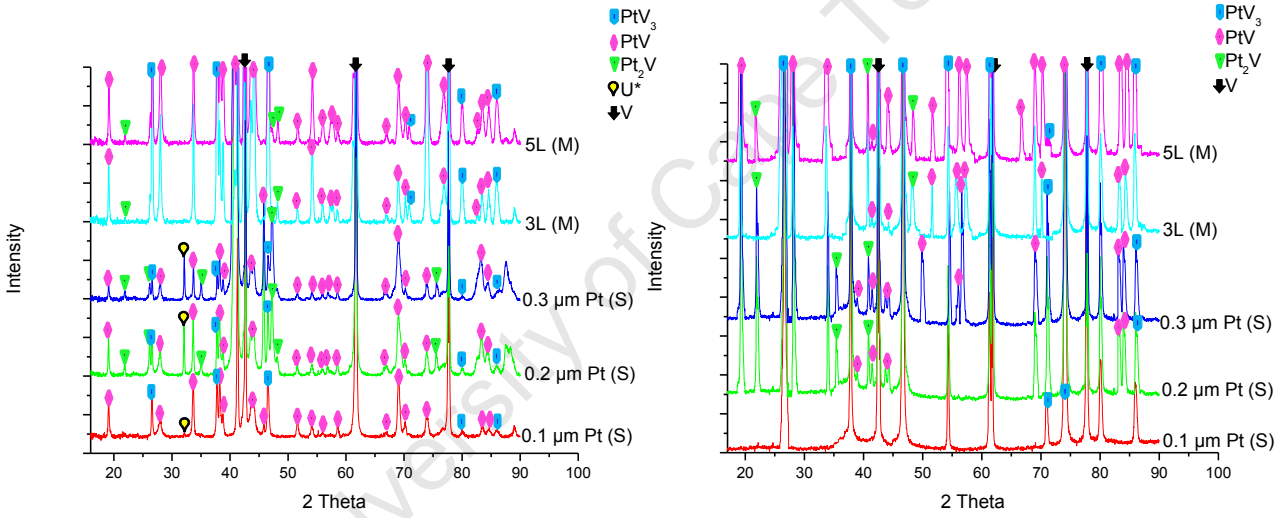

Figure 5.2.4: Single and multilayer coatings of Pt on V-substrate, heat treated at 800°C (A) and 900°C (B) for 8 hours. (S) = single layers and (M) = multilayers at alternating 0.1 µm Pt and 0.05 µm V.

As shown in figure 5.2.4 A and B, heat treatment of 3L and 5L multilayers resulted in formation of higher peak intensities of ordered phases compared to heat treatment of single layer coatings. The difference between single and multilayer coatings is accordingly that, for the same heat treatment temperature and time, the volume fraction of each phase formed is greater in multilayer coatings than in single layer coatings, even if the total Pt coating thickness is the

same. This suggests that diffusion in multilayer coatings is more efficient than in thick single layer coatings; probably because in thin multilayer coatings, the diffusion distance is short.

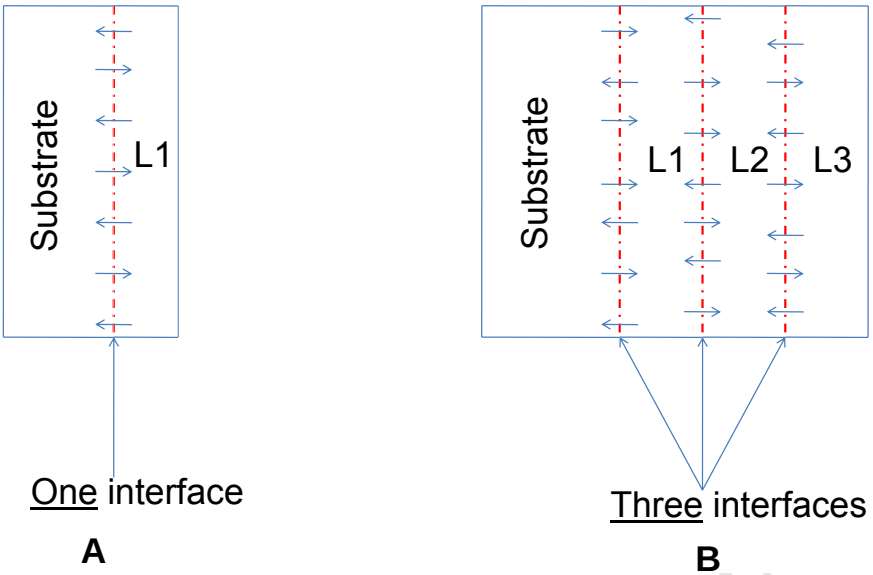

Figure 5.2.5: A schematic diagram showing interfaces across which diffusion takes place. A = single layer (L1) Pt-coating on V substrate. B = multilayer coatings made up of L1 and L3 = Pt and L2 = V, on V substrate.

As shown in figure 5.2.5 A, there is only one interface across which Pt and V can diffuse in single layer coatings; but in multilayer coatings, diffusion takes place across more than one interface as shown in figure 5.2.5 B. This means that with more than one interface, the diffusion distance is shorter, which therefore results in faster phase formation compared to the longer diffusion distance.

5.2.2 Single and multilayer coatings on Pt substrates

Heat treatments of single and multilayer V coatings on Pt substrates resulted in a different sequence of phase formation compared to when V was used as a substrate with Pt coatings. The peak intensities observed after heat treatments of single and multilayer coatings on Pt substrates

at 600°C and 700°C were very small and, as explained in section 5.2.1 above, such peaks were considered as an indication of phase nucleation only. Higher temperature heat treatments resulted in formation of greater peak intensities; hence the following discussion is based on heat treatments at 800°C and 900°C for different times.

5.2.2.1 Differences in phase formation between platinum and vanadium substrates coated with a 0.3 µm single layer

A general difference between the two substrates used in this research project is that Pt rich ordered phases were found preferentially when Pt was used as a substrate and V rich ordered phases were formed when V was used as a substrate as shown in Chapter 4.

A single layer coating of 0.3 µm is used for comparison of substrates here, because the multilayer coatings on V and Pt substrates are not directly comparable (different coating thicknesses were applied as explained in chapter 3). A single layer coating of 0.3 µm Pt on V substrate (discussed in section 5.2.1 above) resulted in formation of PtV_3, PtV and Pt_2V peaks after heat treatment at 800°C for 8 hours. Changing the substrate to Pt coated with a single layer of 0.3 µm V resulted in formation of Pt_3V, Pt_2V and PtV after the same heat treatment time and temperature as shown in figure 4.2.8. Therefore, for the same heat treatment temperature, time, and thickness of coated layer, Pt_3V is formed preferentially when Pt is used as a substrate whereas PtV_3 is formed when V is used as a substrate. This suggests that, with all other factors kept the same, the phases formed are determined by the type of substrate/coating used. This observation was unexpected because according to the Pt-V phase diagram and the EHF rule, PtV_3 is expected to be the first phase formed for both substrate types (because PtV_3 has the composition closest to the liquidus composition). Details on first phase formation as determined by the EHF rule and the Pt-V phase diagram are discussed later in section 5.3.3.

5.2.2.2 Similarities in phase formation on platinum and vanadium substrates

Besides the fact that Pt rich ordered phases formed preferentially, the trend in phase formation as discussed in section 5.2.1 above was also seen during heat treatments of V coatings on Pt substrates. For instance, figure 4.2.8 shows that increase in time of heat treatment from 4 hours to 8 hours at 800°C resulted in growth of the Pt_3V peaks and formation of Pt_2V and PtV peaks. This showed the expected time effect on phase formation, whereby growth and also nucleation of new peaks is expected with increase in time of heat treatment.

Heat treatment of V coatings on Pt substrates at 900°C, for 2 hours and 4 hours, resulted in only peaks of the Pt_3V phase. The implication of this is that, in order to form the Pt_3V phase from the limited volume of V available, the Pt_2V and PtV phases were decomposed at 900°C. This behaviour was also noted after heat treatments of 0.1 μm Pt single layers on V substrate, whereby the PtV phase was formed up to 800°C and was decomposed at 900°C (figure 4.2.1).

Heat treatments of multilayer coatings on Pt substrates and V substrates showed a similar effect of time and temperature on phase formation as in single layers. Figure 4.2.11 and 4.2.12 provide evidence of this observation for Pt substrates: increasing heat treatment time from 4 hours to 8 hours at 800°C and from 2 hours to 4 hours at 900°C resulted in an increase in the intensity of peaks of ordered phases previously formed, in addition to formation of new peaks. But an increase in temperature from 800°C to 900°C generally resulted in fewer peaks of ordered phases. Peaks of V rich ordered phases, in particular, were formed less as the heat treatment temperature increased: at 900°C, V rich ordered phase are decomposed whereas the Pt rich ordered phases remain stable. Comparing the two substrates, V rich ordered phases formed preferentially when V was a substrate, and Pt rich ordered phases formed preferentially when Pt was a substrate. This shows that phase formation is determined by the substrate used.

5.2.2.3 The effect of time at temperature on phase formation

The volume fraction of phases formed increases with an increase in time at temperature; and peak intensities of ordered phases also increase with increased time of heat treatment. For instance, figure 4.2.11 shows that more peaks with high intensities were formed after heat treatment at 800°C for 8 hours compared to heat treatment at the same temperature for 4 hours. The effect of time at temperature on diffusion can be explained by a schematic diagram shown in figure 5.2.6 below.

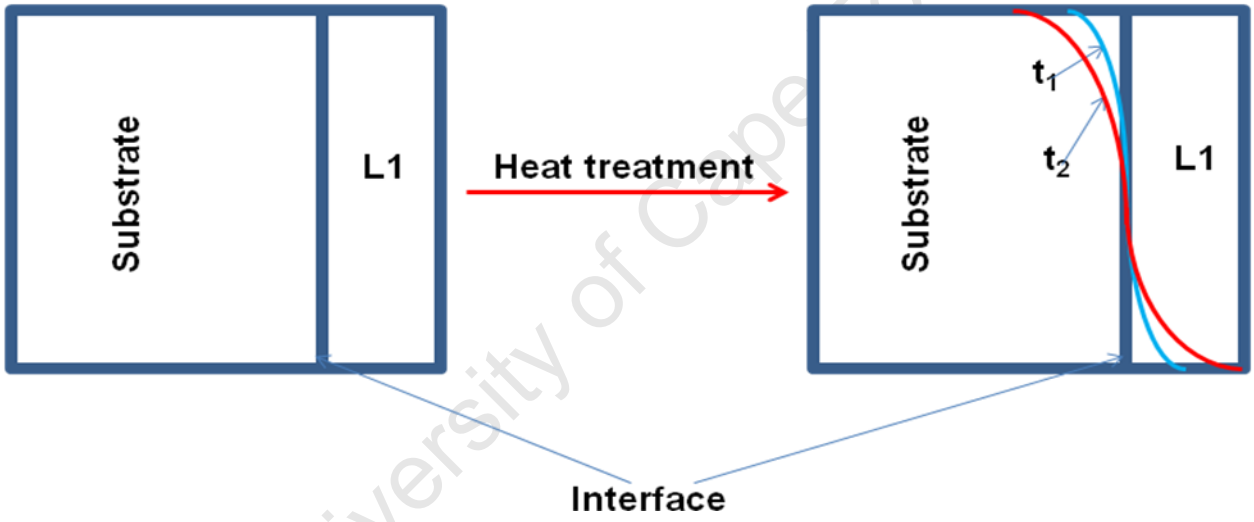

Figure 5.2.6: A schematic diagram showing interdiffusion as a result of increase in time of heat treatment (t = time and L = coated layer).

During heat treatment of a diffusion couple, an increase in time of heat treatment results in an increase in the distance travelled by unlike atoms within each element, driven down the concentration gradient. For instance, if the substrate represents element A and L1 represents element B, upon heat treatment, B-atoms diffuse into A and A-atoms into B. An increase in time of heat treatment from t_1 to t_2 results in B-atoms travelling further into A and *vice versa*. The implication of this is that, increase in time of heat treatment results in a larger interdiffused zone between coating and substrate, which allows formation of a larger volume of ordered phases.

5.2.2.4 The effect of number of coating layers on phase formation

Figure 5.2.7 shows a comparison of results obtained from single and multilayer coatings on Pt substrates heat treated at 800°C and 900°C for 8 hours.

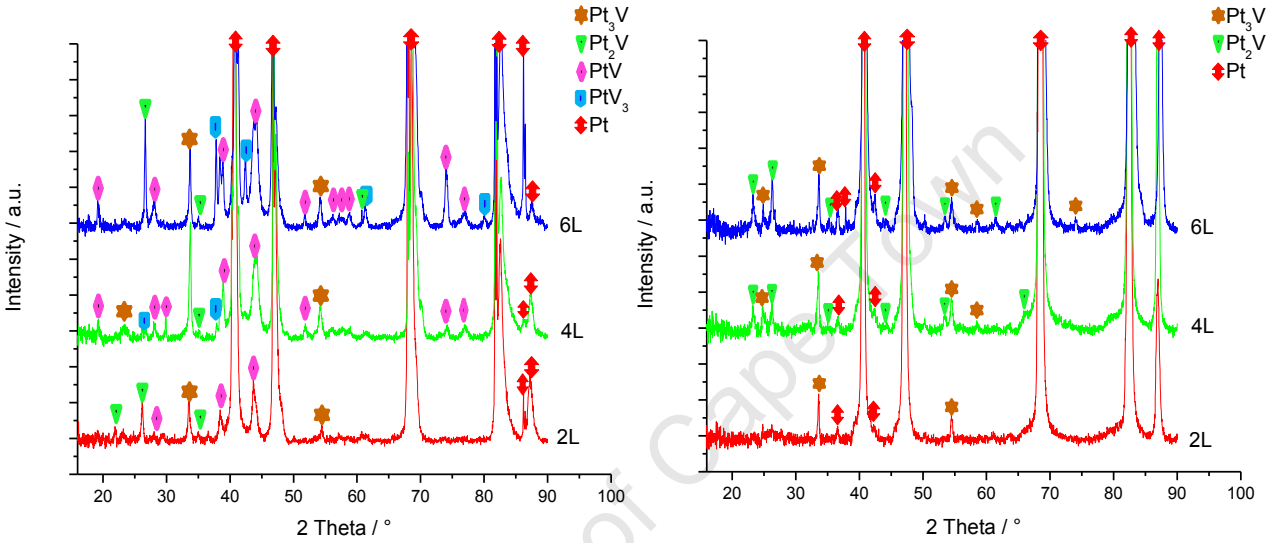

Figure 5.2.7: Single and multilayer coatings of V on Pt substrate, heat treated at 800°C for 8 hours (A) and 900°C for 8 hours (B). (2L = single layer of 0.3 µm V. 4L and 6L = multilayers of alternating 0.3 µm V and 0.07 µm Pt).

As shown in figure 5.2.7, volume fraction of ordered phases increases with an increase in number of coated layers. Based on the discussion in section 5.2.1, an increase in the number of layers results in more than one, or larger, interdiffused layer which allows formation of a larger volume of ordered phases; hence the observed increase in intensity and total number of peaks of ordered phases with increase in number of coating layers.

5.3PHASE FORMATION IN RELATION TO THE Pt-V PHASE DIAGRAM

Section 5.3.1 will focus on phase formation in relation to the Pt-V equilibrium phase diagram shown in figure 5.3.1. A discussion of first phase formation follows in section 5.3.2. Finally, section 5.3.3 presents discussion on phase formation sequence.

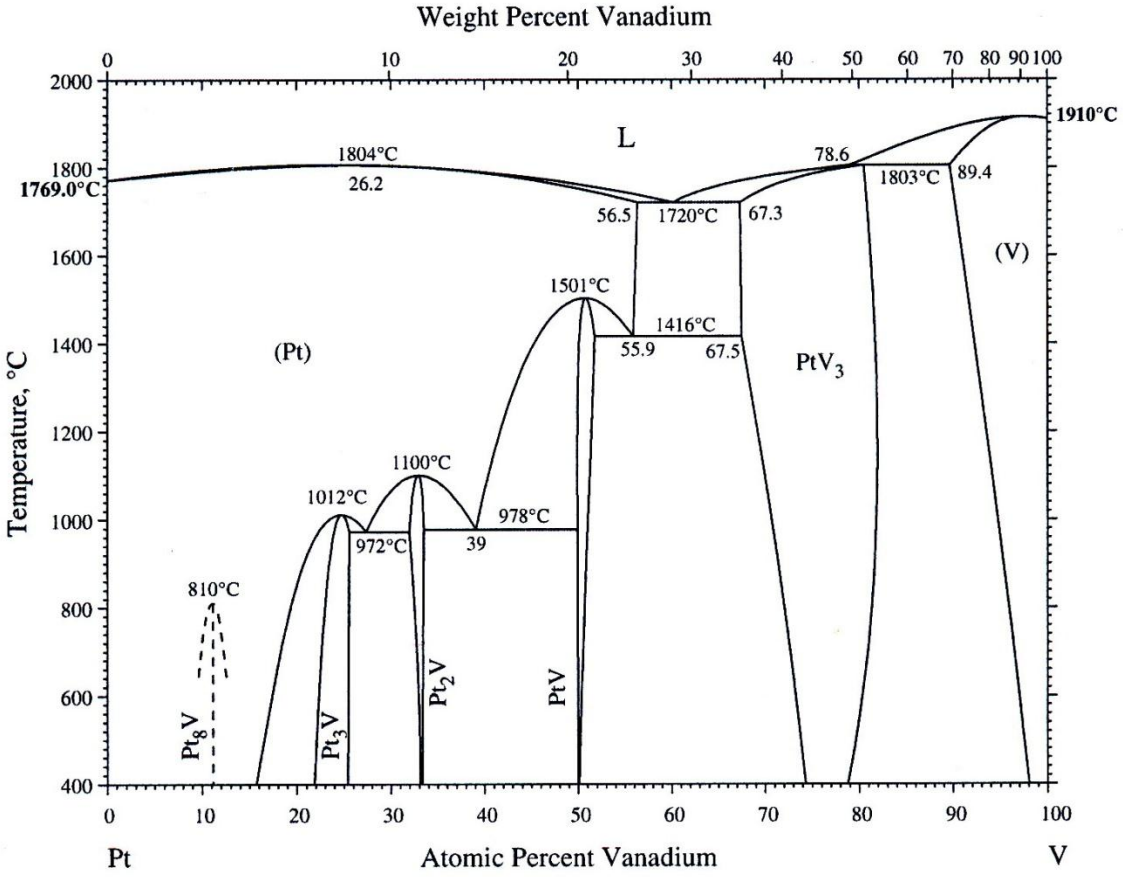

Figure 5.3.1: Equilibrium phase diagram of platinum-vanadium system (after Waterstrat [32] with Pt_8V information by Nxumalo *et al.* [6]).

Table 5.3.1: Summary of temperature and alloying requirements for the formation of Pt-V ordered phases (after Waterstrat [32]).

Ordered structure	Pt composition (at. %)	V composition (at. %)	Heat treatment temperature (°C)
Pt_3V	74 - 78	22 - 26	400 - 1000
Pt_2V	67	33	400 - 1100
PtV	50	50	400 - 1500
PtV_3	21 - 26	74 - 79	400 - 1800
Pt_8V	89	11	- 810

5.3.1 Overall phase formation

Table 5.3.1 shows a summary of the combinations of temperature and composition at which the five ordered Pt-V phases are stable, as per the phase diagram. (Note that the lowest phase diagram temperature is 400°C; the phases are expected to be stable also at lower temperatures). The aim of the experiments carried out in this project was to characterize the phase transformations which are observed after heat treatment of Pt and V coatings on V and Pt substrates. This led to the selection of 600°C, 700°C, 800°C and 900°C heat treatment temperatures, which resulted in formation of four Pt-V ordered phases, Pt_8V not being observed. Although the four ordered phases Pt_3V, Pt_2V, PtV and PtV_3 are stable at all heat treatment temperatures, they were not all observed after each heat treatment.

Pt_8V ordered phase has previously been shown to have exceptionally slow kinetics of formation [6]. It was therefore unlikely to form under heat treatment conditions investigated in this work. Furthermore, Pt_8V has a large tetragonal unit cell, which further reduces its probability of formation under these experimental conditions.

According to Pretorius *et al.* [1, 3, 4], formation of a new phase is preceded by consumption of the previous phase. This means that if heat treatment temperature increases for instance, some of the ordered phases formed at the lower temperature will be consumed to initiate formation of new ordered phases which are (either thermodynamically or kinetically) favored at the higher temperature. This is because ordered phases are formed in sequence and following formation of

the first phase, the second phase forms at the intersection between the first phase and the unreacted element and this phase is expected to form at the expense of the first phase.

5.3.2 The effect of composition on phase formation

In a bulk diffusion couple, "composition" refers to the relative fraction of the two inter-acting elements. In a thin film system however, the "composition" of interest relates to the volume of coating available for phase formation. In the Pt-V system, this effect was seen after gradually increasing the thickness of the Pt coating on the V substrate. Figures 4.2.1, 4.2.2 and 4.2.3 respectively show that there was a higher overall phase formation after heat treatment of 0.2 µm Pt and 0.3 µm Pt at different temperatures compared to 0.1 µm Pt. A specific illustration of this can be made using the XRD spectrum showing heat treatment at 900°C for 8 hours for the three different coating thicknesses. At 0.1 µm Pt coating, the only peaks seen were those of the PtV_3 ordered phase, but the heat treatment of 0.2 µm Pt and 0.3 µm Pt resulted in additional peaks of the PtV and Pt_2V phases. This demonstrates that at 0.1 µm Pt, the concentration of Pt was not high enough to enable the formation of PtV and Pt_2V phases, of which the Pt requirements are 50 at.% and 67 at.% respectively. As can be seen from the phase diagram, PtV and Pt_2V phases are expected to form in a very narrow composition range but the likelihood of these ordered phases forming increases with an increase in the Pt coating thickness.

The disadvantage of increasing the coating thickness is that it requires higher temperatures, or longer times, to achieve a complete diffusion of thick coatings because the diffusion distance is longer. This was seen after heat treatment of different Pt coating thicknesses at the same temperature and time, as seen in figure 4.2.4 (600°C, 8 hours) and figure 4.2.5 (700°C, 8 hours). The spectra in both figures show few peaks of ordered phases for the 0.3 µm Pt coating compared to the 0.1 µm Pt and 0.2 µm Pt coatings. At higher temperatures such as in figure 4.2.6 (800°C, 8 hours) and figure 4.2.7 (900°C, 8 hours), phase formation is consistent, increasing with increase in thickness of Pt coating. Besides high temperature requirements, thick coatings are also a disadvantage because they can have poor adhesion with the substrate as shown by

morphology characterization in section 4.1. Thick coatings show discontinuous adhesion with substrate as shown in figure 5.2.2 and this result in no interdiffusion at the site of the voids.

But if the ultimate desire is to form Pt rich ordered phases, then the thick Pt coatings are advantageous. Firstly, it has been illustrated by results obtained in this project that the formation of Pt rich ordered phases is directly proportional to the thickness of Pt coating. For instance, figure 4.2.1 shows that the thickness of 0.1 µm Pt heat treated at 900°C for 8 hours resulted in only PtV_3 peaks forming. But when the coating thickness was increased to 0.2 µm Pt and 0.3 µm Pt and heat treated at the same temperature and time as shown in figure 4.2.2 and 4.2.3 respectively, PtV and Pt_2V peaks were formed in addition to PtV_3 peaks. This therefore shows that in thin coatings the Pt was not enough to enable formation of PtV and Pt_2V phases. A series of heat treatments from 600°C to 900°C as shown in figures 4.2.1, 4.2.2 and 4.2.3 also shows that at 0.1 µm Pt, Pt_2V phase was not formed. The PtV peaks which started forming at 700°C, increased at 800°C but were not seen at 900°C. This therefore shows that the Pt concentration available at 0.1 µm coating was only enough to form PtV in addition to PtV_3, and that the Pt coating was consumed with an increase in temperature. This was confirmed by compositional analysis of 0.1 µm Pt coatings, shown in figure 4.1.6, which shows higher Pt content after heat treatment at 600°C for 8 hours compared to the heat treatment at 900°C for 8 hours.

In addition, increasing Pt coating thickness can be regarded as an advantage as it has been shown that an increase in coating thickness resulted in an increase in the volume of ordered phases. This was shown by the increase volume fraction of peaks formed at various angles. (For instance, comparing the phase formation at 0.2 µm and 0.3 µm Pt, the same ordered phases were formed but at a higher volume fraction of peaks at 0.3 µm Pt coating than at 0.2 µm Pt coating.) Thick coatings could offer particular benefits if the intended application requires wear resistance.

5.3.3 First phase formation

The EHF model [1, 3, 4, 46-50] states that the first phase to form is controlled by the lowest temperature eutectic. This is in agreement with Brown and Ashby [49] who state that the greatest mobility of atoms, which leads to the most effective mixing at a reaction interface upon heating, is expected to take place at the composition of the lowest eutectic (or liquidus) of the binary system. From the Pt-V phase diagram shown in figure 5.3.1, the first phase expected to form is PtV_3 because its composition is closest to that of the lowest eutectic temperature. PtV_3 was indeed the first ordered phase formed after heat treatment of Pt on V substrate in this project. From figure 4.2.1, heat treatment of 0.1 µm Pt on V substrate at 600°C for 8 hours shows small peaks of PtV_3 only. Given that 600°C was the lowest temperature studied in this project, this shows that PtV_3 was the first to nucleate. The EHF model [1, 3, 4] also states that the first phase formed will increase in volume until the limiting element is completely consumed. Figure 4.2.1 shows that the PtV_3 peaks which nucleated at 600°C increased in intensity at 700°C, i.e. the PtV_3 phase increased in volume.

According to the EHF model [1, 3, 4], the effective concentration at the growth interface is independent of the relative thicknesses of the interacting components. In the present work, this means that the formation of PtV_3 as the first ordered phase should be independent of the thickness of coatings, and also of which element is substrate. According to the results obtained in this project however, changing the substrate to Pt does not result in PtV_3 as the first ordered phase to form. Instead, heat treatment of single and multilayer coatings on Pt substrates showed Pt_3V as the first ordered phase formed, as shown in figure 4.2.8. The intensity of these peaks increased with increase in heat treatment time and temperature.

When Pt was used as a substrate, the only configuration which exhibited the PtV_3 phase was the 6L multilayer coating heat treated at 800°C for 4 hours, as shown in figure 4.2.12. Even for this sample, the intensity of the PtV_3 peaks was smaller than that of Pt_2V and Pt_3V peaks. The PtV_3 phase in this case is likely to have formed only because the 6L multilayer had (0.3 µm) more V than the 4L multilayer, i.e. a greater volume of V to enable formation of PtV_3.

5.3.4 Sequence of phase formation in Pt-V thin film systems

Phase formation in thin films is sequential; according to the EHF rule [1, 3, 4]. Results obtained from the heat treatment of coatings in this research project displayed a sequential phase formation, but not always the sequence expected. Tables 5.3.2 to 5.3.5 show the sequence of ordered phases formed on V and Pt substrates.

5.3.4.1 Phase formation sequence in Pt single-layer coatings on V substrates

Table 5.3.2: Sequence of phase formation in single layer coatings of Pt on V substrate as heat treatment temperature and coating thickness increases.

Single layer coatings	600°C	700°C	800°C	900°C
0.1 µm Pt	PtV_3	PtV_3, PtV	PtV_3, PtV	PtV_3
0.2 µm Pt	PtV_3, PtV	PtV_3, PtV	PtV_3, PtV, Pt_2V	PtV_3, PtV, Pt_2V
0.3 µm Pt	PtV_3, PtV	PtV_3, PtV, Pt_2V	PtV_3, PtV, Pt_2V	PtV_3, PtV, Pt_2V

The lowest temperature heat treatment of a 0.1 µm Pt single layer on V resulted in the formation of PtV_3. This is expected to use up the entire limiting element (Pt coating). Increasing either temperature or coating thickness however resulted in phase formation in the sequence PtV_3, PtV, Pt_2V. This is inconsistent with the EHF model [1, 3, 4], which predicts that after the first phase formation (PtV_3), the next phase to form at at the V/PtV_3 interface is a V rich phase (because the effective concentration of the unreacted element (V) is greater than the composition of PtV_3). Pretorius *et al.* [1, 3, 4] showed that for the Al/Zr coating system, $ZrAl_3$ was the first and only phase formed from thin Zr on thick Al, consistent with the EHF model. Similarly, since PtV_3 is the most V rich ordered phase that can be formed in the Pt-V system, no further interaction is expected to take place and PtV_3 should be the first and only phase to form. This was not the case in this project: for thin Pt on thick V, PtV_3 was the first but not the only phase formed as seen in

table 5.3.2 and table 5.3.3. The disappearance of the PtV peak for the a 0.1 µm Pt single layer on V is an outlier which will be discussed in section 5.4 below. The Pt_3V phase was not observed.

5.3.4.2 Phase formation sequence in multilayer coatings on V substrates

Table 5.3.3: Sequence of phase formation in multilayer coatings on V substrate as heat treatment temperature and number of layers increase.

Multilayer coatings	600°C	700°C	800°C	900°C
3L	__	PtV_3, PtV	PtV_3, PtV, Pt_2V, Pt_3V	PtV_3, PtV, Pt_2V, Pt_3V
5L	__	PtV_3, PtV	PtV_3, PtV, Pt_2V, Pt_3V	PtV_3, PtV, Pt_2V, Pt_3V

Heat treatments of multilayer coatings on V substrates showed no formation of ordered phases after heat treatment at 600°C, two phases at 700°C and three phases after heat treatment at 800°C and 900°C (figure 4.2.9 and figure 4.2.10). The phase formation sequence is thus PtV_3, PtV, Pt_2V which was the same as seen in single layer coatings. The sequential phase formation as expected in coating studies was therefore demonstrated in both single and multilayer coatings but not necessarily in the order predicted by the EHF rule.

5.3.4.3 Phase formation sequence in V single layer coatings on Pt substrates

Table 5.3.4: Sequence of phase formation in single layer coatings of V on Pt substrate as heat treatment temperature increases.

Single layer coatings	600°C	700°C	800°C	900°C
0.3 µm V	__	__	Pt_3V, Pt_2V, PtV	Pt_3V

Heat treatment of single layer coatings of 0.3 µm V on Pt substrate at 600°C and 700°C resulted in no formation of ordered phases. Figure 4.2.8 shows that peaks of ordered phases only started to form after heat treatment at 800°C for 4 hours. After this heat treatment Pt_3V peaks were observed; increasing heat treatment time to 8 hours resulted in growth of the Pt_3V peaks and formation of Pt_2V and PtV peaks. Increasing heat treatment temperature to 900°C resulted in disappearance of the latter two phases, suggesting that decomposition of the Pt_2V and PtV phases has occurred at this temperature; the peaks of Pt_3V phase remained. Therefore with Pt as a substrate, the phase formation sequence was Pt_3V, Pt_2V, PtV: the EHF rule for phase formation sequence was not followed. The order of phase formation was also the inverse of that in V substrates.

5.3.4.4 Phase formation sequence in multilayer coatings on Pt substrates

Table 5.3.5: Sequence of phase formation in multilayer coatings on Pt substrate as heat treatment temperature and number of layers increase.

Multilayer coatings	600°C	700°C	800°C	900°C
4L	__	__	Pt_3V, Pt_2V, PtV, PtV_3	Pt_3V, Pt_2V
6L	__	__	Pt_2V, Pt_3V, PtV, PtV_3	Pt_3V, Pt_2V

Similarly to a single V layer on Pt, heat treatments at 600°C and 700°C of multilayers showed no formation of ordered phases. The first peaks of ordered phases were seen after heat treatment of the 4L multilayer at 800°C for 4 hours as shown in figure 4.2.11. The Pt_3V peaks seen at this heat treatment temperature showed higher intensity than the Pt_2V peaks, which suggests formation of Pt_3V as the first phase. Increasing heat treatment time to 8 hours resulted in increased intensity of Pt_3V peaks and formation of PtV and PtV_3 peaks. The peak intensity of PtV was higher than that of PtV_3, therefore placing PtV third, and PtV_3 fourth, in the phase formation sequence.

Further increasing heat treatment time and/or temperature resulted in decomposition of PtV and PtV_3 peaks, leaving Pt_3V and Pt_2V as the only remaining ordered phases at 900°C. The Pt rich ordered phases were therefore formed preferentially when Pt was used as a substrate. Therefore as seen in single layer coatings of V on Pt substrate, the EHF rule for phase formation sequence is not followed in multilayer coatings and the order of phase formation is inversely related to that observed when V was used as a substrate.

5.4EVALUATION OF THE EHF MODEL USING THE Pt-V SYSTEM

Calculated data on Effective Heat of Formation (ΔH´) for predicting phase formation in the Pt-V binary system is not recorded in the literature. In this work however, the EHF equation was used to estimate ΔH´ to predict phase formation in Pt-V system. The equation is stated as follows [1, 3, 4].

ΔH´ = ΔHº x (effective concentration of limiting element/compound concentration of limiting element)

The lowest temperature on the liquidus curve of the Pt-V phase diagram is 1720ºC. The effective concentration at the composition of this lowest eutectic is 60.7 at.% V, 39.3 at.% Pt. Therefore, table 5.3.6 below shows the ΔH´ values calculated at this concentration.

Table 5.3.6: ΔH´ values calculated for limiting Pt (Pt < V) and limiting V (Pt > V).

Phase	Compound concentration [51]	ΔHº kJ(mol. at.)$^{-1}$ [43, 51]	Limiting element	ΔH´ kJ(mol. at.)$^{-1}$	Limiting element	ΔH´ kJ(mol. at.)$^{-1}$
PtV_3	$Pt_{0.25}V_{0.75}$	-20	Pt	-31.4	V	-16.2
PtV	$Pt_{0.5}V_{0.5}$	-36	Pt	-28.3	V	-43.7
Pt_2V	$Pt_{0.667}V_{0.333}$	-38	Pt	-22.4	V	-69.3
Pt_3V	$Pt_{0.75}V_{0.25}$	-29	Pt	-15.2	V	-70.4

According to calculations shown in table 5.3.6, the effective heat of formation (ΔH´) is different depending on which element is the coating (limiting). Phase formation sequence is therefore expected to be PtV_3, PtV, Pt_2V, Pt_3V if Pt is the coating and Pt_3V, Pt_2V, PtV, PtV_3 if V is the coating.

According to the EHF model [1, 3, 4], whatever the configuration of a system, mixing at the interface will always be controlled by the lowest temperature eutectic of the system and the effective concentrations will be expected to be as close as possible to that of the lowest eutectic within the concentration range of the two interacting phases. Phases are then expected to react with each other to form a phase with the most negative effective heat of formation with a composition lying between that of the interacting phases.

The EHF and the W-B models correctly predict the first phase formation. But for subsequent phase formation, the EHF rule states that:

"*After the first phase formation in metal-metal binary systems, the next phase to form at the interface between the compound phase and the remaining element is the next phase richer in the unreacted element, which has the most effective heat of formation."*

The W-B states that:

"The second phase is the compound with the smallest ΔT that exists in the phase diagram between the composition of the first phase and unreacted element."

Therefore, phase formation sequence in Pt-V system is more consistent with the W-B model because it only considers ΔT differences existing in the phase diagram, whereas the EHF model fails for Pt-V system because it says subsequent phases form richer in the unreacted element, which means for Pt < V (Pt coating), after the formation of PtV_3, the next phase will be richer in V, but PtV_3 is the most V rich ordered phase.

According to the Pt-V phase diagram, vanadium is expected to diffuse into platinum more readily than platinum into vanadium, because the platinum-based solid solution accommodates vanadium to a greater degree than vanadium accommodates platinum.

5.4.1 Thin Pt-coatings on thick V-substrates (Pt < V)

The Pt < V system studied in this research project showed that PtV_3 was formed first upon heat treatment of Pt coatings on V substrate, as predicted by the EHF model. According to this model, no other phase is expected to form until the entire limiting element (Pt coating) is used up for the formation of PtV_3; the second phase is then formed at the expense of the first phase. This continues for subsequent phase formation. In the P < V system however, when the second phase (PtV) forms, the peak intensity of the first phase (PtV3) does not decrease as expected; instead it increases with increasing temperature, growing while the second phase is forming. In other words, in the Pt < V system, the second and subsequent phases do not "wait" for the first phase to use up the entire coating.

Based on the results of the present work, it is proposed that phases nucleate in sequence, but formation of a subsequent phase does not require consumption of the previous phase. Formation of these ordered phases is, rather, dependent on the availability of coating. This is proposed to take place as follows: PtV_3 is nucleated first but does not use up the entire coating before PtV forms second; if the coating is limited such as in 0.1 µm Pt, no other phase forms. Instead, these two phases grow at the expense of the Pt coating as heat treatment temperature increases. A further increase in temperature favors formation and growth of PtV_3 over PtV because at high temperature, we expect a high diffusion rate. Also, since the Pt-V phase diagram suggests faster diffusion of V into Pt than Pt into V, the interdiffusion zone is highly concentrated with vanadium, therefore promoting formation of a V rich phase (PtV_3). This is could be the reason why the PtV phase disappears at 800ºC to only leave PtV_3 at 900ºC as shown in figure 4.2.1.

The coating thickness is important in the Pt-V system because if increased to 0.2 µm and 0.3 µm, growth of the second (PtV) and third (Pt_2V) phase is maintained even with the faster vanadium diffusion into platinum as mentioned above. Only the order in which the second and subsequent phases are formed is controlled by lowest temperature eutectic as predicted by the EHF model. The importance of coating thickness can be illustrated using figure 5.3.2 on phase formation.

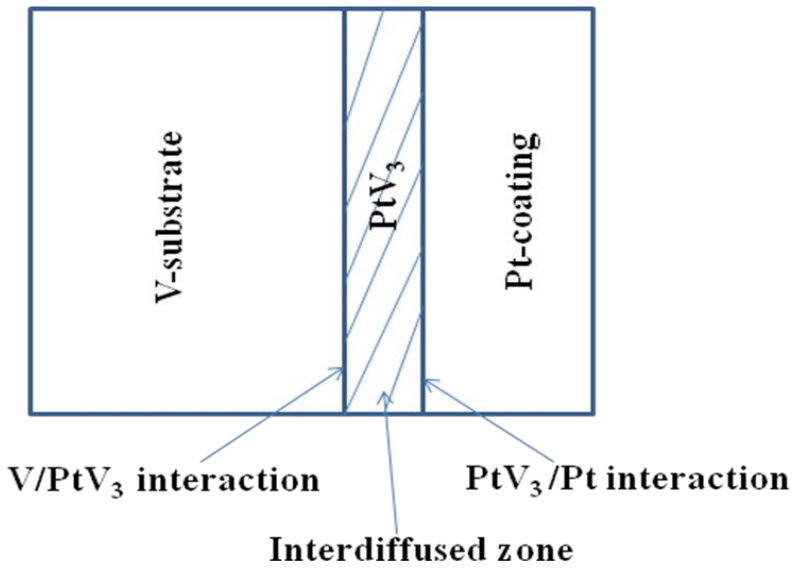

Figure 5.3.2: A schematic diagram showing consumption of the coating element for phase formation.

In thicker coatings such as 0.2 µm Pt and 0.3 µm Pt studied in this project, the first phase is formed but does not consume all the coating in order to grow. On one side of the interdiffused zone (V/PtV_3 interaction) as shown in figure 5.3.2 above, the effective concentration favors formation of V rich phases and since PtV_3 is the most V rich phase that can be formed, no other phase will form. Vanadium would therefore have to diffuse across the interdiffused zone to interact with elemental platinum to form a different phase or PtV_3. But that means the diffusion distance is longer for the vanadium. A shorter alternative diffusion distance would then be on the other side of the interdiffused zone (PtV_3/Pt interaction) which is more likely to result in formation of other phases richer in platinum (PtV, Pt_2V and Pt_3V). So this means having formed PtV_3, the rest of the coating is used to form phases richer in platinum and the volume of PtV_3 phase does not decrease because it is maintained by the faster diffusing vanadium, which for a thinner coating, dominates and eventually PtV_3 becomes the only phase formed as shown in figure 4.2.1 for the 0.1 µm Pt coating.

This is likely to happen in the Pt-V system because, applying the EHF concept for Pt-coating (limiting) on V-substrate (excess/unreacted), after the first phase formation (PtV_3), the effective

concentration of the unreacted element (V) is greater than the composition of PtV_3. This means the next phase to form at V/PtV_3 interface is a V-rich phase, but because PtV_3 is the most V-rich phase that can be formed, no interaction is expected to take place and PtV_3 becomes the first and only phase to form [3]. (Pretorius used thin Zr on thick Al to illustrate this and says $ZrAl_3$ will be the first and only phase formed). This was not the case in the Pt-V system because with PtV_3 being the most V rich phase for thin Pt on thick V, PtV_3 was the first but not the only phase formed.

A noticeable phase formation trend in the Pt-V system is that, once a particular phase is formed, it keeps growing depending on availability of coating, and this contradicts the EHF model which predicts that the first phase will be consumed to form the second phase which in turn will be consumed to form the third phase. Consumption/decomposition of ordered phases in the Pt-V system was only seen when coating thickness was limiting. In this case, the ordered phases are consumed in a reverse order in which they were formed. This means the phase formed last in a sequence (most Pt rich) will be the first to decompose, while phases richer in V remain stable. Therefore from the three phases Pt_2V, PtV and PtV_3, the Pt_2V phase will be consumed as temperature increases to form PtV and PtV_3. If only PtV and PtV_3 were formed, then PtV will be consumed to form PtV_3. The process is also likely to be influenced by the faster diffusion of V into Pt, hence the preferred V richer phases.

In the Pt-V system then, coating thickness and the faster diffusion of V into Pt than Pt into V take dominant control of phase formation. The EHF model fails for this system because after the first phase formation, it predicts formation of phases richer in the unreacted element (V), which was not the case in Pt-V system. The results in this project rather show that after formation of PtV_3 as the first (correctly predicted) phase, subsequent phases formed were respectively richer in Pt than V. In summary, for Pt < V, the sequences of phase formation was PtV_3, PtV, Pt_2V and Pt_3V.

5.4.2 Thin V-coatings on thick Pt-substrates (Pt > V)

Phase formation in the Pt > V configuration is directly opposite that in the Pt < V configuration. For thin V coatings on thick Pt substrates, the first phase formed was Pt_3V. The EHF model fails for this configuration because it predicts that the first phase should be the one closest to the liquidus temperature, which is PtV_3.

The sequence of phase formation in the Pt > V configuration was Pt_3V, Pt_2V, PtV, PtV_3. The amount of coating element determined phase formation just as in the Pt < V configuration. For instance, comparing 4L with 6L multilayers of this configuration (Figure 4.2.11 and figure 4.2.12 respectively), PtV_3 was only formed after heat treatment at 800ºC/8hrs in 4L multilayer, whereas in 6L multilayer it was nucleated at 800ºC/4hrs and grew as heat treatment temperature and time increased. This emphasizes the determining effect of coating thickness over the EHF model on phase formation in the Pt-V system.

6. CONCLUSIONS

1.

- Four ordered Pt-V phases (PtV_3, PtV, Pt_2V and Pt_3V) which were previously only formed in bulk Pt-V alloys, were successfully formed in the Pt-V coated system.

2.

- The kinetics and thermodynamics of ordered phase formation in Pt-V coatings were found to be affected by heat treatment time, temperature, coating thickness and number of coating layers. Volume fraction of ordered phases was found to increase with an increase in magnitude of these factors.
- For single layer coatings, roughness and damage such as cracking and delamination of coatings were found to increase with increase in heat treatment time, temperature and coating thickness. But for the same amount of coating material separated into multilayers, roughness and damage such as cracking and delamination was minimal. This was a result of less residual strains in thin multilayer coatings than in thick single layer coatings.
- Phase transformation in multilayer coatings was found to be more efficient than in single layer coatings because for the same amount of coating material, a higher volume fraction of ordered phases were formed from multilayer coatings than single layer coatings. This is because diffusion distance is shorter in multilayer coatings than in think single coatings.
- Finally, based on the sequential phase formation in coating systems as opposed to simultaneous phase formation in bulk alloys, experimental parameters such as heat treatment time, temperature, coating thickness and number of coatings can be controlled for optimum formation of desired ordered phases.

3.

- The EHF model was successful in predicting first phase formation in the Pt-V system only when the configuration was thin Pt coating on thick V substrate (Pt < V). Results in this research project have demonstrated this in all single layer and multilayer coatings.

- In terms of phase formation sequence in the Pt-V system, the EHF model was also successful in predicting that subsequent phase formation is controlled by the lowest temperature eutectic of a system, in that the effective concentrations are expected to be as close as possible to the concentration of the lowest eutectic. The Pt-V phase diagram shows that PtV_3 has the closest composition to that of the lowest eutectic hence is expected to be the first phase formed. The next closest effective concentration favors formation of PtV followed by Pt_2V and finally Pt_3V. In this regard, the results obtained in this project demonstrated correctly the phase formation sequence as PtV_3, PtV, Pt_2V and Pt_3V according to the EHF model and the Pt-V phase diagram.
- For the Pt-V system, the model fails in two ways. First, for the Pt < V configuration, Pt is limiting and following first phase formation, the next phase is expected to be V rich. But in the Pt-V system, ordered phases were successively formed richer in Pt. Secondly; phases formed first are expected to decrease in volume to form subsequent phases. In Pt-V system however, subsequent phases were formed and grew along with the phases initially formed but only until the coating was limiting, in which case the most Pt-rich phase (formed last) was the first to be consumed.
- Changing the configuration to a thin V coating on thick Pt substrate rendered the EHF model unsuccessful on two counts. Firstly, the first phase formed was Pt_3V instead of PtV_3 as predicted by the EHF model. Secondly, the model fails because it predicts that following first phase formation in Pt > V, the next phase formed will be richer in the unreacted element. But following Pt_3V as the first phase formed in Pt > V configuration, subsequent phases were formed successively richer in V as Pt_2V, PtV and PtV_3, which was a direct opposite to when the configuration was Pt < V, and depending on amount of coating available, the most V rich phase (formed last in the sequence) was the first to be consumed with increase in heat treatment temperature and time.
- Even though attempts were made to minimize contamination, it is possible that prediction of phase formation according to the EHF model was affected by post-deposition contamination.

Finally, according to the EHF model, phases formed first are expected to decrease in volume to form subsequent phases. In the Pt-V system however, the first phase remained stable while other phases were formed, in both the Pt < V and Pt > V configuration.

LIST OF REFERENCES

[1] R. Pretorius, T. K. Marais, and C. C. Theron, "Thin film compound phase formation sequence: An effective heat of formation model," *Materials Science Reports,* vol. 10, pp. 1-83, 1993.

[2] D. A. Porter and K. E. Easterling, *Phase Transformations in Metals and Alloys*: Nelson Thornes, 1992.

[3] R. Pretorius, R. de Reus, A. M. Vredenberg, and F. W. Saris, "Use of the effective heat of formation rule for predicting phase formation sequence in Al-Ni systems," *Materials Letters,* vol. 9, pp. 494-499, 1990.

[4] R. Pretorius, "Prediction of silicide formation and stability using heats of formation," *Thin Solid Films,* vol. 290-291, pp. 477-484, 1996.

[5] Z. W. Lu and B. M. Klein, "Theoretical studies of the stability of ordered A8B compounds," *Physical Review B,* vol. 50, pp. 5962-5970, 1994.

[6] S. Nxumalo and C. I. Lang, "Thermodynamic stability of Pt8V," *Journal of Alloys and Compounds,* vol. 425, pp. 181-184, 2006.

[7] R. Taylor, S. Curtarolo, and G. Hart, "Predictions of the Pt8Ti Phase in Unexpected Systems," *Journal of the American Chemical Society,* vol. 132, pp. 6851-6854.

[8] S. Nxumalo, M. P. Nzula, and C. I. Lang, "Order hardening of Pt8X alloys," *Materials Science and Engineering: A,* vol. 445-446, pp. 336-340, 2007.

[9] D. M. Solina, R. W. Cheary, P. D. Swift, S. Dligatch, G. M. McCredie, B. Gong, and P. Lynch, "Investigation of the interfacial structure of ultra-thin platinum films using X-ray reflectivity and X-ray photoelectron spectroscopy," *Thin Solid Films,* vol. 372, pp. 94-103, 2000.

[10] I. Fuke, V. Prabhu, and S. Baek, "Computational Model for Predicting Coating Thickness in Electron Beam Physical Vapor Deposition," *Journal of Manufacturing Processes,* vol. 7, pp. 140-152, 2005.

[11] K. Holmberg and A. Matthews, *Coatings Tribology: Properties, Techniques, and Applications in Surface Engineering*: Elsevier, 1994.

[12] W. D. Sproul, "Physical vapor deposition tool coatings," *Surface and Coatings Technology,* vol. 81, pp. 1-7, 1996.

[13] P. H. Mayrhofer, C. Mitterer, L. Hultman, and H. Clemens, "Microstructural design of hard coatings," *Progress in Materials Science,* vol. 51, pp. 1032-1114, 2006.

[14] C. Quiñones, W. Vallejo, and F. Mesa, "Physical and electrochemical study of platinum thin films deposited by sputtering and electrochemical methods," *Applied Surface Science,* vol. 257, pp. 7545-7550.

[15] K. Tammeveski, T. Kikas, T. Tenno, and L. Niinistö, "Preparation and characterization of platinum coatings for long life-time BOD biosensor," *Sensors and Actuators B: Chemical,* vol. 47, pp. 21-29, 1998.

[16] K. Tu and R. Rosenberg, *Preparation and properties of thin films*: Academic Press, 1982.

[17] H. Lüth, *Surfaces and interfaces of solids*: Springer-Verlag, 1993.

[18] H. Lüth, *Surfaces and interfaces of solid materials*: Springer, 1995.

[19] H. Lüth, *Solid Surfaces, Interfaces and Thin Films*: Springer, 2001.

[20] Y. Ma and P. B. Balbuena, "Pt surface segregation in bimetallic Pt3M alloys: A density functional theory study," *Surface Science,* vol. 602, pp. 107-113, 2008.

[21] D. L. Beke and I. A. Szabó, *Diffusion and stresses: proceedings of the 1st International Workshop on Diffusion and Stresses, held in Balatonfüred, Hungary, May 28-31, 1995*: Scitec Publications, 1996.

[22] A. S. Ostrovsky and B. S. Bokstein, "Grain boundary diffusion in thin films under stress fields," *Applied Surface Science,* vol. 175-176, pp. 312-318, 2001.

[23] Y. C. Chen, Y. G. Zhang, and C. Q. Chen, "General theory of interdiffusion growth in diffusion couples," *Materials Science and Engineering: A,* vol. 368, pp. 1-9, 2004.

[24] V. H. Garcia, P. M. Mors, and C. Scherer, "Kinetics of phase formation in binary thin films: the Ni/Al case," *Acta Materialia,* vol. 48, pp. 1201-1206, 2000.

[25] W. M. Holmes, C. De Panfilis, and K. J. Packer, "Diffusion in thin films on the surface of a porous solid," *Magnetic Resonance Imaging,* vol. 19, pp. 525-526, 2001/5// 2001.

[26] V. Branger, V. Pelosin, K. F. Badawi, and P. Goudeau, "Study of the mechanical and microstructural state of platinum thin films," *Thin Solid Films,* vol. 275, pp. 22-24, 1996.

[27] D. Schryvers and S. Amelinckx, "New long period superstructure in Pt3V with M = 3/2," *Materials Research Bulletin,* vol. 20, pp. 367-372, 1985.

[28] D. Schryvers and S. Amelinckx, "Order-disorder phenomena in the platinum rich part of the Pt-V phase diagram," *Acta Metallurgica*, vol. 34, pp. 43-54, 1986.

[29] D. Schryvers, G. Van Tendeloo, and S. Amelinckx, "On the short range order state in Pt3V," *Materials Research Bulletin*, vol. 20, pp. 361-366, 1985.

[30] S. P. Parker, *Solid-state physics source book*. New York: McGraw-Hill, 1988.

[31] A. J. Appleby and G. Editor-in-Chief: Â Jürgen, "CHEMISTRY, ELECTROCHEMISTRY, AND ELECTROCHEMICAL APPLICATIONS| Platinum Group Elements," in *Encyclopedia of Electrochemical Power Sources* Amsterdam: Elsevier, pp. 853-875, 2009

[32] H. Okamoto, "Pt-V (Platinum-Vanadium)," *Journal of Phase Equilibria and Diffusion*, vol. 30, pp. 666-667, 2009.

[33] M. P. Nzula, C. I. Lang, and D. J. H. Cockayne, "The formation of Pt8Cr in Pt 10 at.% Cr," *Journal of Alloys and Compounds*, vol. 420, pp. 165-170, 2006.

[34] F. Liu, S. J. Song, F. Sommer, and E. J. Mittemeijer, "Evaluation of the maximum transformation rate for analyzing solid-state phase transformation kinetics," *Acta Materialia*, vol. 57, pp. 6176-6190, 2009.

[35] A. Van der Ven, H.-C. Yu, G. Ceder, and K. Thornton, "Vacancy mediated substitutional diffusion in binary crystalline solids," *Progress in Materials Science*, vol. 55, pp. 61-105.

[36] H.-C. Yu, D.-H. Yeon, A. Van der Ven, and K. Thornton, "Substitutional diffusion and Kirkendall effect in binary crystalline solids containing discrete vacancy sources and sinks," *Acta Materialia*, vol. 55, pp. 6690-6704, 2007.

[37] R. J. Borg and G. J. Dienes, *An introduction to solid state diffusion*. Boston: Academic Press, 1988.

[38] G. Kostorz, *Phase transformations in materials*: Wiley-VCH, 2001.

[39] K. Tu and R. Rosenberg, *Treatise on Materials Science and Technology: Preparation and properties of thin films*: Academic Press, 1982.

[40] O. Lebacq, A. Pasturel, D. N. Manh, A. Finel, and R. Caudron, "Electronic structure, cohesive properties and phase stability in Ni3V, Pd3V, and Pt3V compounds," *Journal of Alloys and Compounds*, vol. 264, pp. 31-37, 1998.

[41] R. M. Tiggelaar, R. G. P. Sanders, A. W. Groenland, and J. G. E. Gardeniers, "Stability of thin platinum films implemented in high-temperature microdevices," *Sensors and Actuators A: Physical,* vol. 152, pp. 39-47, 2009.

[42] M. Topić, C. A. Pineda-Vargas, R. Bucher, H. E. du Plessis, B. Breedt, V. Pischedda, S. Nxumalo, and C. I. Lang, "High temperature study on thin aluminium coatings deposited onto thick platinum substrates," *Surface and Coatings Technology,* vol. 203, pp. 3044-3048, 2009.

[43] Q. Guo and O. J. Kleppa, "The standard enthalpies of formation of the compounds of early transition metals with late transition metals and with noble metals as determined by Kleppa and co-workers at the University of Chicago - A review," *Journal of Alloys and Compounds,* vol. 321, pp. 169-182, 2001.

[44] J. Chakraborty, U. Welzel, and E. J. Mittemeijer, "Mechanisms of interdiffusion in Pd-Cu thin film diffusion couples," *Thin Solid Films,* vol. 518, pp. 2010-2020.

[45] S. B. Lee, J. M. Rickman, and K. Barmak, "Phase transformation kinetics and self-patterning in misfitting thin films," *Acta Materialia,* vol. 51, pp. 6415-6427, 2003.

[46] P. Mogilevsky and E. Y. Gutmanas, "First phase formation at interfaces: effective heat of formation model for ternary systems," *Materials Science and Engineering: A,* vol. 208, pp. 203-209, 1996.

[47] P. Mogilevsky and E. Y. Gutmanas, "On thermodynamics of first-phase formation during interfacial reactions," *Materials Science and Engineering: A,* vol. 221, pp. 76-84, 1996.

[48] H. Moore, D. Olson, and R. Noufi, "Use of the effective heat of formation model to determine phase formation sequences of In-Se, Ga-Se, Cu-Se, and Ga-In multilayer thin films," *Journal of Electronic Materials,* vol. 27, pp. 1334-1340, 1998.

[49] C. C. Theron, O. M. Ndwandwe, J. C. Lombaard, and R. Pretorius, "First phase formation at interfaces: Comparison between Walser-Bené and effective heat of formation model," *Materials Chemistry and Physics,* vol. 46, pp. 238-247, 1996/12// 1996.

[50] M. Wittmer, M. A. Nicolet, and J. W. Mayer, "The first phase to nucleate in planar transition metal-germanium interfaces," *Thin Solid Films,* vol. 42, pp. 51-59, 1977.

[51] C. P. Wang, A. Q. Zheng, and X. J. Liu, "Thermodynamic assessments of the V-Ge and V-Pt systems," *Intermetallics,* vol. 16, pp. 544-549, 2008.